Nuclear Magnetic Resonance Studies of Protein Conformation

I. Ribonuclease S

II. Hemoglobin

Thesis

by

Wray Hughes Huestis

In Partial Fulfillment of the Requirements

For the Degree of

Doctor of Philosophy

California Institute of Technology

Pasadena, California

1972

(Submitted 26 May 1972)

Acknowledgments

I would like to thank Dr. Michael Raftery, who suggested the studies described in this Thesis, and whose subsequent policy of noninterference contributed greatly to their educational value and to my enjoyment of them. I also owe thanks to Dr. Gregory Ketabgian, whose skilled and tireless needle provided the hemoglobin, and to John Racs for help in amino acid analyses. I thank David L. Huestis for assistance in computer analysis of coupled ionization systems.

I appreciate financial support from the National Science Foundation in the form of Fellowships, and from the California Institute of Technology in the form of teaching assistantships.

To John Howe Scott, with my thanks

Abstract

Fluorine nuclear magnetic resonance techniques have been used to study conformational processes in two proteins labeled specifically in strategic regions with covalently attached fluorinated molecules. In ribonuclease S, the ϵ-amino groups of lysines 1 and 7 were trifluoroacetylated without diminishing enzymatic activity. As inhibitors bound to the enzyme, changes in orientation of the peptide segment containing the trifluoroacetyl groups were detected in the nuclear magnetic resonance spectrum. pH Titration of one of the histidines in the active site produced a reversal of the conformational process.

Hemoglobin was trifluoroacetonylated at the reactive cysteine 93 of each β chain. The nuclear magnetic resonance spectrum of the fluorine moiety reflected changes in the equilibrium position of the β chain carboxy terminus upon binding of heme ligands and allosteric effectors. The chemical shift positions observed in deoxy- and methemoglobin were pH dependent, undergoing an abnormally steep apparent titration which was not observed in hemoglobin from which histidine β 146 had been removed enzymatically. The abnormal sharpness of these pH dependent processes is probably due to interactions between several ionizing groups.

The carbon monoxide binding process was studied by concurrent observation of the visible and nuclear magnetic resonance spectra of trifluoroacetonylated hemoglobin at fractional ligand saturations throughout the range 0-1.0. Comparison of the ligand binding process observed in these two ways yields evidence for a specific order of ligand binding. The sequence of events is sensitive to the pH and organic phosphate concentration of the medium, demonstrating the delicately balanced control system produced by interactions between the hemoglobin subunits and the effectors.

Table of Contents

INTRODUCTION

Nuclear magnetic resonance, a physical tool which has yielded extensive information in structural analysis of molecules of moderate size, has been used to a lesser extent in direct structural and conformational studies of macromolecules such as proteins. The large numbers of nonequivalent protons in a native protein produce a ^{1}H-nmr* spectrum of great complexity with limited resolution of individual resonances even at the highest available magnetic fields. Despite this drawback extensive information on the molecular properties of lysozyme, ribonuclease A and cytochrome c has been obtained from examination of high field methyl group resonances and low field aromatic resonances at 220 MHz by McDonald and Phillips (1969). In addition, the properties of myoglobin (Shulman et al., 1969; Kurland et al., 1968) and hemoglobin (Kurland et al., 1968; Wüthrich et al., 1968) have been examined by ^{1}H-magnetic resonance spectroscopy at 220 MHz through studies of high and low field resonances which arise from interactions of methyl groups with porphyrin rings. Thus, for some proteins whose catalytically or conformationally important residues are unusually shielded or de-shielded, useful assignments and analyses can be made, but an examination of the growing catalogue

---

*Abbreviation: nmr, nuclear magnetic resonance.

of protein spectra serves to show that many interesting proteins are not so fortuitously designed. If nmr is to be generally applicable to direct investigation of protein molecules, methods must be devised for simplifying their spectra to permit unequivocal identification of individual resonances and thereby allow interpretation of spectral changes induced by processes of interest.

The approach employed in these investigations was observation of the ^{19}F-nmr spectrum of a protein modified by covalent attachment of a small fluorinated probe moiety. The probe molecule was introduced specifically into a catalytically or conformationally strategic site on the protein in a way which did not interfere with enzymatic activity. Fluorine is well suited to this purpose, for it is relatively small and easy to introduce as part of small molecules of a variety of reactive specificities. Fluorine nmr absorption occur at frequencies where there is no proton interference, yet they may be observed without drastic modification of proton nmr equipment. Fluorine labeling is particularly useful for study of mammalian proteins, since the in vivo labeling techniques used for study of some bacterial proteins (Katz et al., 1968; Markley et al., 1968; Putter et al., 1969) are impractical for most applications in more complicated organisms.

Ribonuclease S and hemoglobin were the proteins chosen for investigation. Ribonuclease S-peptide can be separated from the remainder of the protein, trifluoroacetylated at its two lysine groups, and then reassociated with the protein to yield an active enzyme with

a simple ^{19}F-nmr spectrum. One of the trifluoroacetylated groups, lysine 7, is found in a helical segment near histidine 12, which is in the active site. Thus the ^{19}F moiety at lysine 7 could be used to detect movements of the helix which resulted when histidine 12 interacted with bound inhibitors. Hemoglobin contains one cysteine residue in each β-chain which is accessible to reaction with thiol reagents under mild conditions. These cysteine residues are found in the $\alpha_1\beta_2$ and $\alpha_2\beta_1$ interfaces in close proximity to several residues which participate in cooperative processes. The fluorinated moiety attached at these positions monitored conformation changes associated with binding of ligands and allosteric effectors.

In both cases, introduction of the fluorine moiety did not interfere with normal activity of the protein.

CHAPTER I

^{19}F-Nuclear Magnetic Resonance Studies of Inhibitor-Induced Conformation Changes in Ribonuclease S

The successful study of conformational processes in proteins by ^{19}F-nmr* depends on the availability of a modification site which can be labeled uniquely with a fluorine probe moiety, and which lies in a region of the protein where mechanistically interesting processes will change its magnetic environment. In addition, precise interpretation of observed effects is possible only if the detailed molecular composition of the fluorine probe site is known, so that application of the technique is most successful in proteins whose crystal structure is known at high resolution.

For these reaons, the protein which was chosen for preliminary investigation by the covalently bound ^{19}F probe technique was ribonuclease S (RNase S). RNase S is formed from bovine pancreatic ribonuclease A by subtilisin cleavage of the amide bond between alanine 20 and serine 21 (Richards and Vithayathil, 1959), the full enzymatic activity of the parent enzyme being retained. RNase S is inactivated by removal of the peptide segment containing residues

---

*Abbreviations used are: nmr, nuclear magnetic resonance; RNase, ribonuclease; 3′-CMP, cytidine-3′-phosphate; 5′-CMP, cytidine-5′-phosphate; 2′-CMP, cytidine-2′-phosphate.

1-20 (RNase S-peptide), but under appropriate conditions the two sections can reassociate with full restoration of enzymatic activity. The fluorine probes selected for this study were trifluoroacetyl groups introduced at lysine residues 1 and 7 of the S-peptide. When trifluoroacetylated ribonuclease S-peptide was associated with ribonuclease S-protein a fully active enzyme was formed. The ^{19}F-nmr spectrum of the modified S-peptide exhibited significant changes on association with the S-protein, and further changes were observed on binding of various inhibitors to this complex.

Experimental

Materials

Ribonuclease S-peptide and S-protein (lot 118B-8110, phosphate-free) were obtained from Sigma Chemical Company. Ethylthioltrifluoroacetate was a product of Pierce Chemical Co. Ribonuclease A, cytidine-2′-phosphate, cytidine-3′-phosphate, cytidine-5′-phosphate, yeast ribonucleic acid, and lysine monohydrochloride were products of Sigma Chemical Co. Phenyl isothiocyanate, trifluoroacetic acid, and N-ethyl morpholine were obtained from Matheson, Coleman and Bell. Aminopeptidase M (lot 51132) was obtained from Henley and Co., and subtilisin Carlsberg (lot 50624) from Novo Industries, Copenhagen.

ϵ-Trifluoroacetyl lysine and α, ϵ-bis(trifluoroacetyl) lysine were synthesized by known methods (Weygand and Geiger, 1956; Schallenberg and Calvin, 1955). ϵ-Trifluoroacetyl lysine--m.p. reported: 226-231° d.; found: 222-230° d. α, ϵ-Bis(TFA)lysine--m.p. reported: 122-123°, found: 121°.

Methods

Ultraviolet absorbances were determined with a Gilford Model 240 spectrophotometer. pH measurements were made using a Radiometer Copenhagen Model 26 or a Sargent Model IR pH meter. ^{19}F-Nmr spectra were recorded using a Varian Model HA-100 spectrometer modified to operate at 94.1 MHz, supplemented by a

Fabritek Model 1062 computer of average transients. Amino acid analyses were performed on a Beckman-Spinco Model 120B amino acid analyser.

RNase enzyme activity was measured using the procedure of Kunitz (1954).

Preparation and Purification of Trifluoroacetylated RNase S-Peptide

Reaction conditions were essentially as described by Goldberger (1967) A solution of RNase S-peptide (15 mg $\equiv 1.5 \times 10^{-5}$ moles lysine residues) in 5 ml of distilled water was adjusted to pH 10 by addition of 5 N NaOH from a micrometer syringe. Ethylthioltrifluoroacetate (1 ml $\equiv 8 \times 10^{-3}$ moles) was added. The pH was monitored continuously and maintained at 10.00 ± 0.05 by addition of 5 N NaOH from the syringe. The reaction was allowed to continue at room temperature for 90 minutes with vigorous stirring. After this time, base consumption had effectively ceased. The pH was lowered to 3.85 by addition of glacial acetic acid, and the resultant solution was subjected to gel filtration on a column (2.5 × 90 cm) of Sephadex G-25 using 0.2 M acetic acid as the eluting solvent. The absorbance of each five ml fraction was determined at 230 nm, and appropriate uv-absorbing fractions were pooled and lyophilized. This procedure typically yielded 8-10 mg of modified peptide.

Amino Acid Analysis of Modified RNase S-Peptide by Total Enzymatic Hydrolysis

To a solution of 0.2 mg of modified S-peptide in 0.5 ml of phosphate buffer (0.1 M, pH 7.0) was added 0.15 mg of subtilisin in 0.1 ml of the same buffer. After the solution had stood for three hours at room temperature, 1.0 mg of aminopeptidase M was added. The solution was allowed to stand for twenty hours at room temperature. The pH of the solution was then adjusted to 2.2 with 6 N HCl, and an aliquot of 0.3 ml of solution was analyzed for amino acid composition. A control solution containing only subtilisin and aminopeptidase M was analyzed identically.

Nmr Spectral Measurements

Nmr solutions were prepared by dissolving 2×10^{-6} moles of modified peptide in 0.5 ml of ammonium formate buffer (0.1 M, pH 4.5), producing a final concentration of 4×10^{-3} M. Solid RNase S protein (2×10^{-6} moles) was added to this solution. Inhibitors were added as solids, producing final concentrations of 4×10^{-3} M for cytidine-5′-phosphate, cytidine-3′-phosphate, and cytidine-2′-phosphate, and 10^{-2} M for phosphate. In studying the effect of pH on the spectrum of RNase inhibited with 3′-CMP, an inhibitor concentration of 7×10^{-2} M was used above pH 6.5. Inhibitors were present in saturating concentrations for all experiments, according to binding constants obtained by Cathou and Hammes (1965) from temperature jump studies on RNase A. Spectra were measured at a probe temperature of 35°C, using a capillary of trifluoroacetaldehyde

hydrate as an external reference standard. Control solutions were prepared exactly as described above, replacing RNase S protein with RNase A.

Modified RNase S was isolated from the solution used for nmr determinations by gel filtration through Sephadex G-25, with 0.1 M ammonium formate, pH 4.5, as eluting buffer. The main body of 280 mμ-absorbing material, found at the same elution volume as RNase A in a previous calibration run, was pooled and lyophilized.

Edman Degradation of Modified RNase S-Peptide

An Edman degradation was carried out by the procedure of Konigsberg and Hill (1962). The nineteen-residue product of the degradation was recovered by gel filtration, eluting from Sephadex G-25 with 0.2 M HOAc as solvent. The phenylthiohydantoin derivative of lysine 1 was not recovered.

Results

The amino acid compositions of modified and native RNase S-peptide are given in Table I. They indicate that at least 80-90% of the lysine residues of the modified peptide were converted to ϵ-trifluoroacetyl lysine. High and low values shown for threonine and glutamic acid, respectively, are due to one glutamine residue which was not chromatographically separated from threonine under the conditions used.

The ^{19}F-nmr spectrum of the modified S-peptide, shown in Figure 1a, consists of a singlet (L) of half-width 2 cps, 9.72 ppm downfield of trifluoroacetaldehyde (external). A second, smaller resonance (K) appears 0.39 ppm downfield of L, and a third (M) appears as a shoulder 0.07 ppm upfield of L. Assignment of the observed resonances was made possible by model studies of ^{19}F-nmr spectra of ϵ-trifluoroacetyl lysine and of α-, ϵ-bis-trifluoroacetyl lysine. The resonances occurred in the same frequency range as those observed for the modified S-peptide. Figure 2a shows the spectrum observed for ϵ-trifluoroacetyl lysine. A mixture of both the singly and doubly acylated amino acids gave the spectrum shown in Figure 2c. In α-, ϵ-bis-trifluoroacetyl lysine, the ^{19}F-nmr resonance of the ϵ-trifluoroacetyl group occurs 4 cps upfield of that due to ϵ-trifluoroacetyl lysine. It was evident from this latter spectrum that the chemical shift of an ϵ-trifluoroacetyl group of lysine is slightly different depending on whether the α-amino group

is trifluoroacetylated or free. On the basis of these model studies of trifluoroacetyl lysine, peak L in Figure 1a was assigned to the ϵ-N-trifluoroacetyl groups of Lys 7 and singly acylated Lys 1 of the modified S-peptide. Peaks K and M in Figure 1a were attributed respectively to trifluoroacetyl groups on the α and ϵ amino groups of doubly acylated Lys 1 of the modified S-peptide. Normally the acylating reagent, ethylthioltrifluoroacetate, is specific for the ϵ-amino group of lysine in proteins (Goldberger, 1967), but a very large excess of the reagent was used to modify the S-peptide and apparently some reaction with the α-amino group resulted.

When a molar equivalent of RNase S-protein was added to the solution of trifluoroacetylated S-peptide, the nmr spectrum changed as shown in Figure 1b. The major peak L appeared to be split into two peaks, L′ and L″, which moved downfield by 0.22 ppm and 0.07 ppm, respectively. In addition, L′ appeared to be broadened to a half-width of 4 cps from an initial value of 2 cps for L. The minor peak M also was shifted 0.07 ppm downfield but peak K was unchanged by the addition of S-protein. According to the original resonance assignments, these changes indicated that the trifluoroacetyl residue on the ϵ-amino groups experienced significantly different environmental changes. As described in the experimental section, the trifluoroacetylated S-peptide-protein complex was subjected to gel filtration and the ^{19}F-nmr spectrum of the reisolated material was found to be identical to that shown in Figure 1b, thus demonstrating that the observed spectral changes were due to complex formation.

As further proof that the observed changes were due to a specific association of modified S-peptide with S-protein it was shown that addition of a mole equivalent of RNase A to modified S-peptide produced no change in the ^{19}F-nmr spectrum of the peptide.

The resonance assignments and interpretation (see Discussion) of these results were tested by examination of the ^{19}F-nmr spectra of S-peptide and RNase S after lysine 1 of the peptide had been removed by an Edman degradation. The spectrum of degraded peptide was qualitatively similar to that of trifluoroacetylated S-peptide; peak L was, however, relatively smaller. Addition of the S-protein (Figure 1c) revealed that component L″ had been removed entirely. It is reasonable to conclude that in the spectrum of trifluoroacetylated ribonuclease S, L′ corresponded to the ϵ-trifluoroacetyl group on Lys 7, L″ to the ϵ-trifluoroacetyl on Lys 1, K to α-trifluoroacetylated Lys 1, and M to the ϵ-trifluoroacetyl group on bis-trifluoroacetylated Lys 1. This result is consistent with the spectral assignments based on model studies (Figure 2) of ϵ- and α-, ϵ-bis-trifluoroacetylated lysine. Also consistent with these assignments are the results of integration of the resonances of the RNase S spectrum. The integral of peak L′, due to ϵ-trifluoroacetyl Lys 7, was approximately equal to the sum of L″ (the resonance of ϵ-trifluoroacetyl lysine 1) and M (due to the ϵ-trifluoroacetyl group of bis-acylated lysine 1). Peaks M and K, which result from bis-trifluoroacetyl Lys 1, were equal in area.

Addition of an inhibitor, phosphate ion, to the trifluoroacetylated RNase S solution produced the change shown in Figure 3b. Resonance L′ was shifted upfield by 0.03 ppm; K, L″, and M were unchanged. Addition of 5′-CMP to a fresh sample of modified enzyme produced a similar change as shown in Figure 3c. Addition of 3′-CMP and 2′-CMP induced more marked changes. As shown in Figure 3d, peak L′ was shifted upfield by 0.07 ppm on binding of 3′-CMP. Furthermore, the presence of two component peaks in L′ was fairly clear. Reexamination of the other RNase spectra (1b; 3b, c) raised the possibility that the apparent width of L′ was due partly to the presence of two poorly resolved resonances. The change induced by 2′-CMP binding (Figure 3e) was similar to that of 3′-CMP; the upfield shift of L′ was ~0.02 ppm greater.

A molecular interpretation of the spectral effects observed upon association of the various inhibitors with the trifluoroacetylated RNase S is difficult due to the complexity of the system, but nonetheless desirable. In order to facilitate such an analysis, the effect of pH on the observed spectral changes was undertaken. The inhibitor chosen for this study was cytidine-3′-phosphate since it most closely resembles the product of the enzyme's action on RNA. The results of this study are shown in Figure 4 and they show that resonance L′ (due to the trifluoroacetyl group on Lys 7) is affected by an ionizable group of pK_a 7.2-7.3 on the enzyme-inhibitor complex. In the absence of the inhibitor, no pH effects in the range 4.5-7.8 were observed.

Trifluoroacetylated RNase S was assayed for enzymatic activity simultaneously with a sample of unmodified RNase S, each being prepared by combination of RNase S-peptide and S-protein in a weight ratio of 1:6. Their activities were identical within the accuracy of the technique; both yielded 110 Kunitz units of activity per milligram of enzyme.

Discussion

The objective of the experiments described here was to devise a technique for detecting the small conformation changes often invoked to explain the kinetics and specificities of enzyme reactions. In the model case, RNase S, a fluorine magnetic resonance probe has been employed to detect the occurrence of conformation changes upon enzyme-inhibitor association.

It was possible, by comparison with model compounds, to assign all the observed ^{19}F resonances in the spectrum of trifluoroacetylated S-peptide, both free and associated with the S-protein. Thus nmr probes were available for the magnetic environments of lysine residues 1 (both α- and ϵ-groups) and 7. The chemical environments of these two residues have been delineated for crystalline RNase S (Wyckoff et al., 1967). Lysine 1 lies exposed to the solvent, near the surface of the protein, while Lys 7 is inside, close to the active site. In addition to the crystal structure data, chemical evidence (Marfey et al., 1965) has suggested that Lys 7 lies very near the active site but does not participate in catalysis or binding. The X-ray data also have shown that in native RNase-S Lys 7 is found in an α-helical segment with His 12, which has been shown by chemical and ^{1}H-nmr evidence to be involved in, though perhaps not essential to, inhibitor binding (Crestfield et al., 1963; Meadows et al., 1967). Since the trifluoroacetylated enzyme remains fully active it is likely the trifluoroacetylated peptide is bound to the

S-protein in a conformation similar to that adopted by unmodified S-peptide.

If inhibitor binding involves movement of His 12, as might be expected in an induced fit binding process (Koshland, 1953), it is likely that the rod-like helical segment including modified Lys 7 would be moved also. Any consequent changes in the magnetic environment of the side chain would be reflected in chemical shift or line shape changes of peak L′ in the magnetic resonance spectrum.

Toward this end the binding at pH 4.5 of the inhibitors phosphate, 2′-CMP, 3′-CMP, and 5′-CMP was studied, and the results are summarized in Figure 3. Phosphate and 5′-CMP produced identical changes in the probe spectrum, causing a 0.03 ppm upfield shift of L′ while not affecting K, L″, or M. Binding of 2′- and 3′-CMP produced more marked changes in resonance L′, corresponding to trifluoroacetyl Lys 7, than did the binding of phosphate or 5′-CMP. The upfield shift obtained upon association of these inhibitors were 0.07 and 0.09 ppm, respectively, and the latter peak was resolved into two components. These two components of peak L′ may not be unique to the complex with 2′-CMP. The resolution of L′ in other spectra was not optimal due to the time required to accumulate the necessary signal intensity and it is possible that the apparent width of L′ in such spectra was due in part to the presence of a shoulder on the lowfield side of the peak. In spectrum 3e, the magnitude of the lowfield component was similar to that of peaks K and M. It is possible that the α-modified S-peptide

associates with S-protein in a slightly different orientation than does exclusively ϵ-modified S-peptide, so that the environment of Lys 7 is slightly altered. If that is the case the environmental difference appears to be magnified on small molecular weight inhibitor binding, but does not produce measurable acitivity loss using RNA as substrate. In all cases, the inhibitor molecule induced a change in the magnetic environment of Lys 7 which appeared to place it in an environment more like that of Lys 1. Examination of a crystal structure model indicates that if as a result of inhibitor binding His 12 were drawn closer to His 119 and Thr 45 (other constituent amino acid residues of the active site cluster), Lys 7 would be pulled away from the Arg 39 region of the protein and exposed more completely to the solvent. The fact that resonances K, L″, and M do not shift on inhibitor binding does not necessarily show that Lys 1 is immobile. In the crystal, the amino terminal is surrounded by a large open region and it could possibly be moved about quite freely without experiencing a detectable change in magnetic environment.

The changes in magnetic environment of Lys 7, as evidenced by chemical shifts of resonance L′, could be caused most reasonably by (1) electric field effects due to ionizable groups in either the inhibitors or the protein; (2) ring current effects in the inhibitors or the protein; or (3) magnetic anisotropy of groups adjacent to Lys 7, such groups being part of either the inhibitors or the protein. Any one or all such effects could be due to (1) proximity of the inhibitors to the trifluoroacetyl group of Lys 7 or (2) a conformation

change in the enzyme. Ring current effects from bound inhibitors are unlikely as the source of the observed spectral changes since phosphate ion caused a similar chemical shift of resonance L′. The effect of pH on the chemical shift of the major component of resonance L′ helps distinguish between the remaining possibilities. It was observed that an ionizable group of pK_a 7.2-7.3 was responsible for the observed chemical shift in the enzyme-inhibitor complex found with 3′-CMP. This is most likely due to the charge on His 119 which has been shown (Meadows and Jardetzky, 1968) to have a pK_a 7.4 when the same inhibitor is complexed with ribonuclease A, while His 12 has a pK_a of 8.0 in the complex. In the free enzyme, these residues have pK_a values of 5.8 and 6.2, respectively. In addition, the pK_a of the phosphate in 3′-CMP is 6.0, which would be lowered upon binding to the highly cationic binding site of RNase S (containing His 12, Lys 41, and His 119). Thus of the three ionizable groups whose pK_a's lie in the range studied, only the His 119 charge produces a measurable effect on the magnetic environment of Lys 7, and then only in the enzyme-inhibitor complex. A calculation from the coordinates of Wyckoff et al. (1970) reveals that the His 119 imidazole nitrogens would be 10-11 Å away from a trifluoroacetyl group on Lys 7, while those of His 12 would be 12-13 Å distant. While the presence of an inhibitor may decrease the Lys 7-His 119 distance, His 12 (and the phosphate group approximately between the histidines) still should be almost as close to Lys 7 as is His 119. In addition, no change was observed in the chemical shift of the

trifluoroacetyl group on Lys 7 in the pH region 8-9 when 3′-CMP was present. This shows that the charge on His 12 has no effect on the observed resonance. It seems unlikely that only His 119 should exert a direct electric field effect on Lys 7. It is also unlikely that the shift of peak L′ is due to hydrogen bonding of some group on the protein to fluorine. Alkyl fluorides hydrogen bond quite poorly as was shown by the proton nmr study of Korinek and Schneider (1957). Hydrogen bonding to trifluoroacetate would be expected to be considerably weaker due to electron withdrawal from the fluorines by the carbonyl group.

A more plausible explanation would be that the charged His 119 affects the relative orientations of segments of the protein as they bind the inhibitor. The decrease in the binding constant of 3′-CMP above pH 5.6 has been attributed (Meadows and Jardetzky, 1968) to the titration of His 119 and His 12. It is likely that the coulombic attraction between protonated His 119 and the phosphate group of the inhibitor could play an important role in binding of this inhibitor, and that when this bond is broken disruption of the binding site may ensue to some extent. A rearrangement of the peptide segments bearing the active site moieties could well alter the environment of Lys 7; for example, if the distance between His 12 and His 119 were increased as His 119 ceased to be strongly bound to the phosphate, Lys 7 could be carried near the face of the protein cleft near Arg 39. Inspection of the RNase S model shows that the trifluoroacetyl group on Lys 7 could be as close as 6 Å to the guanidino group of Arg 39.

The ^{19}F-nmr data presented here indicate that inhibitor binding causes a small change in the position of His 12 of the S-peptide which results in its being brought closer to His 119 in the complexed form. When His 119 (pK_a 7.2-7.3) is deprotonated in the complex, His 12 (pK_a 8.0 in the complex) moves back toward its position in the free enzyme. No information is obtainable from the present studies on movements of His 119 since no probe was attached which would monitor such effects.

The use of ^{19}F probes would seem to be a sensitive method for detecting protein conformation change as evidenced from the results obtained from both (a) association of trifluoroacetylated RNase S-peptide with the S-protein and (b) the association with the protein-peptide complex of various inhibitors. While this method is restricted to proteins where suitable chemical modifications are possible, its sensitivity should allow detailed investigations of such systems, hopefully permitting interpretation at the atomic level.

References

Cathou, R. E., and Hammes, G. G. (1965), J. Amer. Chem. Soc. 87, 4674.

Crestfield, A. M., Stein, W. H., and Moore, S. (1963), J. Biol. Chem. 238, 2413.

Crespi, H. Z., Rosenberg, R. M., and Katz, J. J. (1968), Science 161, 795.

Goldberger, R. F. (1967), Methods in Enzymology, Vol. XI, C. H. W. Wirs (ed.), p. 319.

Gross, E., and Witkop, B. (1966), Biochem. Biophys. Res. Commun. 23, 720.

Katz, J. J., Strain, H. H., Lenssing, D. L., and Doughtery, R. C. (1968), J. Amer. Chem. Soc. 90, 784.

Konigsberg, W., and Hill, W. J. (1962), J. Biol. Chem. 237, 2547.

Korinek, G. J., and Schneider, W. G. (1957), Can. J. Chem. 35, 1157.

Koshland, D. E., Jr. (1953), Biol. Revs. 28, 416.

Kunitz, M. (1946), J. Biol. Chem. 164, 563.

Kurland, R. J., Davis, D. G., and Ho, C. (1968), J. Amer. Chem. Soc. 90, 2700.

Markley, J. L., Putter, I., and Jardetzky, O. (1968), Science 161, 1249.

Marfey, P. S., Uziel, M., and Little J. (1965), J. Biol. Chem. 240, 3270.

McDonald, C. C., and Phillips, W. D. (1969), J. Amer. Chem. Soc. 91, 1513.

Meadows, D. H., Markley, J. L., Cohen, J. S., and Jardetzky, O. (1967), Proc. Natl. Acad. Sci. (U.S.) 61, 1307.

Meadows, D. H., and Jardetzky, O. (1968), Proc. Natl. Acad. Sci. (U.S.) 61, 406.

Putter, I., Baretto, A., Markley, J. L., and Jardetzky, O. (1969), Proc. Natl. Acad. Sci. (U.S.) 64, 1396.

Richards, F., and Vithayathil, P. (1959), J. Biol. Chem. 234, 1459.

Schallenberg, E. F., and Calvin, M. (1955), J. Amer. Chem. Soc. 77, 2779.

Shulman, R. G., Wüthrich, K., Yamane, T., Antonini, E., and Brunori, M. (1969), Proc. Natl. Acad. Sci. (U.S.) 63, 623.

Weygand, R., and Geiger, R. (1956), Chem. Ber. 89, 647.

Wüthrich, K., Shulman, R. G., and Peisach, J. (1968), Proc. Natl. Acad. Sci. (U.S.) 60, 373.

Wyckoff, H. W., Hardman, K. D., Allewell, N. M., Inagami, T., Johnson, L. N., and Richards, F. M. (1967), J. Biol. Chem. 242, 3984.

Wyckoff, H. W., Tsernoglou, D., Hanson, A. W., Knox, J. R., Lu, B., and Richards, F. M. (1970), J. Biol. Chem. 245, 305.

Table I

Amino Acid Composition of Trifluoroacetylated RNase S-Peptide from Total Enzymatic Hydrolysis

Amino acid	mμ moles	Ratio**	Native peptide
Asp*	1333	1.0	1
Met sulfone	trace		
Thr	3905	3.0	2
Ser	3930	3.0	3
Glu	2659	2.0	3
Pro	–	–	–
TFA-lysine	2263	1.74	–
Ala	5030	3.9	5
Cys	–	–	–
Val	–	–	–
Met	1162	0.9	1
Ilu	13	.01	–
Leu	–	.04	–
Tyr	–	–	–
Phe	1526	1.2	1
His	1191	0.9	1
Lys	316	.24	2
Arg	1511	1.2	1

* Taken as 1.0 for mole ratio determination.

** Values expressed in residues per molecule.

Figure 1. ^{19}F-Nmr spectra of trifluoroacetylated RNase S. (a) Trifluoroacetylated RNase S-peptide; (b) trifluoroacetylated RNase S-peptide associated with RNase S-protein; (c) trifluoroacetyl peptide-protein complex after removal of Lys 1 from the peptide.

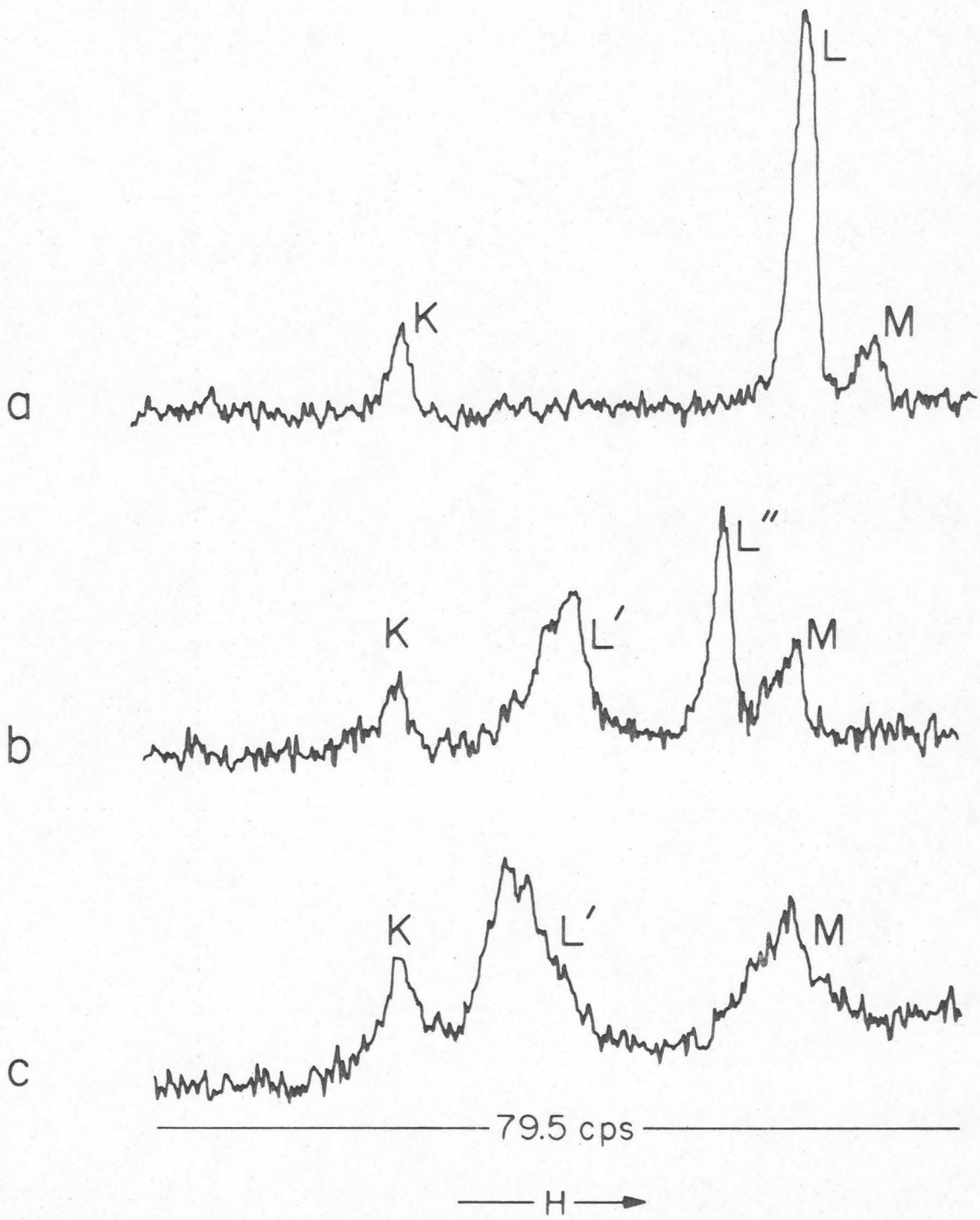
a
K
L
M
b
K
L′
L″
M
c
K
L′
M
79.5 cps
H

Figure 2. ^{19}F-Nmr spectra of trifluoroacetylated lysine. (a) ϵ-Trifluoroacetyl lysine; (b) α, ϵ-bis-(trifluoroacetyl)-lysine; (c) a mixture of ϵ-mono and α, ϵ-bis-(trifluoroacetyl)lysine.

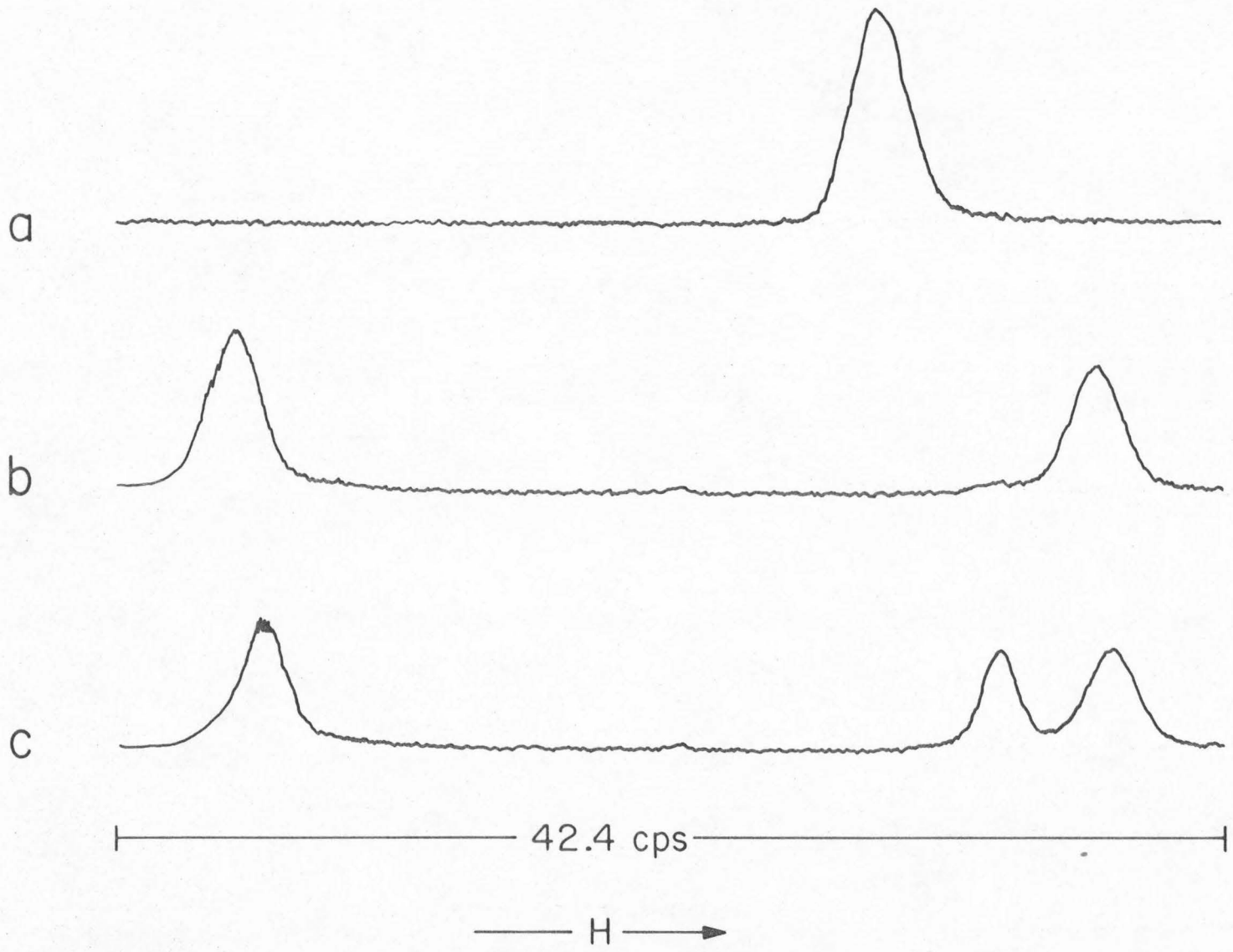
a
b
c
42.4 cps
H

Figure 3. ^{19}F-Nmr spectra of trifluoroacetylated RNase S (4×10^{-3} M) in the presence of various inhibitors. (a) Free RNase S; (b) $+10^{-2}$ M phosphate; (c) $+4 \times 10^{-3}$ M 5′-CMP; (d) $+4 \times 10^{-3}$ M 3′-CMP; (e) $+4 \times 10^{-3}$ M 2′-CMP.

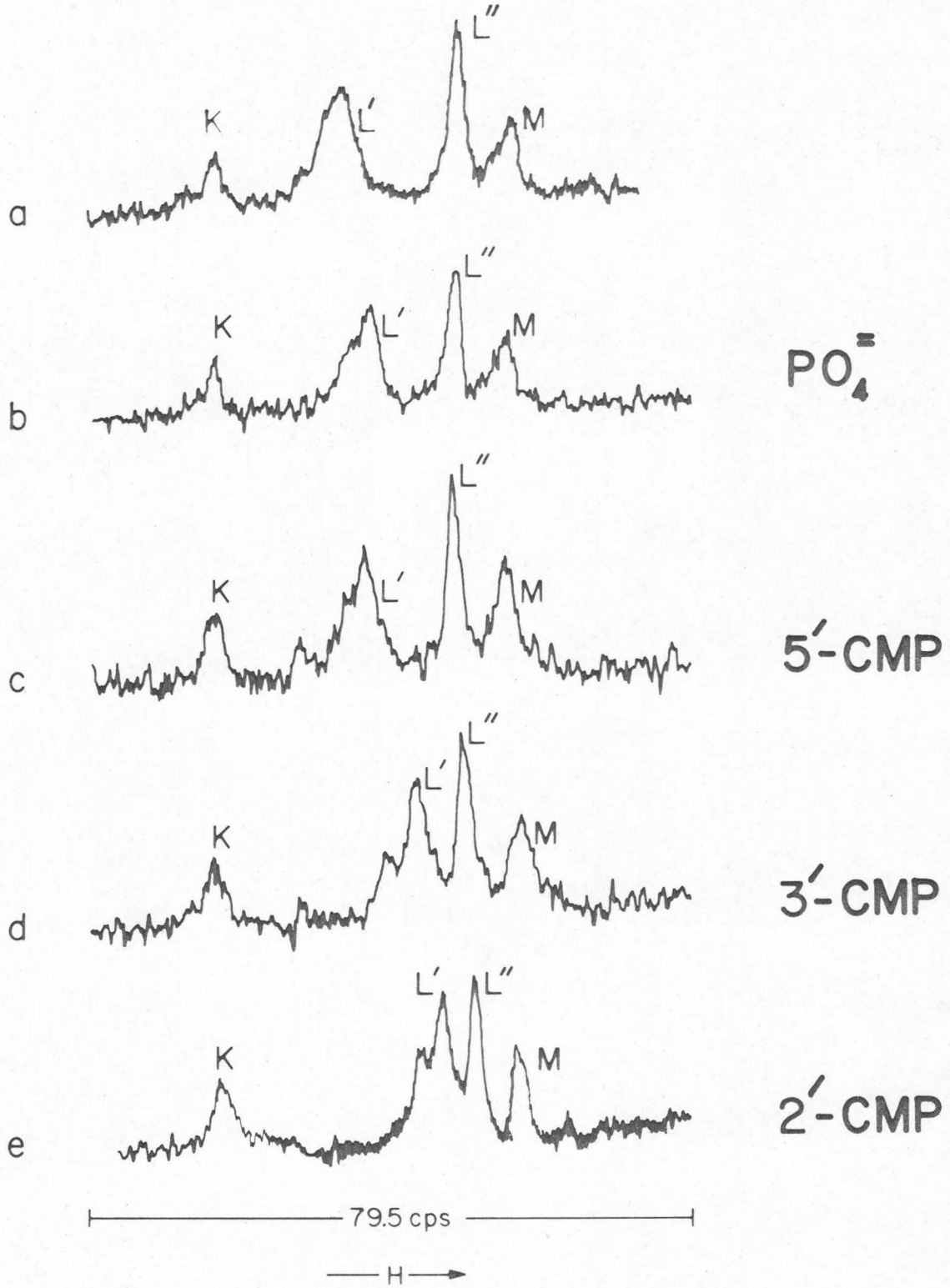
a
K
L′
L″
M
b
K
L′
L″
M
$PO_4^{=}$
c
K
L′
L″
M
5′-CMP
d
K
L′
L″
M
3′-CMP
e
K
L′
L″
M
2′-CMP
79.5 cps
H

Figure 4. Chemical shift of ϵ-trifluoroacetyl Lys 7 (peak L′) on binding of 3-CMP as a function of pH. o, position of peak L′ in free RNase S; Δ, position of peak L′ in RNase S saturated with 3′-CMP. The solid line is the theoretical titration curve of an ionizable group of pK 7.25.

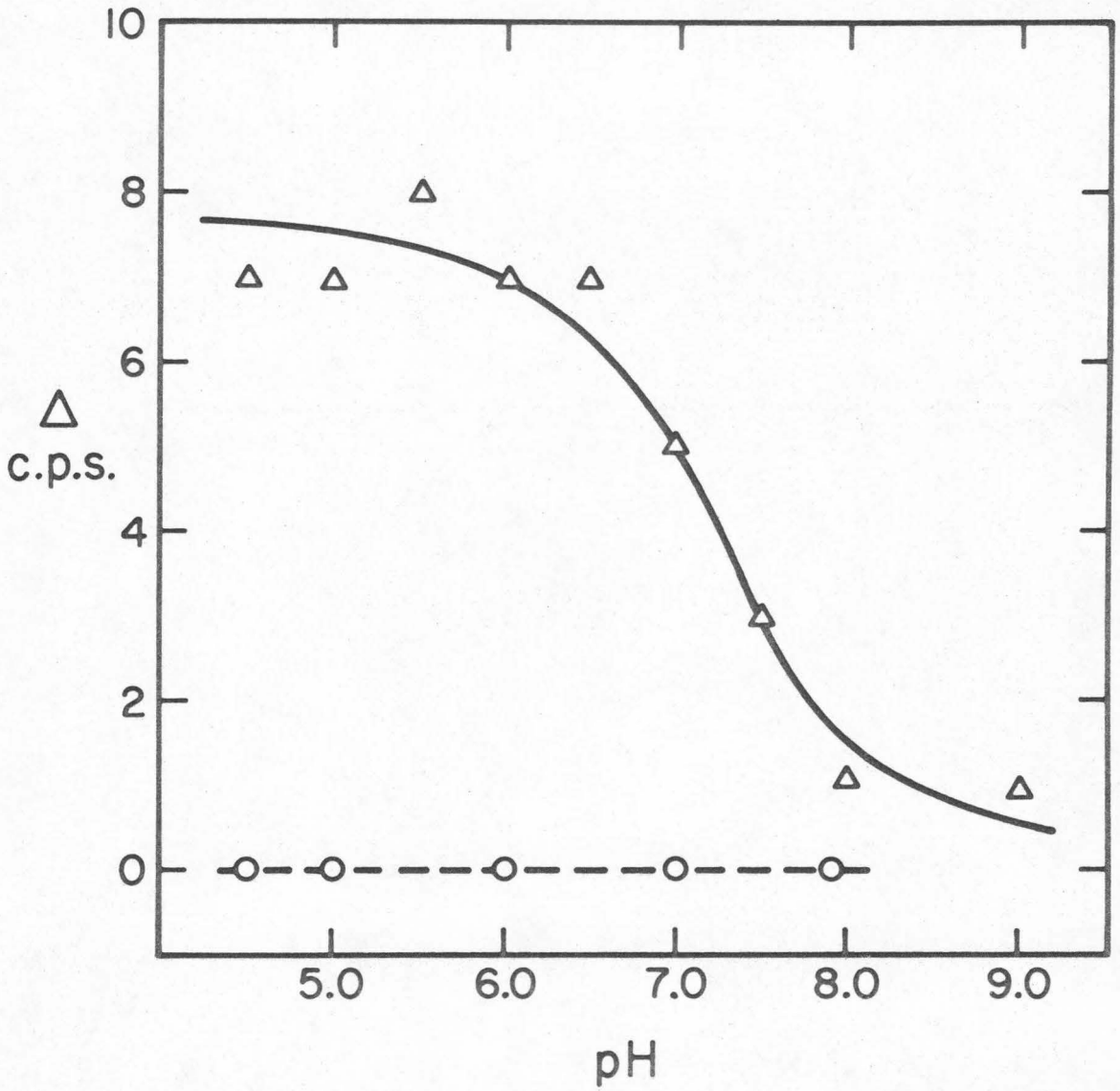
10
8
6
4
2
0
Δ
c.p.s.
5.0
6.0
7.0
8.0
9.0
pH

CHAPTER II

Study of Conformational Processes in the $\alpha_1 \beta_2$ Contact Region of Hemoglobin

Hemoglobin, the oxygen transport protein of vertebrate respiratory systems, is the most extensively studied allosteric protein. Its unusual substrate binding kinetics were recognized by Bohr in 1906, since which time a research effort of unparalleled magnitude has tried to untangle its complexities. The resulting mass of information on hemoglobin's interactions with heme ligands and allosteric effectors (protons, carbon dioxide, organic phosphates) has not produced a consensus on the precise mechanism of the oxygen binding process. However, it is generally agreed that the allosteric properties result in some way from the existence of high and low oxygen affinity forms of the protein, which differ from one another in quaternary and/or tertiary structure. Contemporary mechanistic studies are generally directed toward precise definition of the differences between these forms and accurate description of the transition process.

Extensive evidence exists for structural differences between liganded and unliganded hemoglobin from crystal forms (Haurowitz, 1938), optical rotation (Briehl, 1962), carboxypeptidase digestion rates (Zito et al., 1969), stability and solubility changes (Cohn and Edsall, 1943), dye binding (Antonini et al., 1963), and rates of

reaction with thiol-specific reagents (Riggs, 1961). Recently, the high resolution crystal structures of met- (Perutz et al., 1968) and deoxyhemoglobin (Muirhead and Greer, 1970) have been determined. This work revealed detailed differences between two forms of the protein, and suggested mechanisms by which the conversion from one form to the other could produce cooperative ligand binding (Perutz, 1970). Although the mechanisms thus far advanced cannot be reconciled with all of the available chemical evidence, knowledge of these crystal structures undoubtedly will be of great value in further studies of the oxygenation process.

In particular, availability of a high resolution crystal structure permits detailed interpretation of phenomena observed by nuclear magnetic resonance spectroscopy. This chapter describes nmr investigations of conformational processes in a critical region of the $\alpha_1\beta_2$ interface. Cysteines 93 of the β chains, the sole cysteine residues in the molecule which are accessible to reaction with thiol-specific reagents under mild conditions, were modified by reaction with bromotrifluoroacetone. Binding of heme ligands, protons, and diphosphoglyceric acid to this trifluoroacetonyl hemoglobin was reflected in the ^{19}F-nmr spectrum of the trifluoroacetonyl group. Analysis of the nmr results in light of crystallographic evidence on the structure of the region permits us to describe conformational processes associated with the allosteric transition.

Experimental

Materials

3-Bromo-1, 1, 1-trifluoropropanone was obtained from Peninsular Chemresearch Inc. 2, 3-Diphosphoglyceric acid was obtained as the pentacyclohexylammonium salt from Calbiochem, and converted to the free acid by shaking with Dowex 50-X8. 5, 5′-Dithiobis-(2-nitrobenzoic acid) was the product of Aldrich Chemical Co. S-Trifluoroacetonyl mercaptoethanol ($HO-CH_2CH_2-S-CH_2-\underset{\underset{O}{\|}}{C}-CF_3$) was synthesized by direct combination of β-mercaptoethanol with 3-bromo-1, 1, 1-trifluoropropanone at room temperature. The white crystalline product was recrystallized from benzene-ligroin and characterized by its infrared and ^{1}H-nmr spectra.

Methods

Hemoglobin concentrations were determined from their absorbance at 540 nm ($E^{1\,cm}_{1\%}$ = 8.5 at 540 nm) using a Gilford Model 240 spectrophotometer. pH Measurements were made using a Radiometer Copenhagen Model 26 pH meter. ^{19}F-Nmr spectra were recorded using Varian Models HA-100 and XL-100-15 spectrometers modified to operate at 94.1 MHz. Both were supplemented by a Fabritek Model 1061 computer of average transients. Spectrum accumulation times were reduced by use of 12 mm o.d. sample tubes. Resonance positions were measured routinely from trifluoroacetic

acid in a capillary tube, or from the H_2O lock signal. Additional controls for bulk diamagnetic susceptibility effects were made by measuring shifts from the internal standard S-trifluoroacetonyl-mercaptoethanol.

Isolation of Human Hemoglobin

Erythrocytes from freshly drawn citrated blood were washed three times with 0.9% NaCl solution. The packed cells were lysed by addition of one volume of distilled water and 0.4 volume of toluene, or by addition of two volumes of distilled water. After being shaken for four minutes, the mixture was centrifuged. The clear hemolysate was removed and dialyzed against distilled water. All steps were carried out at 4°C. Hemoglobin stock solutions were stored as the carboxy derivative at 4°C, and used within one week of preparation.

Preparation of ^{19}F-Labeled Hemoglobin

A solution oxyhemoglobin (600 mg in 6 ml $H_2O \equiv 1.86 \times 10^{-5}$ moles Cys β93) was added to 6 ml sodium phosphate buffer (0.4 M pH 7.15). 3-Bromo-1-trifluoropropanone (50 μl = 90 mg $\equiv$ 4.7×10^{-4} moles) was added and the solution was stirred at room temperature for 30 minutes, during which time the pH was maintained at 7.15 by addition of 1 M sodium hydroxide. A slight precipitate was removed by centrifugation, and the reaction mixture was subjected to gel filtration on a Bio-Gel P-2 column (2.5 × 50 cm, eluting solvent 0.1 M NaCl) to remove excess reagent, organic phosphates and phosphate. For nmr studies the hemoglobin solution

was concentrated to 10% by ultrafiltration employing an Amicon apparatus.

Sulfhydryl group determinations were carried out by the method of Ellman (1959). Oxygen affinities and Hill coefficients were determined for Hb and Hb^{TFA}* by a modification of the procedure of Riggs and Wohlbach (1956). Equilibria were determined at 25° in 0.1 M sodium phosphate at pH 7.0.

Deoxyhemoglobin (Hb^{TFA}-deO_2) was prepared from oxyhemoglobin (Hb^{TFA}-O_2) by repeated washing with nitrogen in a tonometer. Methemoglobin (Hb^{TFA}-III) was prepared by addition of $K_3Fe(CN)_6$ (600 μl of 0.1 M solution $\equiv 6 \times 10^{-5}$ moles) to oxyhemoglobin (400 mg $\equiv 2.4 \times 10^{-5}$ moles Fe^{II}) in 10 ml sodium phosphate buffer (0.01 M, pH 7.0). The solution was allowed to stand at room temperature for 30 minutes, then the Hb^{TFA}-III was purified by passage through a Bio-Gel P-2 column (2.5 × 50 cm) with 0.1 M NaCl as eluting solvent. Cyanmethemoglobin (Hb^{TFA}-III CN) was prepared by the same procedure, with a 100-fold excess of KCN (in 1 ml H_2O, pH 7) being added at the same time as the $K_3Fe(CN)_6$. Determinations of Hb^{TFA}-III and Hb^{TFA}-III CN were carried out by the method of Tomita et al. (1968).

---

*Abbreviations used are: DPG, diphosphoglycerate; PMB, p-mercuribenzoate; TFA, trifluoroacetonyl; Hb-deO_2, deoxyhemoglobin; Hb-O_2, oxyhemoglobin; Hb-CO, Hb-III, Hb-III CN, carboxy-, met-, and cyanmethemoglobin, respectively; and Hb^{TFA}, trifluoroacetonylated hemoglobin.

Carboxyhemoglobin (Hb^{TFA}-CO) was prepared by washing Hb^{TFA}-O_2 with carbon monoxide in a tonometer.

Preparation of Functional Derivatives

Hb^{TFA} was carbamylated at its amino termini by reaction with isocyanate, as described by Kilmartin and Rossi-Bernardi (1969). Des-His β146 hemoglobin was prepared by carboxypeptidase B digestion of purified β chains, according to the procedure of Kilmartin and Wootton (1970). Des-Tyr β145-His β146 hemoglobin was prepared by carboxypeptidase A digestion of hemoglobin, as described by Antonini et al. (1961). Des-His β146 and des-His β146-des Tyr β145 derivatives of Hb^{TFA}-III were prepared by oxidation of the corresponding oxy derivatives, as described previously.

Nmr Spectral Measurements

Solutions used for nmr studies typically contained 300 mg of hemoglobin in 3 ml of 0.1 M NaCl solution. pH Adjustments were made by slow addition of 0.1 M HCl or NaOH, with stirring. The pH of each solution was measured before and after the spectrum was recorded. Deoxyhemoglobin solutions were transferred from tonometer to argon-filled nmr tubes with a syringe. Diphosphoglyceric acid (0.16 M in H_2O, pH 7.0) was added to hemoglobin solutions in aliquots adequate to insure >95% saturation at each pH, while avoiding oversaturation which might have resulted in non-specific binding (Garby et al., 1969). Molar ratios of DPG:hemoglobin required to meet these criteria were calculated from the

binding data of Benesch and Benesch (1970) and Garby et al. (1969).

Results

Characterization of Trifluoroacetonylated Hemoglobin

The extent of modification of the exposed –SH groups of hemoglobin was determined spectrophotometrically, using the 5, 5′-dithiobis-(2-nitrobenzoic acid) method of Ellman (1959). Hb^{TFA}-O_2 was found to contain fewer than 0.1 moles of exposed –SH groups per mole of tetramer, as compared with 1.9 moles/mole tetramer for native Hb-A.

The oxygen equilibrium curves of Hb and Hb^{TFA} are shown in Figure 1. The functional effect of introduction of the trifluoroacetonyl groups was not great: oxygen affinity was increased very slightly, and the Hill coefficient was reduced from 2.7 to 2.5.

Nmr Spectra of Trifluoroacetonylated Hemoglobin

The spectrum of Hb^{TFA}-O_2 consisted of a singlet which appeared 483 cps upfield of trifluoroacetic acid. * Deoxygenation to Hb^{TFA}-deO_2 produced a shift to higher field of 52 cps in the ^{19}F resonance, which appeared at +535 cps. In Hb^{TFA}-III (methemoglobin) the resonance was found at +525 cps; for Hb^{TFA}-CO and Hb^{TFA}-III CN resonances appeared at +470 and +460 cps, respectively (Figure 2).

---

* Shifts are given relative to trifluoroacetic acid, for Hb^{TFA} 1.5×10^{-3} M in 0.1 M NaCl, pH 6.75.

Effect of Phosphate and Diphosphoglyceric Acid on Spectra of Hb^{TFA}

Addition of diphosphoglyceric acid (DPG) to Hb^{TFA} shifted the ^{19}F resonance to higher field (Figure 3). Below pH 7, the presence of 0.5 mole equivalent of DPG shifted the resonance to +540 cps, and 1.0 mole equivalent of DPG shifted it to +547 cps--a total of +12 cps. Further, in 0.1 M phosphate buffer the Hb^{TFA} signal appeared at +540 cps in the absence of DPG. The presence of DPG or phosphate did not change the chemical shift of the Hb^{TFA}-O_2 resonance when other salts (e.g., 0.1 M NaCl) were present.

pH Dependence of the ^{19}F-Nmr Spectrum

The effect of pH on the chemical shift of labeled hemoglobin is shown for various ligands in Figure 4. The position of the ^{19}F resonance of Hb^{TFA}-O_2 was constant in the pH range 6.0-8.5. The resonance position for Hb^{TFA}-CO and Hb^{TFA}-III CN also were essentially constant for the pH range 7.0-8.0. The chemical shift of Hb^{TFA}-deO_2 underwent a significant change (Figure 4) in this pH range. A plot of chemical shift change vs. pH had the appearance of a titration curve (pK_a = 7.4) occurring over an abnormally short pH range. This pH effect was again evident in DPG-bound Hb^{TFA}-deO_2 (Figure 7); the titration curve showed an apparent pK_a of ~7.4, but was even steeper. The resonance position of Hb^{TFA}-III also changed by ~30 cps with pH, apparently reflecting the titration of a group of pK_a 7.8 (Figure 10).

To examine possible direct effects of pH on the ^{19}F probe moiety, the ^{19}F chemical shift of a model compound, S-trifluoroacetonylmercaptoethanol (I) was studied as a function of pH.

$$HO-CH_2CH_2-S-CH_2-\underset{\underset{O}{\|}}{C}-CF_3$$

I

As is shown in Figure 4, the ^{19}F resonance position was invariant from pH 6.0 to pH 8.0, above which a small downfield shift was apparent which was not observed in spectra of protein bound probes.

Source of the pH Dependence of the Chemical Shifts

By application of several chemical modifications, it was possible to identify which of several ionizable groups in the vicinity of Cys β93 was directly involved in the pH-dependent chemical shift of Hb^{TFA}-deO_2. Carbamylation of the amino termini with isocyanate produced a small overall chemical shift change in both oxy and deoxy derivatives (2-3 cps), but no change in the titration curve for Hb^{TFA}-deO_2. Binding of diphosphoglyceric acid (DPG) to Hb^{TFA}-deO_2, which raises the pK_a of histidine β143 (DeBruin et al., 1971), did not alter the pH dependence of the nmr shift, although the titration curve appeared sharper (Figure 7) and an overall chemical shift change was present. Removal of His β146 resulted in disappearance of the pH-dependent chemical shift change, with the chemical

shift previously observed above pH 8 being present over the entire pH range (Figure 6). The same result was obtained by removal of His β146 and Tyr β145 by carboxypeptidase A digestion.

The nmr spectrum of des His β146 Hb^{TFA}-III showed that loss of the histidine altered the environs of Cys β93 profoundly (Figure 11). The overall chemical shift changed, and its pH dependence above pH 7.5 was eliminated. A pH dependent shift change of pK_a 7.1 remained, indicating the influence of an ionization process which was not evident in either oxy or deoxyhemoglobin. Removal of Tyr β145 eliminated all pH dependence (Figure 11).

Discussion

Binding of heme ligands and allosteric effectors to Hb^{TFA} produces changes in its ^{19}F-nmr spectrum which reflect molecular events in the vicinity of the trifluoroacetonyl groups. Although Cys $\beta 93$ is not a critical residue in allosteric processes, its proximity to several vital groups in the $\alpha_1\beta_2$ interface makes it a useful position for a conformation sensitive nmr probe. Its neighbors in the F helix are His $\beta 92$, the proximal heme ligand, and Asp $\beta 94$, which is bound electrostatically to the side chain of His $\beta 146$ in deoxy (but not oxy) hemoglobin. Unlike some of the bifunctional (Benesch and Benesch, 1961; Arndt et al., 1971) or rather large (McConnell, 1967; Moffat, 1971) sulfhydryl derivatives previously used to study interactions in this region, the trifluoroacetonyl group produces minimal perturbations of the protein's properties. Hb^{TFA} exhibited an oxygen affinity almost identical with that of native HbA and a Hill coefficient of 2.5 (Figure 1). Therefore it is probable that the processes being observed are very nearly normal.

Conformational Processes Near Cys $\beta 93$ Induced by Ligand Binding

The structural differences between liganded and unliganded hemoglobin in the vicinity of Cys $\beta 93$ have been described in detail by Perutz (1970). A schematic representation of these differences is shown in Figure 5. In unliganded hemoglobin, the carboxy terminal segment of the β chain is immobilized in the crevice of the $\alpha_1\beta_2$

interface by "salt bridges" (i. e., electrostatic interactions) between the terminal histidine β146 and two other residues. The histidine carboxyl group is bridged to the ϵ-amino group of Lys α_1 40, and the side chain imidazolium group is similarly bonded to the carboxyl side chain of Asp $\beta_2$94, approximately 4Å from Cys β93. A steric requirement for the formation of these two bonds is that the phenolic side chain of Tyr $\beta_2$145 must fit into a pocket between the F and G helices of the β chain. According to Perutz, a crucial event in the cooperative binding process is a conformation change which squeezes the F and H helices together, forcing Tyr β145 out of its pocket. This breaks the salt bridges of His $\beta_2$146, causing release of protons (the Bohr effect) and destabilization of the deoxy structure. Thus transition to the oxy structure and ligand binding are expedited. (Chemical evidence will be presented which suggests that this model gives undue emphasis to electrostatic bonds at the expense of energetic contributions from Tyr β145's hydrophobic interactions. Such considerations have no bearing on the described sequence of events.) In the "oxy" structure, the carboxy terminal segment has no fixed position, but moves about freely in the solvent. Evidence from spin label studies (Deal et al., 1971) indicates that both "bound" and "free" conformations of this segment can exist to some extent in both oxy- and deoxyhemoglobin, depending on conditions of pH and ionic strength. The process should therefore be regarded as the shifting of position of a conformational equilibrium rather than as a transition between two fixed states. This equilibrium is of central

importance in the cooperative mechanism, since carboxypeptidase A removal of Tyr β145 and His β146 abolishes cooperativity (n = 1.0) (Antonini, 1964).

The Carboxy Terminus Equilibrium in Hb^{TFA}

The His β146 imidazole is anchored 4-5 Å away from Cys β93 by its bond to Asp β94, near enough for the ^{19}F moiety to be influenced by the imidazole ring current or charge. Hence it is likely that the nmr differences of liganded and unliganded Hb^{TFA} reflect the shifting position of the carboxy terminus equilibrium, and that the pH dependence of the Hb^{TFA}-deO_2 resonance is produced by deprotonation of the histidine's imidazole group. The Hb^{TFA}-deO_2 resonance moves downfield toward the position of Hb^{TFA}-O_2 as the pH is raised, which would be expected from either removal of the imidazole charge on deprotonation, or movement of the aromatic ring away from the F helix as the salt bridge is broken. These alternatives are indistinguishable from presently available data; application of the simultaneous ^{19}F-^{1}H-nmr technique of Millett and Raftery (1972) will permit precise interpretation of the observed effect.

The role of His β146 was confirmed by the nmr behavior of Hb^{TFA}-deO_2 from which the histidine had been removed by carboxypeptidase B. In this derivative the pH dependent portion of the chemical shift was absent (Figure 6), and the 15 cps chemical shift difference observed above pH 8 for normal Hb^{TFA} appeared over the entire pH range. X-Ray data have shown that removal of His β146

does not produce extensive structural disruption (Perutz et al., 1971), nor is cooperative ligand binding much reduced (n = 2.5). Hence the pH dependent portion of the Hb^{TFA}-deO_2 chemical shift is primarily a local consequence of the proximity of His β146.

The remaining 15 cps chemical shift difference between liganded and unliganded Hb^{TFA} is less easily assigned. Removal of Tyr β145 or carbamylation of ϵ-amino Val β1 had no effect. The spin state of the iron, which is high spin paramagnetic in deoxyhemoglobin and low spin diamagnetic in most liganded species, is not likely to be a major factor, for reasons which will be discussed in reference to Hb^{TFA}-III. A change in orientation of the α chain might produce minor changes in chemical shift on deoxygenation, although the α chain is fully 10 Å away from Cys β93 in oxyhemoglobin. No specific identification can be made at present, beyond the conclusion that the conformation of Hb^{TFA}-deO_2 is generally different from that of Hb^{TFA}-O_2 in this region.

His β146 and the Alkaline Bohr Effect

The foregoing results indicate that the pH-dependent process observed in Hb^{TFA}-deO_2 involves His β146. If the observed process directly reflects the titration of that imidazole, the demonstrated pK_a of 7.4 is ~0.7 pH units higher than the probable pK_a of His β146 in oxyhemoglobin. (This pK_a is assigned by analogy with values measured in smaller peptides terminating in histidine (Perrin, 1965).) Such a pK_a rise is substantiated by other estimates (Kilmartin and

and Wootton, 1970) of the fractional contribution of His β146 to the Bohr effect. However, as the ensuing discussion will show, the observed pH-dependent process is likely to much more complicated than a single group titration.

Mammalian erythrocytes contain diphosphoglyceric acid (DPG) and hemoglobin in approximately equal concentrations (5×10^{-3} M). At neutral pH and physiological salt concentrations, DPG binds strongly ($K_{diss} \cong 10^{-5}$) to unliganded but not liganded hemoglobin. Bound DPG decreases the oxygen affinity while increasing the Bohr effect and cooperativity (DeBruin et al., 1971; Tyuma and Shimizu, 1970; Tyuma et al., 1971). Extensive studies of this interaction have been conducted by these investigators, and there is general agreement that the "specific" DPG binding site is between the β chains in the cluster of positive charges formed by lysines β82, histidines β143, and the amino groups of valine β1. The increased cooperativity and decreased oxygen affinity produced by this binding have been attributed (Perutz, 1970) to stabilization of the deoxy structure by the salt bridges which DPG forms between the β chains. The cationic groups involved in the salt bridges exhibit raised pK_a's, which increases the Bohr effect. In high concentrations, most small anions can mimic these effects.

In the presence of a 1:1 molar ratio of DPG, the ^{19}F-nmr signal of Hb^{TFA} shifted to higher field by ~12 cps in the pH range 6-8, while exhibiting the same sort of pH dependence observed in stripped Hb^{TFA}-deO_2 (Figure 7). An exact interpretation of this

shift is difficult. A conformation change probably has occurred, as evidenced by the change in chemical shift at all pH values, but since no crystallographic evidence is yet available on the Hb·DPG complex, the exact nature of the change is not clear. The titration curve itself indicates that none of the DPG-binding groups is being observed directly, since no pK_a change occurs. However, the unusual steepness of the curve suggests that the His β146-linked process is influenced indirectly by these groups. A model for the interaction of ionizing groups in a protein is discussed in the next section.

Coupled Ionizations in Deoxyhemoglobin

The pH-dependent process observed in Hb^{TFA}-deO_2 has the superficial appearance of a titration curve, but upon closer examination it is seen to be abnormally steep. The chemical shift changes over a pH range of about one pH unit, compared with the two pH units over which 80% of a normal ionization is observed. This sharpness is accentuated when DPG is bound to the deoxyhemoglobin (Figure 7). Similar properties appear in the pK_a = 7.1 ionization observed in des-His β146 methemoglobin (Figure 11). No precedent has been reported for unusually sharp titrations of ionizable groups in native proteins. Individual carboxyl and imidazole groups have been titrated in the active sites of lysozyme (Parsons, 1972) and ribonuclease (Meadows and Jardetzky, 1968), but normal curves were obtained. The microscopic environments of ionizable groups in proteins have been observed to induce abnormal pK_a values, but shortened ionization

ranges have not been reported.

The steepness of these titrations is best explained as the result of interactions between the observed ionization and other ionizable groups in the protein. If a pH-dependent process occurs during the deprotonation of His β146 which causes its pK_a to change, the shape of the titration curve will be abnormal. The critical requirement for a steep titration is that the pK_a of the observed group decreases in the pH range in which it ionizes. This can be accomplished by a conformation change in the protein which is governed by a second ionization in the same pH range, or by a direct interaction with the second group.

Consider a system of two such interacting groups, represented as HA$\sim\sim$BH, in which the pK_a of HA is controlled by the ionization state of BH and vice versa.*

$$\frac{[H^+][^-A\sim\sim BH]}{[HA\sim\sim BH]} = K_{A1} \qquad (1)$$

$$\frac{[H^+][^-A\sim\sim B^-]}{[HA\sim\sim B^-]} = K_{A2} \qquad (2)$$

$$\frac{[H^+][HA\sim\sim B^-]}{[HA\sim\sim BH]} = K_{B1} \qquad (3)$$

---

*Thermodynamic consistency requires that $\Delta K_A = \Delta K_B$, hence $K_{A1} K_{B2} = K_{A2} K_{B1}$.

$$\frac{[H^+][^-A\sim B^-]}{[^-A\sim BH]} = K_{B2} \qquad (4)$$

For this coupled ionization, the fraction S of A which is not ionized can be expressed as a function of $[H^+]$ and the K's as follows:

$$S = \frac{[H^+]^2 + [H^+]K_{B1}}{[H^+]^2 + [H^+](K_{A1} + K_{B1}) + K_{B1}K_{A2}} \qquad (5)$$

This equation generates abnormally steep titration curves when $pK_{A1} > pK_{A2}$. Computer analysis of the slopes of calculated curves at S = 0.5 showed that the steepest titration in this system occurs for equivalent groups ($pK_{A1} = pK_{B1}$ and $pK_{A2} = pK_{B2}$) when the $\Delta pK = pK_1 - pK_2$ is large. (Plots with $\Delta pK > 4$ pH units are visually indistinguishable.) Such a curve is shown in Figure 8(2) for $\Delta pK = 4$ units, the constants having been chosen to place the observed pK_a at 7.4. The slope of this plot at S = 0.5 is twice as great as that of a normal acid titration curve. Curves of any desired slope less than this maximum and greater than a normal curve can be obtained by specifying smaller positive ΔpK's. Intermediate slopes also result when groups A and B are nonequivalent, with the additional effect that the calculated curves may be asymmetrical.

Greater maximum slopes can be obtained by extending the model to include more interacting ionizations. Systems of three and four equivalent interacting groups were analyzed as described for the

double coupled model (see Appendix I for further discussion). Figure 8(3) and 8(4) shows examples of calculated curves produced by interaction of three and four ionizations. Maximum slopes at S = 0.5 are three and four times the slope of a normal titration curve for three and four interacting ionizations, respectively. For either model, appropriate constants will produce curves of any desired steepness less than the maximum.

The nondeterminacy of these models is illustrated by the following fitted curves of the titration data of stripped Hb^{TFA}-deO_2. Reasonable fits of these data are produced by the double coupled ($pK_1 = pK_{A1} = pK_{B1} = 9.4$, $pK_2 = pK_{A2} = pK_{B2} = 5.4$), triple coupled ($pK_1 = 8.6$, $pK_2 = 7.4$, $pK_3 = 6.2$), or quadruple coupled ($pK_1 = 8.3$, $pK_2 = 7.7$, $pK_3 = 7.1$, $pK_4 = 6.5$) symmetrical models. The slope of these curves at S=0.5 is about 1.5 times as steep as that of a normal titration. These fits also illustrate that the higher the order of interaction, the smaller the ΔpK's which are required to generate a desired slope. The data from titration of DPG-complexed Hb^{TFA}-deO_2 can be fitted from at least four coupled groups ($pK_1 = 9.4$, $pK_2 = 8.6$, $pK_3 = 6.2$, $pK_4 = 5.4$). The slope is steeper than a normal titration by a factor of four.

The numerous models which fit these data are functionally indistinguishable, since the observed ionization actually occurs at the central pH (7.4) and the intrinsic pK_a's are unobservable.

Present knowledge of individual ionization processes in hemoglobin is inadequate to permit application of these models to actual

events in the protein. The β chain of human hemoglobin contains nine histidines, two cysteines (one in Hb^{TFA}), and one α-amino group which could be expected to ionize in the pH range of interest. Speculation about interactions among these groups is futile until more is known about the roles of individual residues in structural changes. It is reasonable to suppose that some or all of the groups which bind DPG are involved in the DPG + Hb^{TFA}-deO_2 titration, but whether DPG binding increases the number of interacting groups or the magnitude of the ΔpK_a's is not known and not predictable from present data. The systematic study of well characterized hemoglobin variants may yield information pertinent to these questions in the future.

Histidine β146 is clearly a party to the observed processes, since they are not observed when the histidine is absent. As Kilmartin has shown (1971), removal of His β146 also removes half of the alkaline Bohr effect. This observation is easily accounted for by a simple pK_a change for the histidine on ligand binding. However, if His β146 is involved in a cooperative ionization system, then its removal will produce widespread disruption of normal ionization equilibria which may account for the missing Bohr protons.

Mechanistic Implications of Ionic Interactions

The observation of "cooperative" ionizations involving critical residues in hemoglobin raises immediate questions about the relation, if any, between cooperative proton binding and cooperative heme

ligand binding. As is discussed in Appendix I, the models developed to calculate abnormally steep titration curves are directly analogous to the Adair equation and Hill equation. It is tempting to suppose that the pH-dependent process observed in Hb^{TFA}-deO_2 is part of the molecular machinery whereby the binding of oxygen to one subunit changes the next subunit to a more receptive form. However, the fact that cooperative oxygen binding is independent of pH between 6 and 9 eliminates the possibility of direct participation of the His β146 imidazole in the oxygen binding mechanism, with or without associated ionization complexes. Indeed, the insensitivity of cooperative oxygen binding to the pH and salt concentration of the medium raises disturbing questions about the role of all ionic forces in its mechanism.

A recent mechanistic proposal (Perutz, 1970) states that a salt bridge between the carboxyl group of His $\beta_2$146 and Lys $\alpha_1$40 constitutes the quaternary structural constraint in the $\alpha_1\beta_2$ interface, which, along with similar electrostatic constraints in the $\alpha_1\alpha_2$ contact, produces cooperative ligand binding in the molecule. The importance of interactions at the $\alpha_1\beta_2$ interface to cooperative transition has long been recognized from the preponderance of invariant residues found there and from the diminished cooperativity found in mutants which exist. The salt bridge model designates the His $\beta_2$146-Lys $\alpha_1$40 interaction as a source of allosteric properties, and attributes lessened cooperativity in variants to weakening of this interaction. For example, the decreased cooperativity and increased oxygen affinity of hemoglobin Hiroshima (His β146 → Asp) have been attributed to loss of

His β146 imidazole-Asp β94 salt bridge stabilization of the carboxyl salt bridge of the residue (Perutz et al., 1971). If the imidazole salt bridge stabilizes the carboxyl bond and thereby contributes to the overall energy of the cooperative transition, then the titration of the imidazole, with or without associated conformation changes, should produce a decline in cooperativity as the pH is raised. This prediction is contrary to what has been observed. Within the accuracy of such experiments, the Hill coefficient of hemoglobin A has been shown to be independent of pH in the range 4.5-9 (Lee and Raftery, 1972; Antonini et al., 1962; Tyuma and Shimizu, 1970), provided salt conditions are kept constant. The His β146 (carboxyl) and Arg α141 salt bridges directly involved in the proposed structural constraints are not titrated in this pH range, but the absence of any effect from removal of the stabilizing His β146 imidazole bond impels a closer examination of the role of its carboxyl bond in the mechanism.

His β146 per se has been shown to be expendable since cooperativity is little impaired when the histidine is removed by carboxypeptidase B digestion (n = 2.5) (Kilmartin and Wootton, 1970). However, removal of the next residue, Tyr β145, by carboxypeptidase A abolishes cooperativity (n = 1.0) (Antonini et al., 1961). The suggestion has been made (Perutz, 1970) that these phenomena are due to the possibility that the Tyr β145 carboxyl group may form the salt bridge to Lys α40 in place of the normal carboxy terminus. A possibility which has not been fully discussed is that the side chain of the tyrosine may play a vital role in the transition, entering into

hydrophobic interactions which are as important energetically as electrostatic ones in maintenance of the constrained deoxy structure.

The influence of the tyrosine side chains on the oxygen affinity of the β chains was discussed in a recent report (Hayashi and Stamatoyannopoulos, 1972) on the properties of mutant hemoglobins Bethesda and Ranier, in which Tyr β145 is replaced by histidine and cysteine, respectively. It was suggested that the phenolic groups contribute to tertiary constraint of the β chains, lowering oxygen affinity as long as the salt bridges of His β146 stabilize the groups in their pockets. The particular substitutions of cysteine and histidine make direct comparison of properties difficult, since the cysteine was shown to form a disulfide bond with Cys β93 and the histidine, being partially charged at physiological pH, would be expected to be less stable than tyrosine if it enters the hydrophobic F-H pocket. In both cases, the mutant residue produces structural perturbations extensive enough to disrupt the salt bridges of His β146 (Greer and Perutz, 1971), so that the altered properties of these hemoglobins cannot be ascribed simply to loss of the tyrosine side chains. However, it is interesting to note that no other examples are known of vertebrate hemoglobins with substitutions at position β145. Mutants with residues such as glycine or alanine, which would produce no steric barrier to formation of the His β146 salt bridges, are not found. This suggests that the phenolic group is not a passive bulk which is pushed in and out of a conveniently shaped notch as salt bridges are broken and formed; rather, that the side chain itself is

involved in energetically important conformational processes. An example of the sort of interactions in which a penultimate tyrosine is involved has been described (Perutz, 1970) in the case of Tyr $\alpha_1 140$. As this tyrosine enters its pocket, it presses on the indole ring of Trp $\beta_2 37$, causing it to tilt over and press on Pro $\beta_2 36$. This inter-chain pressure pushes the β chain toward its deoxy conformation and presumably helps to keep it there.

The behavior of the allosteric parameters P_{50} and n as functions of pH and ionic strength lend credence to the suggestion that subtle hydrophobic interactions such as these are no less important than electrostatic ones in the energetics of the cooperative transition. It has long been recognized that neutral salt concentration has profound influence on oxygen affinity and the Bohr effect, but not on cooperativity. Very high concentrations (e. g., 1-4 M) of neutral salt supress the Bohr effect to a marked degree (Antonini et al., 1962), and a 50-fold increase in sodium chloride concentration can produce a ten-fold increase in log P_{50} for stripped hemoglobin (Benesch et al., 1969). Binding of diphosphoglyceric acid (DPG), which in 1:1 molar ratio decreases oxygen affinity dramatically, is regarded as a specialized and more effective instance of the general salt effect, and indeed very high concentrations of either DPG or neutral salt can eliminate any effect from addition of the other (Benesch et al., 1969). All of the studies cited have shown no dependence of the Hill coefficient on neutral salt concentration in the range $<10^{-2}$ M to 5 M. Some implications of these findings have been discussed, particularly in

reference to the role of DPG. The data point consistently to binding of negative salt ions in a cavity between the β chains of deoxyhemoglobin, involving six positively charged groups on the protein (His β143, Val β1, Lys β82). This binding, whether by DPG or other anions such as chloride, stabilizes the deoxy form and thus lowers the oxygen affinity. Addition of further neutral salt to deoxyhemoglobin which is saturated with DPG lowers the oxygen affinity further, but only to a small degree. Thus it appears that most of the effective ion binding is confined to the DPG binding site. The only further effect of high salt concentrations is the supression of the Bohr effect (Antonini et al., 1962), a phenomenon which is not surprising since high ionic strength should stabilize the protonated forms of the primary Bohr residues (His β146, Val α1) in their oxy conformation.

In view of the sensitivity of the Bohr and DPG electrostatic interactions to salt concentration, an ionic strength effect on the salt bridges of the proposed cooperative mechanism would be expected. If the quaternary structural constraints afforded by the interchain salt bridges are in fact the most important energetic factors in the conformation transition, it is interesting that variation of the ionic strength of the medium has so little effect on the Hill coefficient. One might expect, in addition, that high external ion concentrations would lead to relative stabilization of the oxy conformation (similar to the effect seen for the Bohr residues), in which the eight charged groups are free in solution. This would result in increased oxygen affinity, rather than the slight decrease which is observed. On the

other hand, high ionic strengths would be expected to oppose exposure of hydrophobic groups such as Tyr β145 to the medium. If indeed these hydrophobic interactions are energetically important in maintenance of the deoxy structure, some destabilization of the oxy (exposed) conformation would be expected from increased solvent ionic strength, resulting in decreased oxygen affinity.

The same considerations apply to the roles of cooperative ionizations. Unless the interacting ionizable groups are protected from the solvent or there is internal compensation for changes in their ionic character with pH and ligand binding, any allosteric property to which they contribute should be sensitive to pH and ionic strength.

Nmr Studies of Methemoglobin

Information obtained from nmr studies of Hb^{TFA}-deO_2 was in general agreement with X-ray data on the conformation of the protein near Cys β93. In three of the liganded forms studied (oxy-, carboxy-, and cyanomethemoglobin), chemical shifts and pH behavior were also consistent with predictions based on the crystal structure. It was surprising to find a radical departure from this pattern in methemoglobin (Hb^{TFA}-III). Methemoglobin is generally classed with the liganded forms since its dye binding properties and crystal form are characteristic of the liganded quaternary structure. However, the chemical shift of Hb^{TFA}-III was observed upfield of other liganded species near that of Hb^{TFA}-deO_2 (Figure 2), and as in HB^{TFA}-deO_2,

the chemical shift was pH dependent (Figure 10). Since evidence already cited suggests that the nmr probe is influenced primarily by conformation changes within the β chain, its behavior in Hb^{TFA}-III suggested that at least in this region of the protein Hb-III differs from Hb-O_2 in tertiary structure.

The crystal structure data are not informative on this question, since the oxyhemoglobin crystals studied were oxidized slowly to methemoglobin during collection of the data (Perutz, 1970). Hence neither crystal structure is known with certainty, if differences exist. Additional uncertainty as to the native conformation of the Cys β93-His β146 region may have been introduced by use of p-mercuribenzoate (PMB) at Cys β93 for two of the three heavy metal derivatives of oxyhemoglobin. PMB-Cys β93 hemoglobin exhibits decreased cooperativity and Bohr effect (Riggs, 1961), which indicate structural disruptions.

The general similarity of Hb^{TFA}-III's nmr behavior to that of Hb^{TFA}-deO$_2$ suggested the possibility that similar processes were being observed. As in the case of Hb^{TFA}-deO$_2$, several nearby histidines (146, 143, 97, 92) and the amino terminus of Val β1 were possible participants. Carbamylation of the amino terminus did not alter the pH behavior of the chemical shift. No specific binding of DPG analogous to the effect seen in Hb^{TFA}-deO$_2$ could be detected in Hb^{TFA}-III, even in the presence of a 100-fold excess of DPG. Hence no information could be obtained on His β143. Removal of His β146, however, changed the pH behavior and chemical shift dramatically

(Figure 11). The pH dependence above pH 7.5 was removed, and an overall chemical shift difference evidenced additional structural differences.

The simplest interpretation of this result is that in Hb^{TFA}-III, His β146 occupies a position near Cys β93 such that its imidazole pK_a is raised above 7.5. This implies retention of the salt bridge to Asp β94. In addition, the oxy quaternary structure of Hb^{TFA}-III requires that the quaternary structural bond between the His β146 carboxyl and Lys α40 be broken. The increased negative charge from the free carboxyl group could further raise the pK_a of the imidazole side chain by as much as 0.5 pH units, according to the model studies cited in Perrin (1965). The binding of cyanide or azide to methemoglobin produces proton release analogous to the Bohr effect (Anusiem et al., 1968), a result which would be expected if the pK_a of His β146 is being lowered by the transition to its liganded conformation.

In order for the Asp β94-His β146 salt bridge to be maintained in methemoglobin, Tyr β145 must be able to occupy its bound position between the F and H helices. In oxyhemoglobin, the salt bridge is destabilized by conformation changes which prevent the entry of Tyr β145 into its pocket, resulting in displacement of the carboxy terminus equilibrium toward the free position. The extent to which this is true of methemoglobin is uncertain. The possibility that methemoglobin exhibits a more hospitable conformation can be inferred from some X-ray evidence on the heme configurations of various liganded species (Hoard, 1966; Perutz, 1970). From these studies a mechanism has

been proposed for the triggering of protein changes on ligand binding by the movement of the iron atom into the plane of the porphyrin ring. By analogy with myoglobin derivatives and iron porphyrin models, Perutz has stated that the iron atom lies 0.75 Å above the heme plane in deoxyhemoglobin, while in oxyhemoglobin it lies within 0.05 Å of that plane. In acid methemoglobin, the distance is 0.3 Å. This intermediate position may be symptomatic of widespread structural characteristics different from either oxy- or deoxyhemoglobin.

Despite some similarities in the nmr behavior of Hb^{TFA}-III and Hb^{TFA}-deO_2, the characteristics of their des-His β146 derivatives indicate that differences exist. The pH-dependent process remaining in des-His β146 Hb^{TFA}-III has no counterpart in the Hb^{TFA}-deO_2 derivative. The process cannot be identified from available data, although its apparent pK_a of 7.1 suggests that the ferric heme may be involved. The pK_a of His β63, the "distal histidine" of the heme, has been determined to be in the pH range 6.7-7.1 (Fabry et al., 1969; George and Hanania, 1953).

Several other ionizations whose pK_a's are known apparently are not involved. The acid-to-alkaline-methemoglobin transition, which occurs when the water molecule at the distal heme ligand position dissociates to hydroxide ion, exhibits a pK_a between 8.15 (from magnetometric titration, Coryell et al., 1937) and 8.3 (from optical difference titrations, Fabry et al., 1969). This latter process produces a spin state change in the hemes from high spin paramagnetic (as in deoxyhemoglobin) to low spin diamagnetic (as in

oxyhemoglobin). (The fact that low spin diamagnetic alkaline Hb^{TFA}-III and high spin paramagnetic Hb^{TFA}-deO_2 exhibit the same chemical shift above pH 8 (Figure 10) indicates that any direct effect of the iron on the nmr probe must be negligible.) The proximal heme ligand, His β92, has a pK_a of 5.1, which is outside the pH range studied (Fabry et al., 1969).

It is possible that the pK_a = 7.1 process observed in des-His β146 Hb^{TFA}-III is not produced by a single ionization. The chemical shift change is considerably steeper than a normal titration curve, suggesting the influence of coupled ionizations such as those observed in Hb^{TFA}-deO_2. Identification of groups involved is not aided by the disappearance of the effect on removal of Tyr β145 (Figure 11). Des-His β146-Tyr β145 Hb^{TFA}-III closely resembles the equivalent derivative of Hb^{TFA}-deO_2. This result is most likely due to disruption of structure by loss of the tyrosine interactions, rather than to any direct effect of the tyrosine. It serves only to emphasize that the carboxy terminal region of Hb^{TFA}-III is different from either oxy or deoxyhemoglobin.

The importance of interactions in this region to the cooperative processes of ferrous hemoglobin suggests that any differences which exist in methemoglobin are likely to have substantial functional consequences. Hence it is significant that previous investigations (Antonini et al., 1964) have shown that the oxidation of deoxyhemoglobin to methemoglobin is not exactly analogous to the ligand binding process. Oxidation is cooperative, but the Hill coefficient is pH

dependent and varies from near 1 below pH 7 to 2.6 above pH 8. Significantly, the midpoint of the transition occurs at about pH 7.4, which suggests the influence of His β146 on the oxidation process. If the salt bridge of His β146 imidazole is retained throughout the oxidation process, it may stabilize deoxy-like structural characteristics and inhibit the conformational processes which produce cooperativity. In that event, breaking of the electrostatic restraint with increasing pH would permit the change to an oxy-like structure (Figure 12) which is necessary for cooperativity. In harmony with this proposal, the oxidation cooperativity is known to be depressed by increased ionic strength (Antonini et al., 1964). The oxidation process thus appears to be governed by electrostatic interactions, in contrast to the oxygen binding process.

Another related feature is the Bohr effect for oxidation, which is larger than that for ligand binding. Part of the increase (the "residual oxidation Bohr effect") cannot be accounted for by the ionization of the water ligand of the ferric heme (Brunori et al., 1969). Any groups in methemoglobin whose pK's differ from those exhibited in deoxy- and oxyhemoglobin are likely to be involved in this phenomenon.

In summary, these studies have revealed dynamic and structural differences between methemoglobin and other liganded forms. The ^{19}F-nmr data permit identification of some, but not all, of these distinctive features. The observed differences suggest mechanisms for the residual oxidation Bohr effect and the pH

dependence of cooperative oxidation of deoxy- to methemoglobin.

References

Antonini, E., Wyman, J., Brunori, M., Taylor, J. F., Rossi Fanelli, A., and Caputo, A. (1964), J. Biol. Chem. 239, 907.

Antonini, E., Wyman, J., Fanelli, A., Rossi, and Caputo, A. (1962), J. Biol. Chem. 237, 2773.

Antonini, E., Wyman, J., Moretti, R., and Rossi Fanelli, A. (1963), Biochim. Biophys. Acta 71, 124.

Antonini, E., Zito, R., Fanelli, A. Rossi, and Caputo, A. (1961), J. Biol. Chem. 236, 60.

Anusiem, A. C., Beetlestone, J. G., and Irvine, D. H. (1968), J. Chem. Soc. A, 960.

Arndt, D. J., Simon, S., and Konigsberg, W. (1971), J. Mol. Biol., in press.

Benesch, R., and Benesch, R. E. (1961), J. Biol. Chem. 236, 405.

Benesch, R. E., and Benesch, R. (1970), Fed. Proc. 29, 1101.

Benesch, R. E., Benesch, R., and Yu, C. I. (1969), Biochemistry 8, 2567.

Briehl, R. W. (1962), Fed. Proc. 21, 72.

Brunori, E., Taylor, J. F., Antonini, E., and Wyman, J. (1969), Biochemistry 7, 2880.

Cohn, E. J., and Edsall, J. T. (1943), "Protein, Amino Acids, and Peptides", Reinhold, New York.

Coryell, C. D., Stitt, F., and Pauling, L. (1937), J. Amer. Chem. Soc. 59, 633.

Deal, W. J., Mohlman, S. G., and Sprang, M. L. (1971), Science 171, 1147.

DeBruin, S. H., Janssen, L. H. M., and Van Os, G. A. J. (1971), Biochem. Biophys. Res. Commun. 45, 544.

Ellman, G. L. (1959), Arch. Biochem. Biophys. 82, 70.

Fabry, T. L., Kim, J., Koenig, S. H., and Schillinger, W. E. (1971), Proc. Johnson Found. Mtg. on Heme and Hemoproteins. Academic Press, New York.

Garby, L., Gerber, G., and deVerdeer, C. H. (1969), European J. Biochem. 10, 110.

George, P., and Hanania, G. (1953), Biochem. J. 55, 236.

Greer, J., and Perutz, M. F. (1971), Nature New Biology 230, 261.

Haurowitz, F. (1938), Z. Physiol. Chem. 254, 266.

Hayashi, A., Stamatoyannopoulos, G. (1972), Nature New Biology, 235, 70.

Hoard, J. L., in Hemes and Hemoproteins (ed., B. Chance, R. W. Estabrook, and T. Yonetani), Academic Press, New York, 1966, p. 9.

Kilmartin, J. V., and Rossi-Bernardi, L. (1969), Nature 222, 1243.

Kilmartin, J. V., and Wootton, J. F. (1970), Nature 228, 766.

Lee, T., and Raftery, M. A. (1972), unpublished results.

McConnell, H., Deal, W. J., and Ogata, R. G. (1969), Biochemistry 8, 2580.

Meadows, D. H., and Jardetzky, O. (1968), Proc. Natl. Acad. Sci. (U.S.) 61, 406.

Millett, F. M., and Raftery, M. A. (1972), Biochem. Biophys. Res. Commun., in press.

Moffat, J. K. (1971), J. Mol. Biol. 55, 135.

Muirhead, H., and Greer, J. (1970), Nature 228, 516.

Parsons, S., and Raftery, M. A. (1972), Biochemistry, in press.

Perrin, D. D. (1965), "Dissociation Constants of Organic Acids in Aqueous Solution", Butterworths, London.

Perutz, M. (1970), Nature 228, 726.

Perutz, M. F., del Pulsinelli, P., Ten Eyck, L., Kilmartin, J. V., Shibata, S., Iuchi, I., Miyaji, T., and Hamilton, H. B. (1971), Nature New Biology 232, 147.

Perutz, M. F., Muirhead, H., Cox, J. M., Goaman, L. C. G., Mathews, F. S., McGandy, E. L., and Webb, L. E. (1968), Nature 219, 29.

Riggs, A., and Wohlbach, R. A. (1956), J. Gen. Physiol. 39, 585.

Riggs, A. (1961), J. Biol. Chem. 236, 1948.

Tomita, S., Enoki, Y., Santa, M., Loshida, H., and Yosuminisu, Yo (1968), J. Nara Med. Assoc. 19, 1.

Tyuma, I., and Shimizu, K. (1970), Fed. Proc. 29, 1112.

Tyuma, I., Shimizu, K., and Imai, K. (1971), Biochem. Biophys. Res. Commun. 43, 423.

Wyman, J. (1948), Adv. Protein Chem. 4, 463.

Zito, R., Antonini, E., and Wyman, J. (1965), J. Biol. Chem. 239, 1809.

Figure 1. Oxygen equilibrium curves for Hb and Hb^{TFA} at 25° in 0.1 M sodium phosphate, pH 7.0.

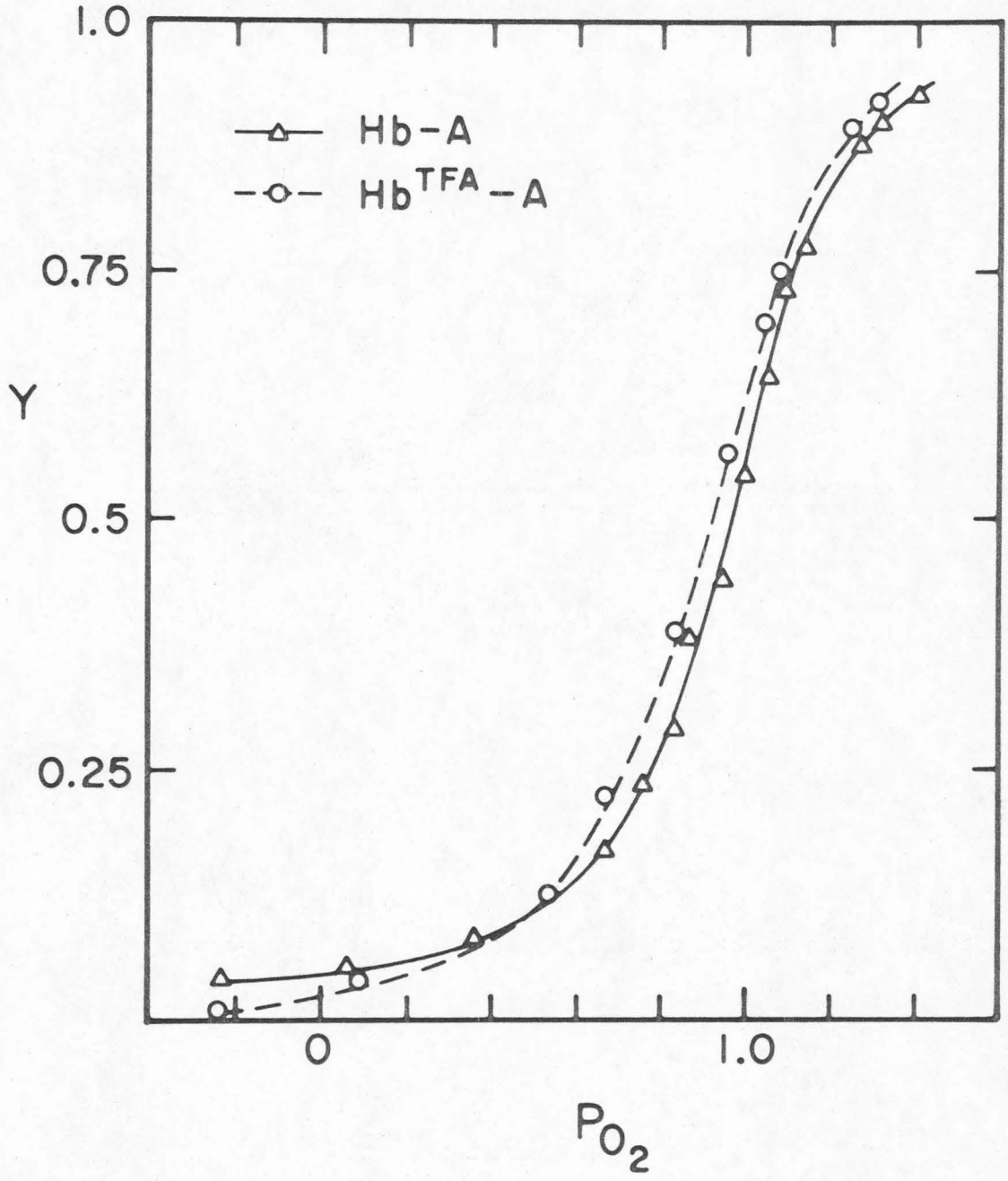
1.0
0.75
0.5
0.25
Y
Hb-A
Hb^TFA-A
0
1.0
P_O2

Figure 2. ^{19}F-Nmr spectra of trifluoroacetonylated hemoglobin for various ligand states.

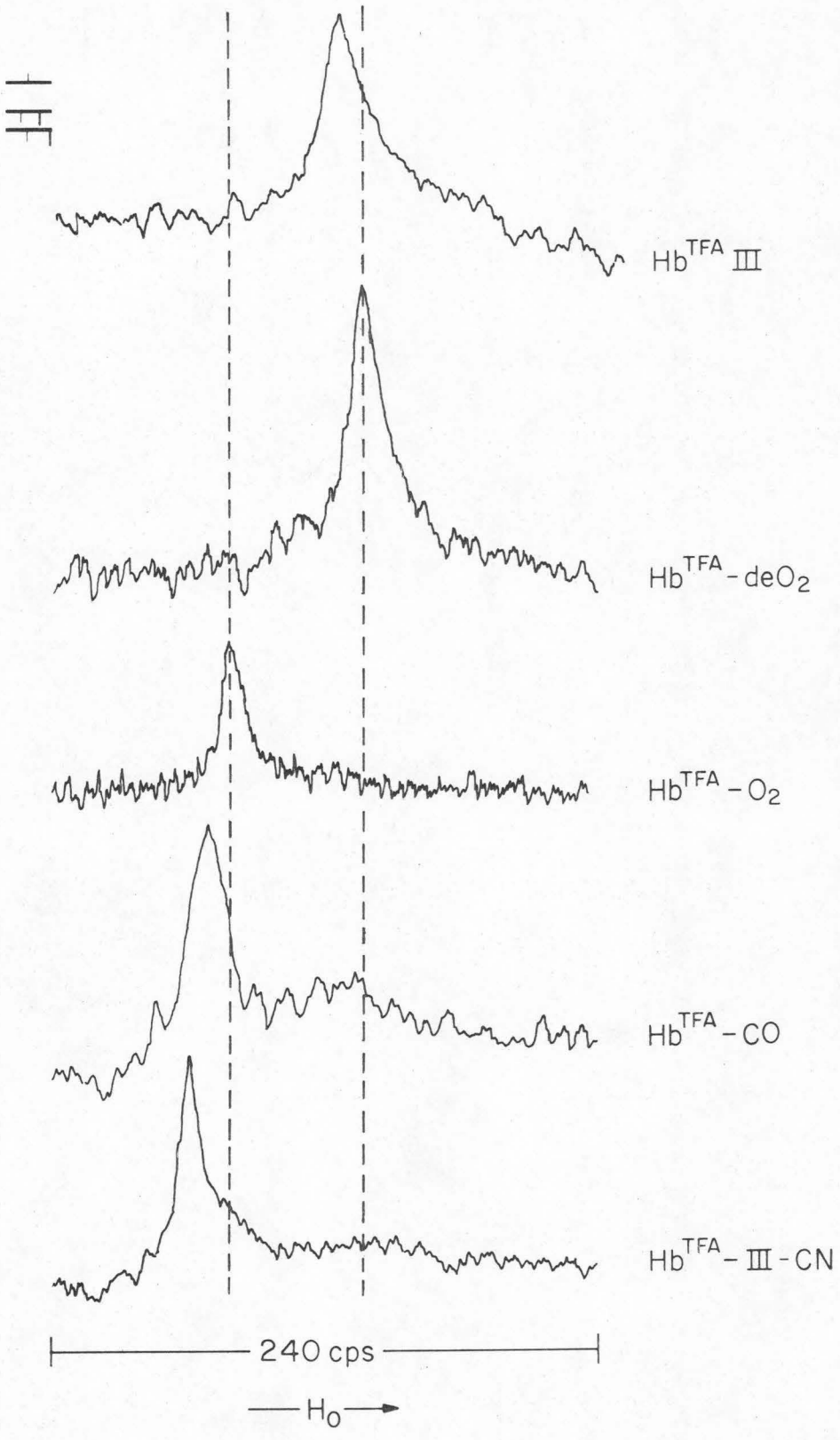
Hb^TFA III
Hb^TFA - deO2
Hb^TFA - O2
Hb^TFA - CO
Hb^TFA - III - CN
240 cps
Ho

Figure 3. ^{19}F-Nmr spectra of trifluoroacetonylated hemoglobin in the presence of DPG, in 0.1 M NaCl at pH 6.75.

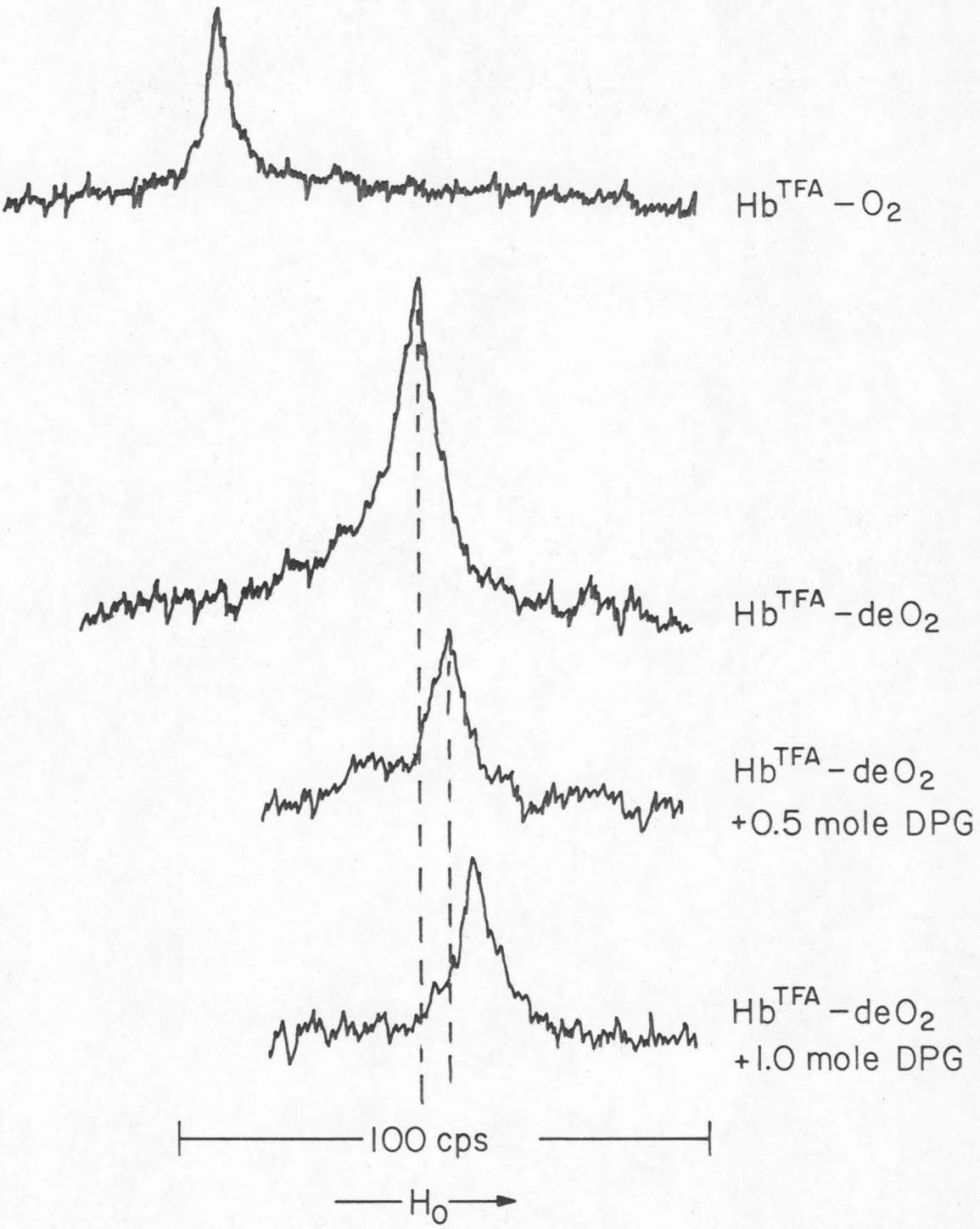
$Hb^{TFA} - O_2$
$Hb^{TFA} - deO_2$
$Hb^{TFA} - deO_2$
+0.5 mole DPG
$Hb^{TFA} - deO_2$
+1.0 mole DPG
100 cps
H_o

Figure 4. Chemical shift of trifluoroacetonylated hemoglobin as a function of pH, for various ligand states (o, Δ, ∇, $\times$) and for S-trifluoroacetonyl-β-mercaptoethanol (•).

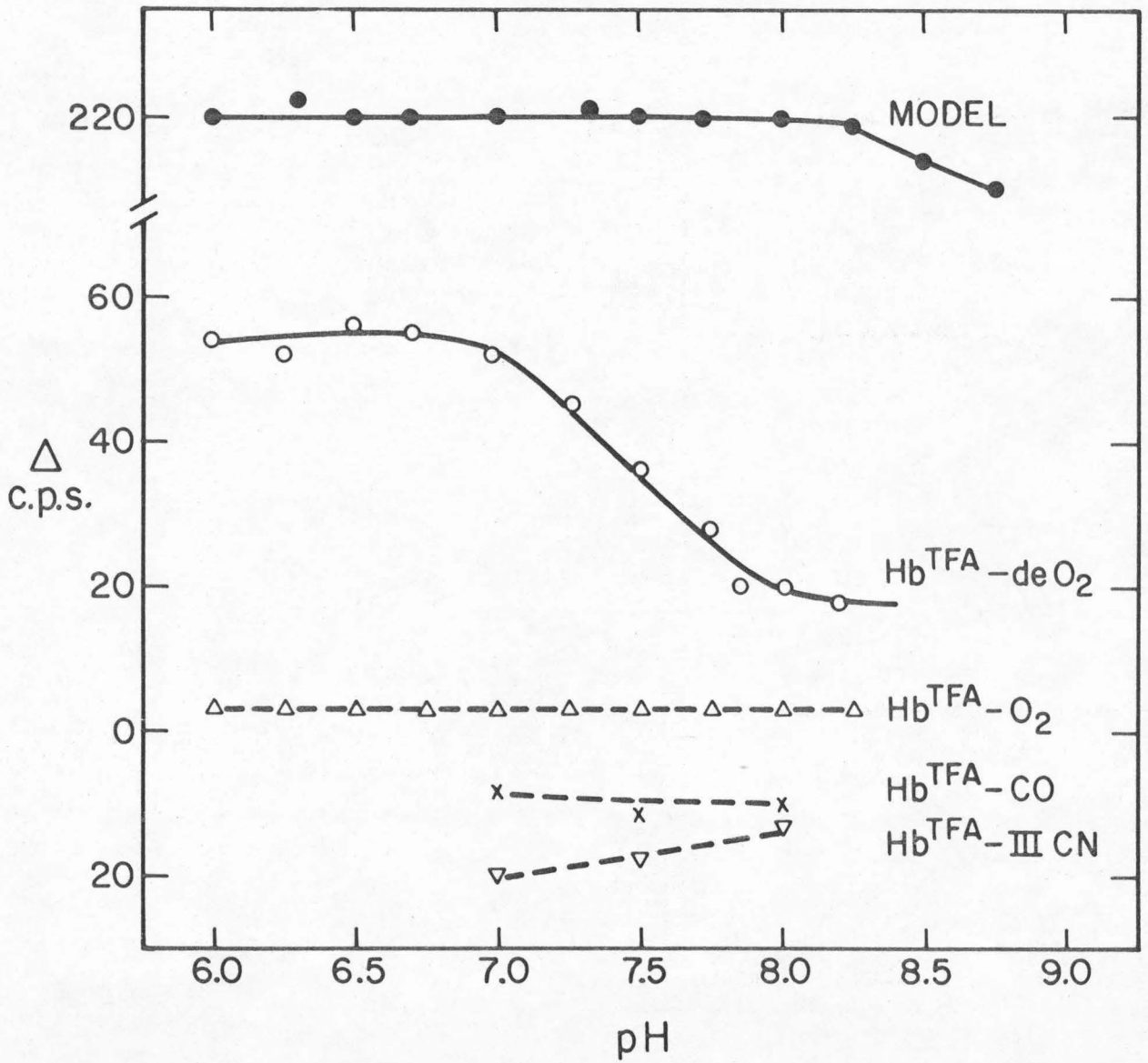
220
60
40
20
0
20
Δ
c.p.s.
MODEL
Hb^TFA – de O2
Hb^TFA – O2
Hb^TFA – CO
Hb^TFA – III CN
6.0
6.5
7.0
7.5
8.0
8.5
9.0
pH

Figure 5. Schematic representation (after Perutz, 1970) of the conformational equilibrium of the C-terminus of the β chain, showing effects of pH and ligand binding in the $\alpha_1\beta_2$ contact region. The position of the ^{19}F probe is indicated by *.

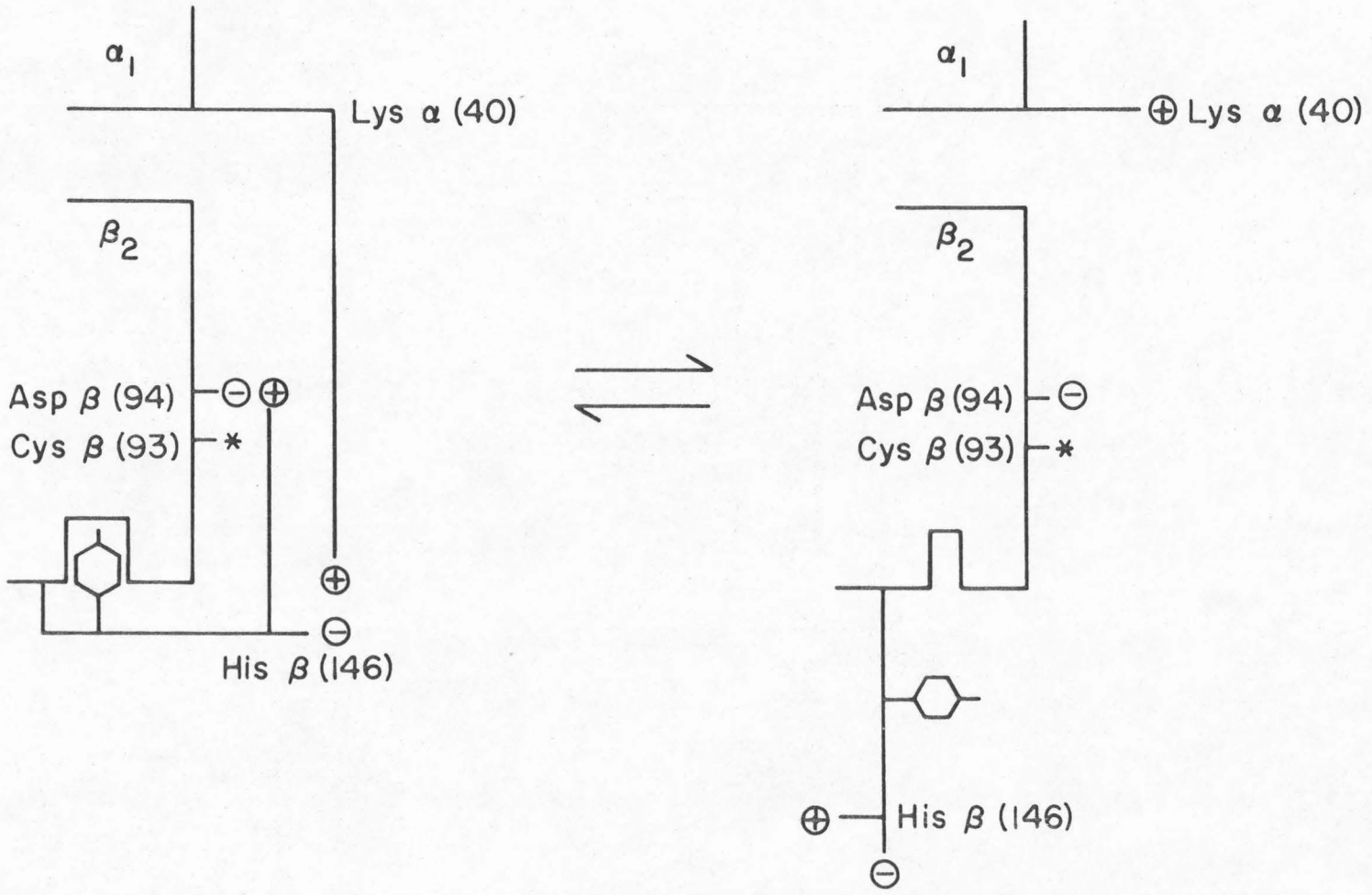

Predominant Deoxy Form

Predominant Oxy Form

Figure 6. Chemical shift of trifluoroacetonylated hemoglobin as a function of pH for Hb^{TFA}-O_2, -Δ-; Hb^{TFA}-deO_2, -o-; Hb^{TFA}-deO_2, des His β146, -●-; Hb^{TFA}-deO_2 des [His β146-Tyr β145], -▲-.

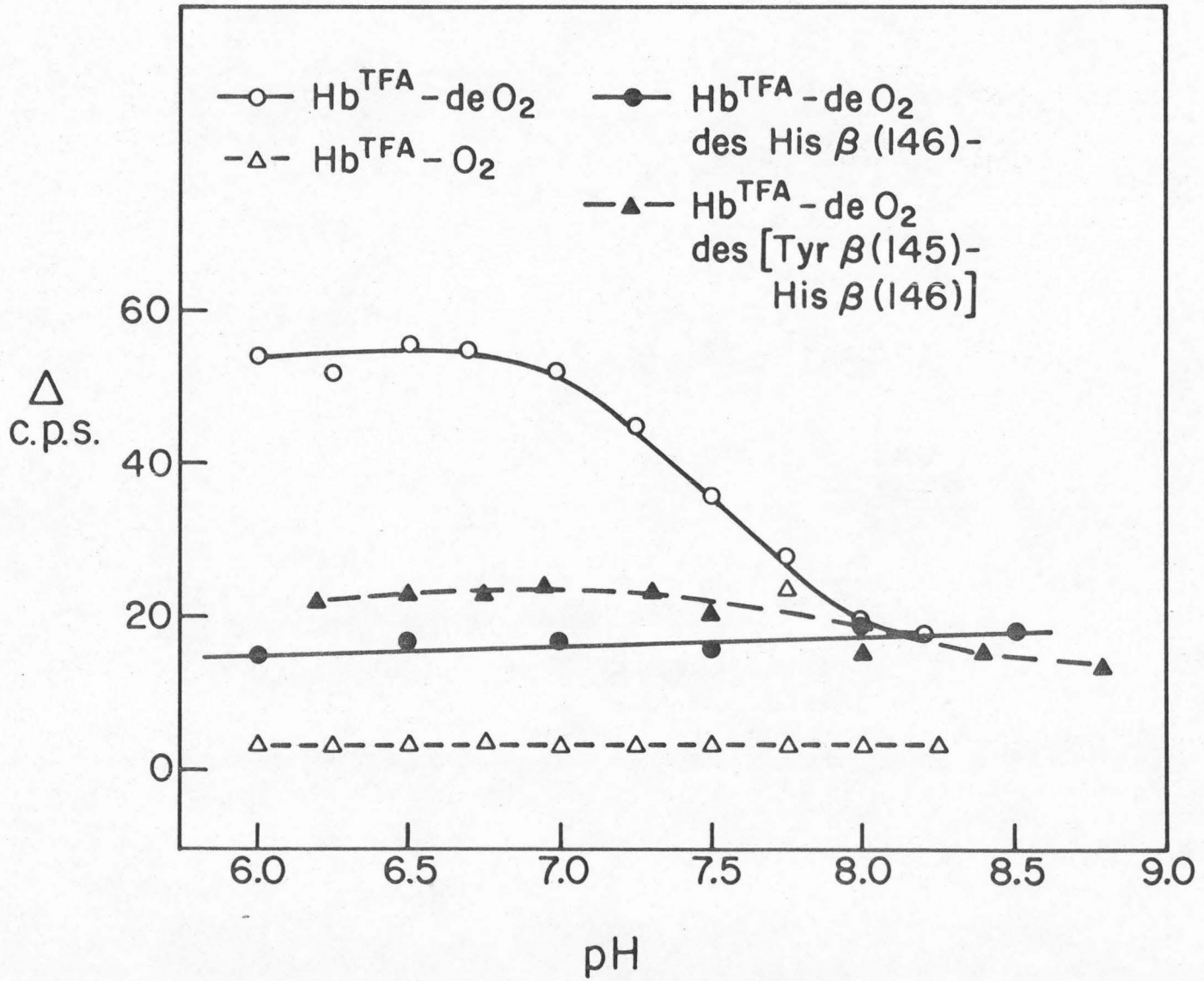
Hb^TFA - de O2
Hb^TFA - O2
Hb^TFA - de O2 des His β (146)-
Hb^TFA - de O2 des [Tyr β (145)- His β (146)]
Δ c.p.s.
60
40
20
0
6.0
6.5
7.0
7.5
8.0
8.5
9.0
pH

Figure 7. Chemical shift of trifluoroacetonylated hemoglobin as a function of pH: (●), Hb^{TFA}-O_2 in presence or absence of DPG; (o), Hb^{TFA}; (Δ), Hb^{TFA} and DPG.

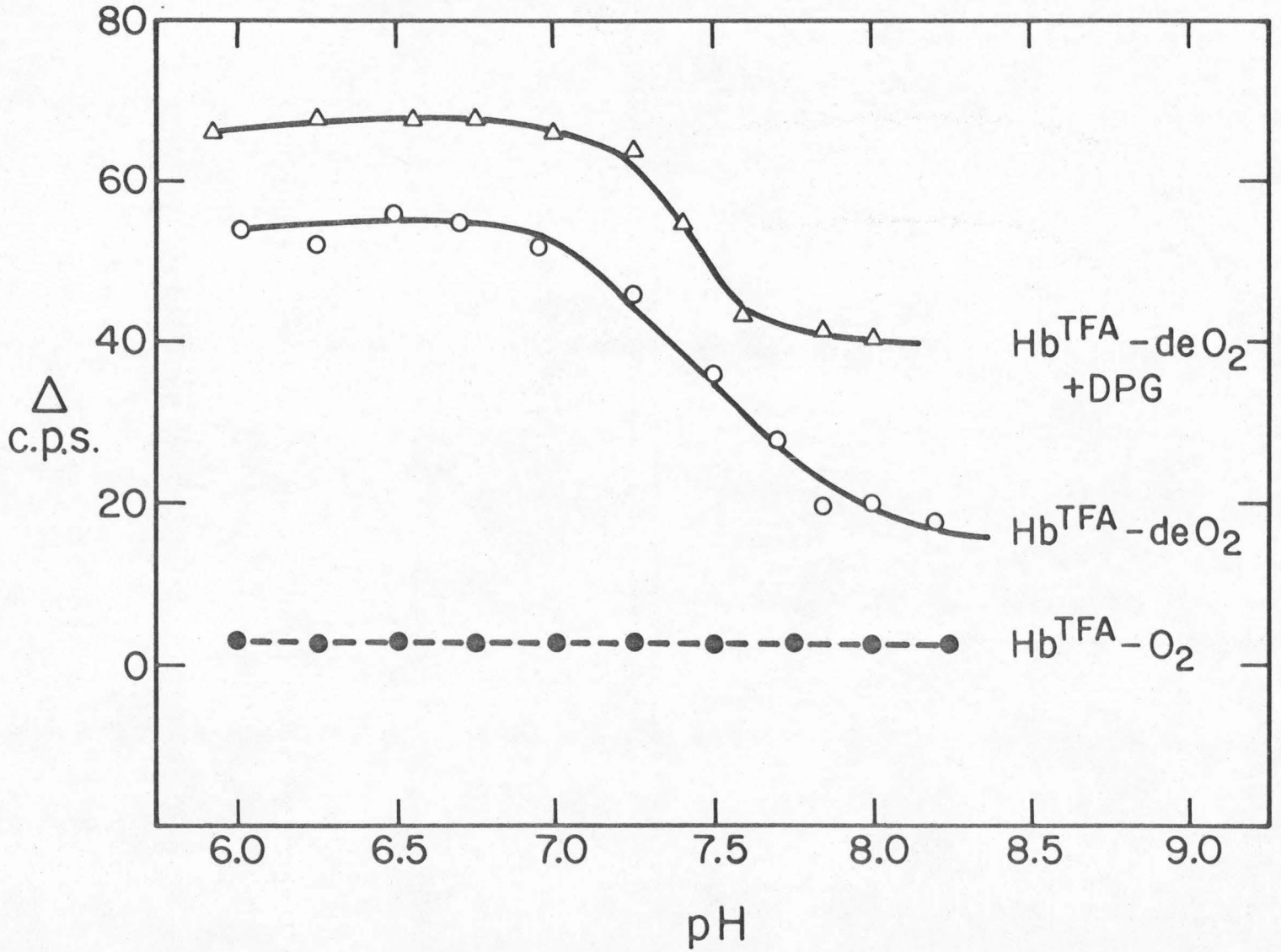
80
60
40
20
0
Δ
c.p.s.
6.0
6.5
7.0
7.5
8.0
8.5
9.0
pH
Hb^TFA - deO2
+DPG
Hb^TFA - deO2
Hb^TFA - O2

Figure 8. Calculated ionization curves for (1) a single acid; (2) a pair of mutually interacting acids ($pK_{a_1} = pK_{b_1} = 9.4$, $pK_{a_2} = pK_{b_2} = 5.4$); (3) three mutually interacting acids ($pK_1 = 9.9$, $pK_2 = 7.4$, $pK_3 = 4.9$); (4) four mutually interacting acids ($pK_1 = 9.9$, $pK_2 = 8.6$, $pK_3 = 6.2$, $pK_4 = 4.9$). The slope at half-titration in each case approaches the theoretical maximum for that order of interaction. All pK's were chosen to place the observed pK_a at pH 7.4.

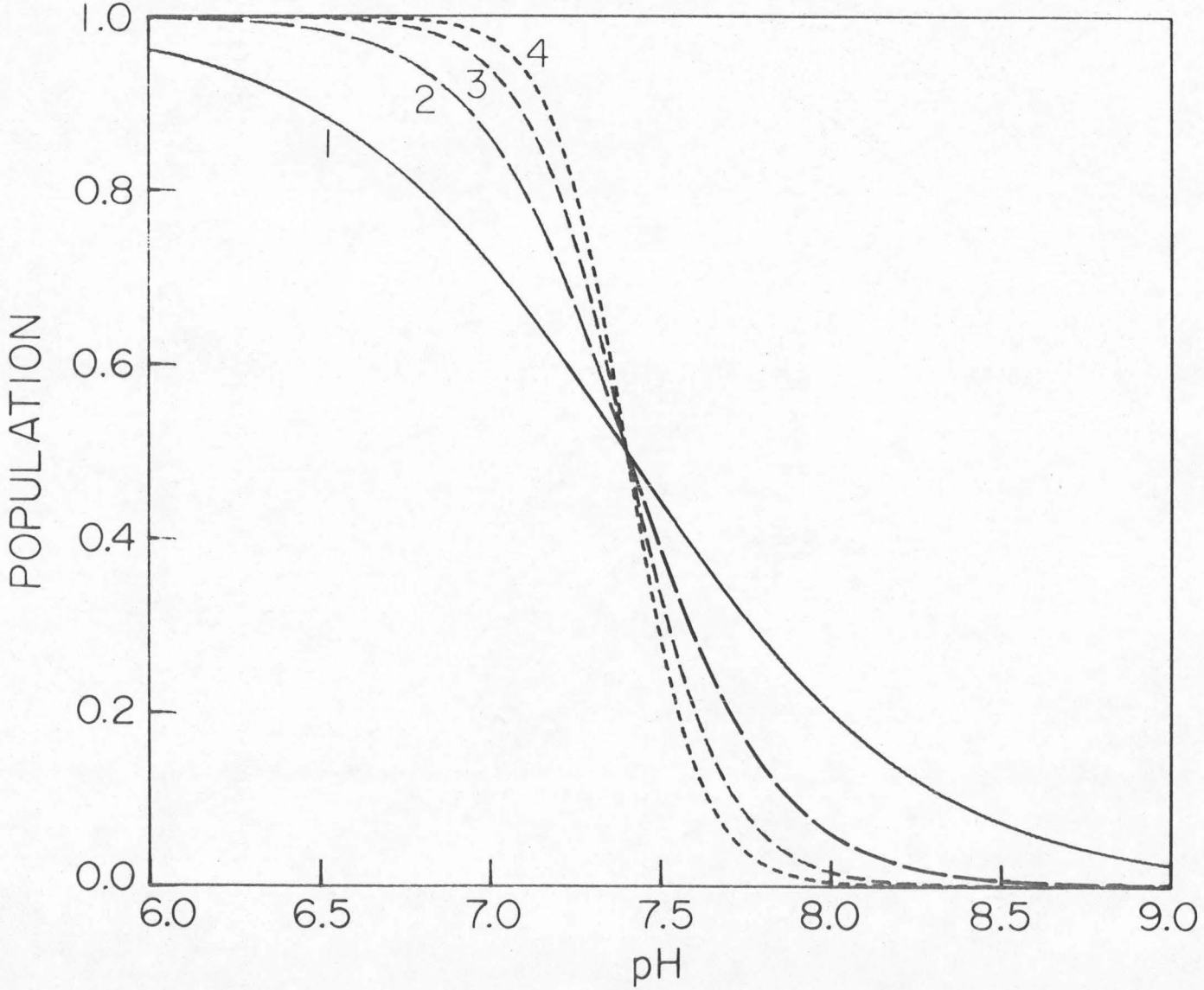
1.0
0.8
0.6
0.4
0.2
0.0
POPULATION
1
2
3
4
6.0
6.5
7.0
7.5
8.0
8.5
9.0
pH

Figure 9. Calculated ionization curves superimposed on experimental titration data for Hb^{TFA}-deO_2, –+–, ($pK_1 = 8.3$, $pK_2 = 7.7$, $pK_3 = 7.1$, $pK_4 = 6.5$); and for Hb^{TFA}-deO_2 + DPG, –□–, ($pK_1 = 9.4$, $pK_2 = 8.6$, $pK_3 = 6.2$, $pK_4 = 5.5$). Solid line is a single acid titration.

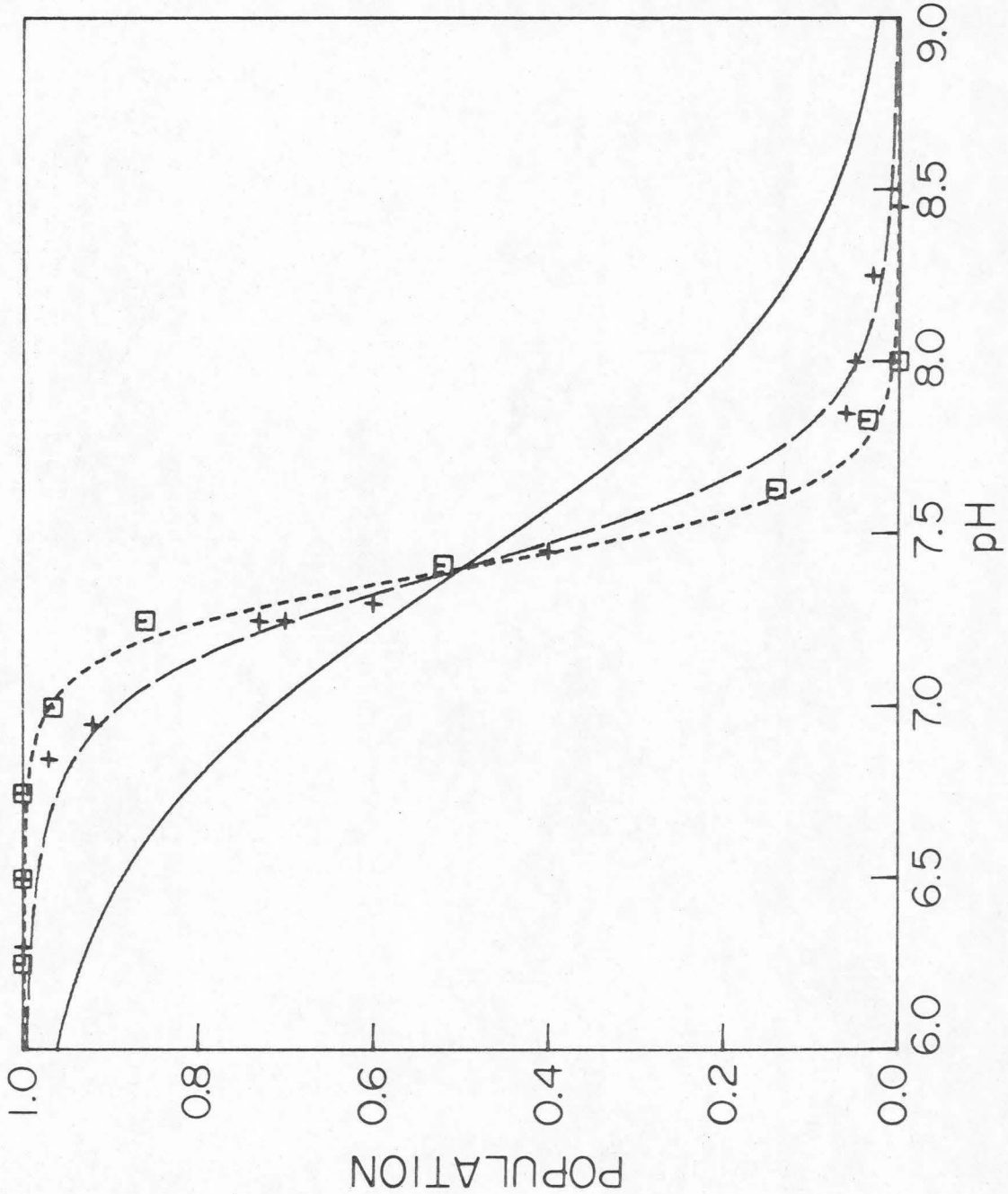
POPULATION
1.0
0.8
0.6
0.4
0.2
0.0
6.0
6.5
7.0
7.5
8.0
8.5
9.0
pH

Figure 10. Chemical shift of trifluoroacetonylated hemoglobin as a function of pH: (●), Hb^{TFA}-O_2; (o), Hb^{TFA}; (∇), Hb^{TFA}-III.

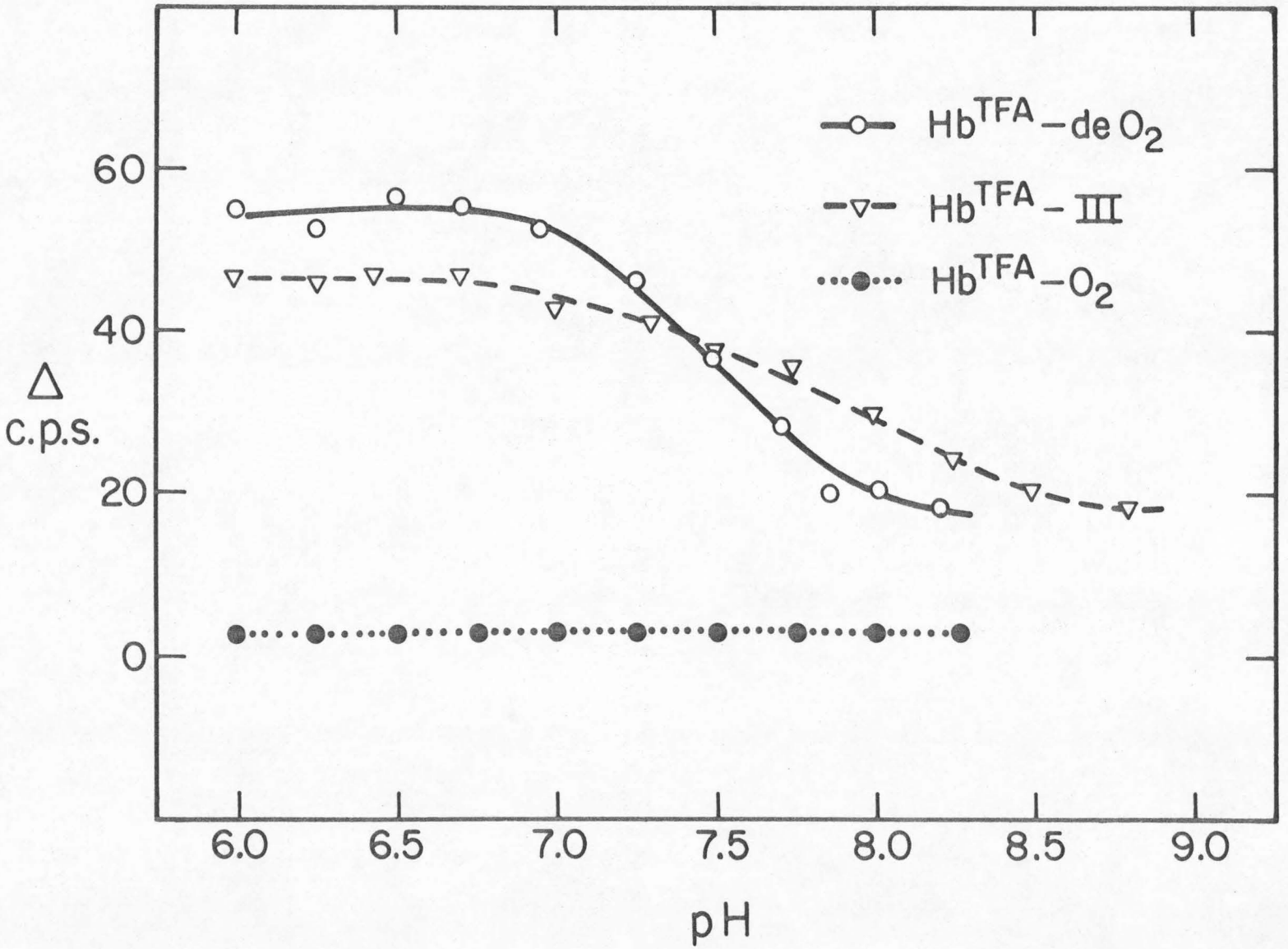
Hb^TFA – de O2
Hb^TFA – III
Hb^TFA – O2
60
40
20
0
Δ
c.p.s.
6.0
6.5
7.0
7.5
8.0
8.5
9.0
pH

Figure 11. Chemical shift of trifluoroacetonylated methemoglobin as a function of pH for Hb^{TFA}-III, Hb^{TFA}-III des His β146, -●-; Hb^{TFA}-III des [His β146-Tyr β145], -o-.

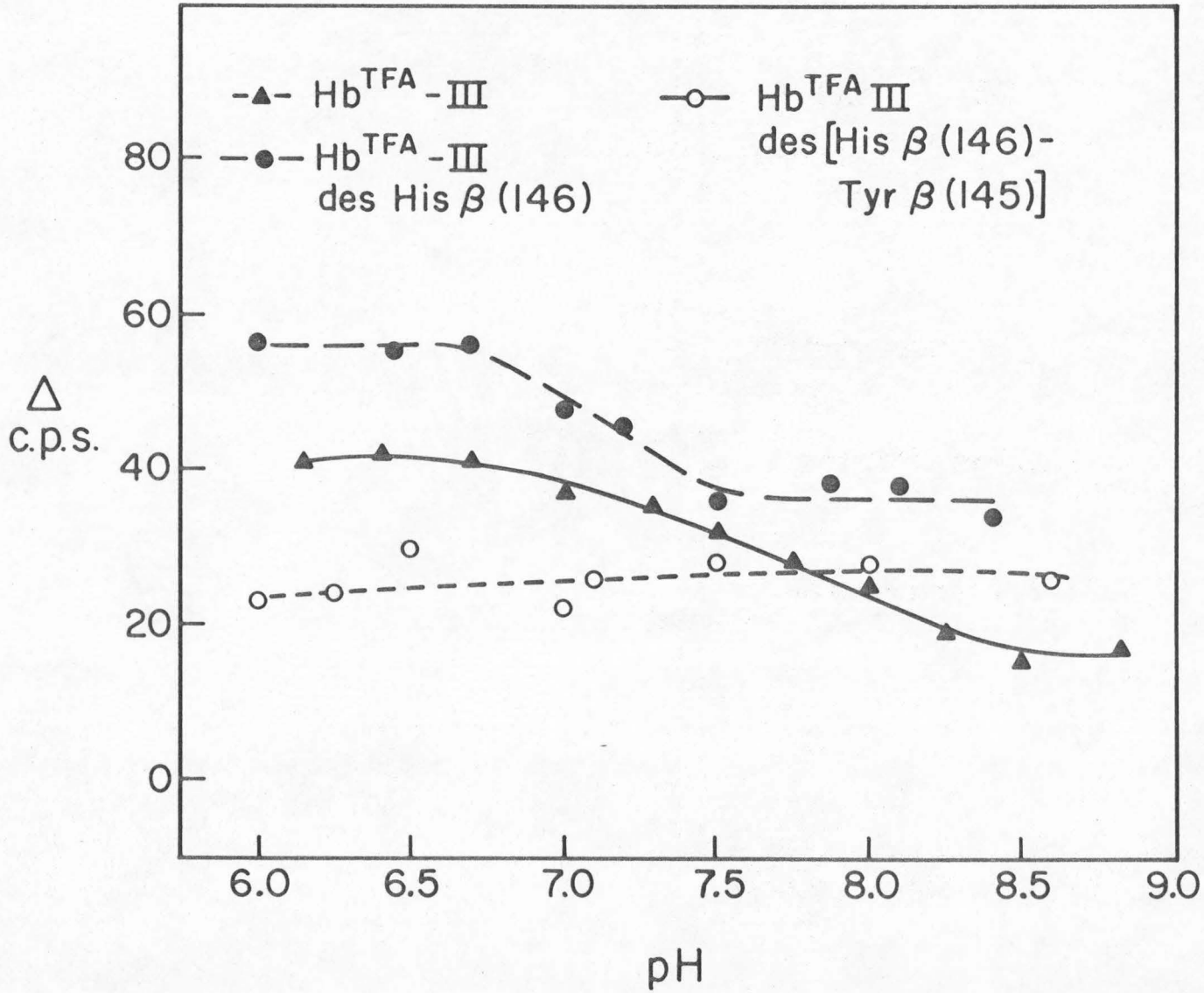
-▲- Hb^TFA -III
-●- Hb^TFA -III des His β (146)
-○- Hb^TFA III des [His β (146)-Tyr β (145)]
80
60
40
20
0
Δ c.p.s.
6.0
6.5
7.0
7.5
8.0
8.5
9.0
pH

Figure 12. Schematic representation (after Perutz, 1970) of proposed conformational equilibria of the β chain C-terminus in deoxy-, oxy-, and methemoglobin.

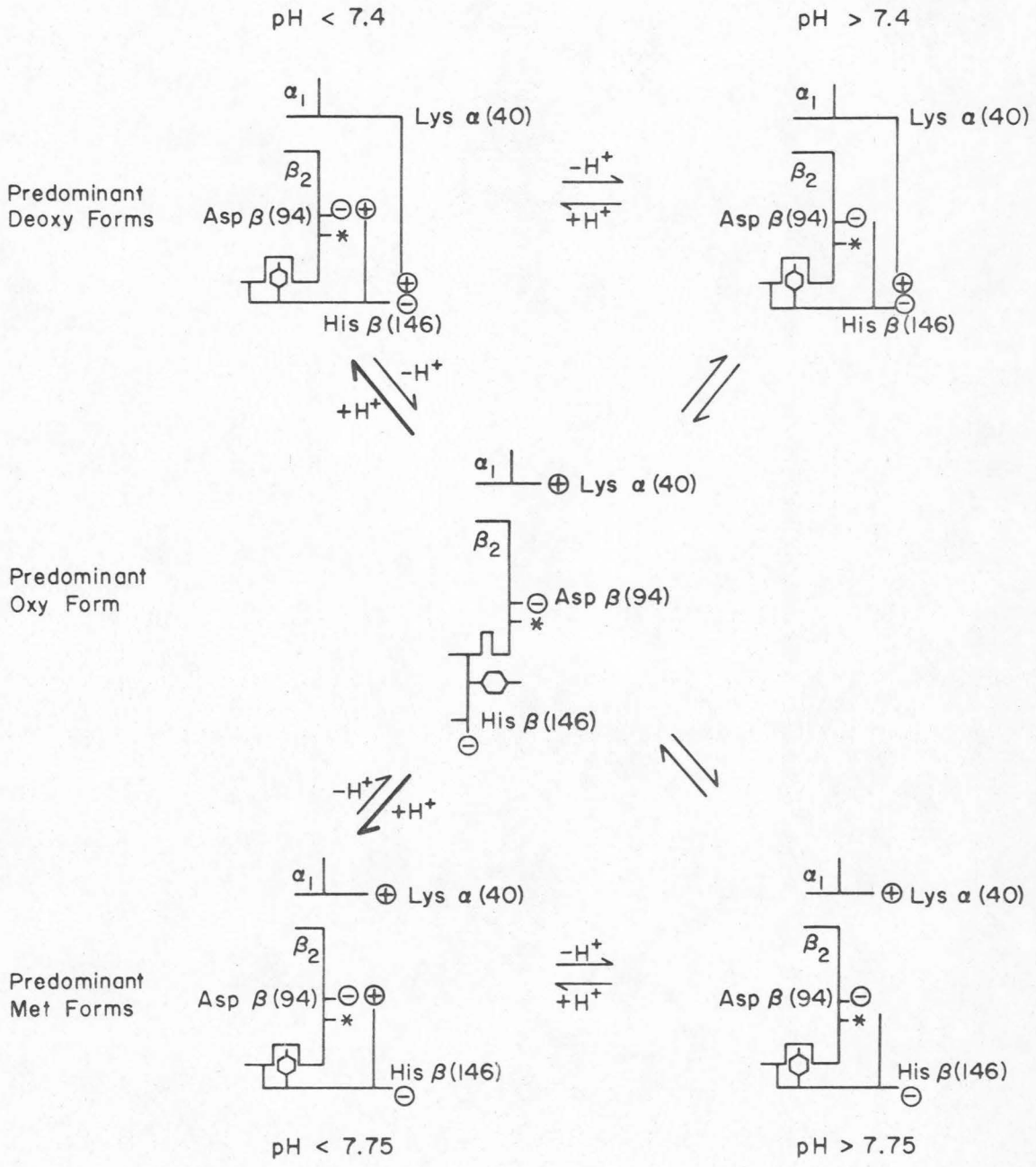
pH < 7.4
pH > 7.4
Predominant Deoxy Forms
α_1
Lys α (40)
β_2
Asp β (94)
His β (146)
$-H^+$
$+H^+$
Predominant Oxy Form
Predominant Met Forms
pH < 7.75
pH > 7.75

CHAPTER III

The Carbon Monoxide Binding Process

The central objective of hemoglobin research is to explain the kinetics of ligand binding in molecular terms. The problem has been approached in two principal ways: 1) kinetic models have been devised which fit kinetic constants to ligand binding data, specifying stages in the reaction sequence when structural changes must occur to produce the required rate enhancements; and 2) structural models propose plausible molecular changes which are likely at certain stages of ligand binding, and which could produce rate enhancements. The chief contributions to the latter approach have come from Perutz and his co-workers, whose delineation of the molecular structures of deoxy- and methemoglobin has permitted informative analyses of the kinds of forces involved in stabilization of the two structures. All models henceforth produced for the allosteric process will be shaped by the knowledge of these endpoints and the energetically plausible paths between them. The intermediate stages of the ligand binding are less accessible to the precise analysis afforded by crystallography, but information on their characteristics can be obtained from spectroscopic studies in solution. The nmr studies of Ogawa and Schulman (1971) on "artificial" intermediates and the work of Ogata and McConnell (1972) on binding of allosteric effectors has yielded valuable information on some of the changes in the molecule during

processes that approximate normal ligand binding.

The structural information yielded by crystallography and magnetic resonance studies is beginning to bring some coherence into analysis of hemoglobin kinetics. It is possible to describe ligand binding very exactly, and to achieve very impressive fits to the most precise data available, in terms of several structural models. The earliest attempts in this direction were made in the mid 1950's by Roughton and Gibson, who obtained kinetic data which was in excellent agreement with the Adair model (Adair, 1925; Gibson, 1959). Later models, which imposed certain restrictions on the kind and sequence of structural changes involved in the allosteric transition (Monod, et al., 1965; Koshland et al., 1966), also were fully consistent with the available data. Refinements of these models in light of structural findings have resulted in some convergence; current proponents of the concerted (Monod) model (Hopfield et al., 1971; Ogata and McConnell, 1972) include in their analyses some aspects which resemble the sequential models (Koshland-Adair). Perutz's structural proposal (1970) for the mechanism of the ligand binding process included features of both ideas.

The basic premise of all of the models is that hemoglobin exhibits high and low ligand affinity forms. The differences arise over the number of structures of each kind which exist, the role (if any) played by the ligand itself in the transition, and the relative energetic importance of the structure in various regions of the molecule to the stability of the various forms.

The experiments described in this Chapter yield information on some of these questions, using the nuclear magnetic resonance spectrum of Hb^{TFA}* to monitor the equilibrium populations of the species present in intermediate stages of ligation.

In Hb^{TFA}, the ^{19}F-nmr probe situated at Cys β93 undergoes observable environmental changes when hemoglobin binds ligands or undergoes structural changes induced by allosteric effectors. These changes primarily reflect the state of the β chain. Comparison of changes in the Cys β93-His β146 region to the overall ligand binding process (observed concurrently from changes in the visible spectrum) permits us to present a model for the sequence of events in ligand binding. The effects of pH and diphosphoglycerate (DPG) were examined, and the model is consistent with the known effects of these factors.

---

*Abbreviations used are: Hb, hemoglobin; Hb^{TFA}, hemoglobin trifluoroacetonylated at Cys β93; nmr, nuclear magnetic resonance; BIC, n-butylisocyanide; CO, carbon monoxide; DPG, diphosphoglyceric acid; bis-tris, 2, 2-bis(hydroxymethyl)-2, 2′, 2″-nitrilotriethanol. Y, the fraction of liganded hemoglobin = $\frac{[Hb\text{-}O_2]}{[Hb]+[Hb\text{-}O_2]}$. α, β, unliganded chains in low affinity conformations; α^*, β^*, unliganded chains in high affinity conformations; α^L, β^L, liganded chains. Y_β, the fraction of liganded β chains = $\frac{[\beta^L]}{[\beta^L]+[\beta]+[\beta^*]}$. DPG, diposphoglyceric acid.

The nmr data obtained do not yield specific structural information on the mechanism of the allosteric binding process, but they do show the order in which the chains bind and demonstrate the existence of a distinct, identifiable species which is intermediate in ligation and structure between the low affinity deoxy form and the fully oxygenated form.

Experimental

Hemoglobin

Human hemoglobin was prepared from freshly drawn citrated blood. The packed erythrocytes were washed three times with 0.9% sodium chloride solution, and lysed with distilled water or distilled water and toluene. The stroma were removed by centrifugation and the supernatant was desalted by gel filtration on a P2 column (2.5 × 45 cm) equilibrated with a buffer containing 0.05 M bis-tris and 0.1 M NaCl at pH 7.0. Hemoglobin solutions were stored at 0° and used within four days of preparation. Hb^{TFA} was prepared as described in Chapter II.

Reagents

Diphosphoglyceric acid was obtained from Calbiochem as the pentacyclohexylammonium salt, and converted to the acid by being stirred with Dowex 50-X8. Para-hydroxymercuribenzoate was obtained from Sigma. Bromotrifluoroacetone was a product of Peninsular Chemresearch, Inc. N-Butyl isocyanide was a product of Aldrich Chemical Company.

Methods

Visible and nmr spectra were measured concurrently at various stages of carboxygenation using an nmr tube with a cuvette fused to the top. The dimensions of this combination cell are shown in Figure 1. The tubes were made to order by Wilmad Glass Co.

During an experiment, the small access hole was sealed by a wide band of rubber which permitted injection of gases into the tube by means of a syringe. Visible absorbances were determined with a Gilford Model 240 spectrophotometer. ^{19}F-Nmr spectra were recorded using a Varian XL-100 spectrometer with fluorine Fourier transform capability. The probe temperature was 27°. The air temperature in the Gilford sample compartment was 26-27°. pH Measurements were made using a Radiometer Copenhagen Model 26 pH meter. Magnitudes of nmr peaks were determined by gravimetric integration.

Carbon Monoxide Binding Experiments

Nmr solutions contained 175 mg of Hb^{TFA} in 5 ml of bis-tris/NaCl buffer (pH 6.75 or 7.40, 0.05 M bis-tris, 0.1 M NaCl). The large solution volume was necessary to prevent a vortex when the tube was spun, since a vortex plug could not be used. A five-fold excess of DPG was introduced as a concentrated solution of the appropriate pH. The hemoglobin solutions were deoxygenated by repeated washing with nitrogen in a tonometer. The solutions were transferred by syringe to the nmr tubes, which had been washed repeatedly with argon. Absorbance of the hemoglobin solutions was recorded at 540 nm before and after the nmr spectrum was recorded for each sample. Aliquots of carbon monoxide were injected into each tube and the tube was rotated manually to expose the solution to the gas mixture. When the absorbance had reached a constant value after each addition, the nmr spectrum was recorded. The binding

experiment at pH 6.75 with DPG was carried out using a 12% hemoglobin solution. Optical absorbances were measured at 650 nm in that instance. Due to the small gas volume in the nmr tube, CO partial pressures were difficult to calculate accurately. The ordinate values in Figure 3 were calculated from oxygenation curves, using the published values for relative oxygen and carbon monoxide affinities.

Binding of n-butyl isocyanide was studied by this method in order to compare the results reported by Gibson and co-workers (Lindstrom et al., 1971) for this ligand to the carbon monoxide binding process. The experimental procedure used was the same one used for carbon monoxide, the butyl isocyanide being introduced by means of a micro syringe.

Preparation of $\alpha_2^{III}CN_{\beta_2}$

The ligand state hybrid $\alpha_2^{III}CN_{\beta_2}$ was prepared as described by Ogawa and Schulman (1971), using isolated α and β chains prepared by the technique of Kilmartin and Wootton (1971). The ligand state hybrid was trifluoroacetonylated by the same procedure used for hemoglobin A. Partial deoxygenation was achieved by washing the solution with nitrogen in a tonometer for over two hours. The temperature was maintained below 10° except when nmr spectra were being recorded, to retard "heme exchange".

Results

The ^{19}F-nmr spectrum of Hb^{TFA} changed with increasing percent carbon monoxide binding (Y) as is shown in Figure 2. In addition to the absorbances characteristic of deoxy- (D) and carboxy-hemoglobin (L), a third species (I) was present in the intermediate ligation range. The chemical shift of the intermediate species was 15 cps upfield of the Hb^{TFA}-CO resonance, and was independent of DPG concentration and of pH in the range 6.75-7.40. The relative magnitude of the peak varied from 5-15% of the total nmr integral, as a function of pH and DPG concentration.

Nmr Studies of the Artificial Intermediate of $\alpha_2^{III}CN_{\beta_2}$

Analysis of the ligand binding data in molecular terms was dependent on positive identification of the subunits influencing the nmr probe. For this purpose, the "artificial intermediate" $\alpha_2^{III}CN_{\beta_2}O_2$ was prepared by published methods (Kilmartin and Wootton, 1971) and trifluoroacetonylated by the usual procedure. The ^{19}F-nmr spectrum of $(\alpha_2^{III}CN_{\beta_2}O_2)^{TFA}$ was identical to that Hb^{TFA}-O_2. Deoxygenation of the intermediate proved to be very difficult; several hours of repeated efforts served only to reduce the Hb^{TFA}-O_2 peak by half. The deoxygenated species which was produced had a chemical shift 30 cps upfield of the oxy peak, which was about 20 cps downfield of the normal position of Hb^{TFA}-deO_2 at the pH used. Addition of a two-fold excess of DPG to the solution

caused the deoxygenated peak to shift upfield by 20 cps, to the normal Hb^{TFA}-deO_2 position. The absence of any signal at the chemical shift position characteristic of Hb^{TFA}-III CN indicated that no observable equilibration of heme ligands had occurred. Thus the species observed at +30 and +50 cps from the oxy peak position was $\alpha_2^{III}CN_{\beta_2}deO_2$, showing that the chemical shift of the fluorine probe is a function of the ligand state and conformation of the β chains.

Comparison of Y with Y_β

The relative magnitudes of the nmr peaks reflect the fractional ligation of the β chains (Y_β). By measuring the visible absorbance change of the nmr sample for each ligand pressure, the total fraction of liganded subunits (Y) corresponding to Y_β was obtained. After the visible absorbance had begun to indicate ligand binding, a lag ensued before liganded species appeared in the nmr spectrum (Figure 3). The fully liganded peak (L) and the intermediate (I) reached detectable concentrations at about Y = .20. Their combined magnitude increased more rapidly than Y for $.20 < Y < .60$. Above Y = .60, the fraction of liganded nmr species was approximately equal to Y. The ligand binding curves (Y vs. log P_{CO}) observed by visible and nmr spectra are shown in Figure 3 for the four sets of conditions studied. There are minor differences in these curves which will be discussed later, but in general they follow the pattern described above.

In Figure 4, the fractional populations of the three nmr species are plotted as functions of Y. The lags in appearance of peaks L and

I and in disappearance of peak D are again demonstrated.

Binding of n-Butyl Isocyanide to Hb^{TFA}

The ligand binding experiments described for carbon monoxide were repeated using the heme ligand n-butyl isocyanide. For the experiment in which DPG was present, the results (Figure 5) were qualitatively similar to those obtained for carbon monoxide binding. An increase in Y of about 0.15 preceded the first appearance of liganded species in the nmr spectrum. In the absence of DPG, no lag was observed. The liganded nmr peak appeared at $Y < 0.05$, and increased linearly with Y throughout its range.

Discussion

The classical models for ligand binding to hemoglobin treated the α and β chains as equivalent binding sites. More recently, kinetic (MacQuarrie and Gibson, 1971) and structural (Perutz, 1970; Davis et al., 1971) evidence has been reported which indicates that the chains are nonequivalent and bind ligands in a preferential order. If the sequence of events involved could be established, the task of assigning cause and effect in structure changes would be expedited.

The nmr studies of the binding process described in this chapter yield evidence for a preferential order of ligand binding. As ligand binding progresses, structural changes in the β chains give rise to three species which produce observable absorptions in the nmr spectrum. The chemical shifts and relative magnitudes of the three nmr peaks permit calculation of the average degree of ligation of each species, and general description of the β chain conformation in each. Differences between the ligation process as observed in the nmr and visible spectra yield indirect evidence on ligation and structural changes of the α chains.

The First Stages of Ligand Binding ($Y < 0.15$)

Partially liganded hemoglobin solutions exhibited nmr absorptions in positions corresponding to deoxyhemoglobin and fully liganded hemoglobin, in addition to an intermediate signal (Figure 2). The liganded (L) and intermediate (I) signals appeared after the visible

absorption change had indicated that about 15% of the chains had bound a ligand (Figure 3). Experiments with the artificial intermediate $\alpha_2^{III}CN\beta_2$, in which the α chains are locked in a liganded state but the β chains can be deoxygenated, showed that chemical shift changes in Hb^{TFA} reflect the ligation and conformation of the β chains. Therefore the absence of changes in the nmr spectrum during early stages of ligand binding indicates that the first ligand binds to an α chain.

This result conflicts with the interpretation of ligand binding experiments reported by Gibson and co-workers (Olson and Gibson, 1971). In stopped flow experiments on the binding of n-butyl isocyanide (BIC) to hemoglobin, these investigators observed an isosbestic point in the Soret region absorption spectrum for $Y < 0.20$. The isosbestic point indicated that a single species, presumably one type of chain, was binding ligand in this ligation range. In experiments conducted in the absence of DPG, no isosbestic point was observed. These results indicated that in the presence of DPG, one type of chain in deoxyhemoglobin exhibited significantly higher ligand affinity than the other type. In the absence of DPG, the α and β chains became equivalent and both bound initial ligands. By analogy with the relative ligand affinities of the isolated chains and by nmr studies of some heme protons, the high affinity chains in DPG-bound hemoglobin were assigned as the β chains (Lindstrom et al., 1971).

To compare these results with our findings on carbon monoxide binding, we studied the nmr and visible spectra of the BIC binding process under the same conditions. In agreement with the prior findings, BIC binding was found to proceed randomly in the absence of DPG (Figure 5). However, in the presence of DPG, BIC binding was very similar to that of CO, with a substantial lag in Y_β relative to Y for $Y < 0.15$. From this result, it appears that the higher affinity chains producing the isosbestic point in Gibson's experiments were α chains. Such a result would be expected from the known stabilizing effect which DPG has on the deoxy form of the β chains. That in turn would decrease the affinity of the α chains indirectly, but it is reasonable to suppose that the β chains would be affected to a greater degree. The comparative experiments on binding of BIC agreed with the conclusion that under most conditions the first ligand binds to an α chain.

Identification of the Intermediate Species

The average number of ligands bound to each of the observable nmr species was determined from log-log plots, as follows. The ratio of magnitudes of any two peaks was plotted versus the carbon monoxide pressure. The average number of ligand molecules by which the two species differ is equal to the slope of the line obtained. For example, if

$$L \underset{}{\overset{K}{\rightleftharpoons}} D + 4\,CO$$

$$K = \frac{[L]}{[D][CO]^4}$$

$$K[CO]^4 = \frac{[L]}{[D]}$$

$$\log \frac{[L]}{[D]} = 4 \log [CO] + \log K.$$

As is shown in Figures 6 and 7, plots of log L/D versus log P_{CO} had slopes of approximately 4 (4.0 and 3.9 by least-squares fits) for pH 7.4 and 6.75, respectively. This indicated that under these conditions peak L represented fully liganded tetramers and peak D was due primarily to deoxy tetramers. (Note that these plots are for $Y > 0.25$, where the magnitude of the lag between Y and Y_β declines.)

A similar log-log plot of I/D yielded a slope of about 3 (2.96 and 2.7 by least-squares fits). As expected, the slopes of L/I versus P_{CO} at the two pH values were 1.0 and 1.3. Therefore the species responsible for peak I contained three liganded subunits. This conclusion was consistent with the relative decrease in magnitude of I relative to D and L when DPG was present. If I were due to a species containing two unliganded β chains, DPG would stabilize it rather than the reverse (Ogata and McConnell, 1972). Hence I must contain three liganded chains and one unliganded β chain.

The chemical shift of I indicated, however, that the unliganded β chain did not exhibit a normal deoxy conformation. In addition, the suppression of the population of I with decreased pH and increased DPG concentration (both of which decrease ligand affinity) suggested that I was likely to be a high affinity form. The chemical shift is consistent with this interpretation. When the pH of a solution containing Hb^{TFA}-deO_2 is raised from 6.75 to 8, the chemical shift position of the D resonance moves from +60 cps away from the L resonance to +30 cps away (see Chapter II). The functional consequence of this pH increase is a four-fold increase in ligand affinity, so the chemical shift position of D at pH 8 is characteristic of a high affinity form. (A similar chemical shift is observed for $\alpha_2^{IIICN}\beta_2$, which has extremely high ligand affinity.) The chemical shift of resonance I is exactly midway between peak L and peak D at pH 8. Hence I is likely to arise from a species in which an unliganded, high affinity β chain is exchanging rapidly with a liganded β chain.

A Model for Carbon Monoxide Binding to DPG-Complexed Hemoglobin

The data presented above are consistent with the ligand binding sequence outlined in Figure 8. (Figure 8 shows the principal species present at each step of the process. However, it should be emphasized that each unliganded species shown is involved in equilibria between high and low affinity forms of each of its subunits. The positions of these equilibria are influenced by pH, DPG concentration, and the ligation states of neighboring subunits.)

At $P_{CO} = O$, deoxyhemoglobin exists primarily with all chains in their low affinity forms. DPG binds to the β chains, stabilizing their low affinity conformation. That, in turn, stabilizes the low affinity form of the α chains, primarily through the numerous electrostatic and nonpolar contacts in the $\alpha_1\beta_2$ interfaces. As the partial pressure of ligand is raised, the first ligands are bound by the small equilibrium concentration of tetramers containing high affinity α chains (α*'s). The conformation of α^L has then changed so that the "salt bridge" links to α_2 and the electrostatic and nonpolar interactions with β_2 are destabilized. This destabilizes the low affinity conformations of α_2 and β_2. In the presence of DPG, however, β_2 is strongly stabilized in its low affinity form by links to β_1. Hence the equilibrium concentration of β^* remains low relative to that of α_2*. The next ligand binds to α_2, placing strains on the $\alpha_2^L\beta_1$ interface interactions and driving the conformational equilibrium of both β chains toward β^*. (Expulsion of DPG results.) Evidence of the shift in this equilibrium is found in the binding constants of DPG analogs, which are half as large for $\alpha_2^{IIICN}\beta_2$ as for $\alpha_2\beta_2$ (Ogata and McConnell, 1972). A ligand then binds to a β^* chain. The resulting three-liganded species is present in relatively large equilibrium concentration, with the β^* exchanging rapidly with β^L chains. Further increase in ligand pressure produces binding at the β^* chain.

This model accounts for the ligand binding data obtained at pH 6.75 and 7.40 for DPG-bound deoxyhemoglobin. The chief difference between these cases is that the concentration of I is smaller

at the lower pH. This is expected, since the stabilizing influence of DPG is enhanced by decreased pH. Thus a higher ligand pressure is required to generate I, but once formed most of it combines immediately with available ligand. Aside from the DPG effect, lower pH stabilizes the low affinity forms of all chains through the Bohr groups. This produces the decreased overall affinity at pH 6.75 which is demonstrated in Figure 3.

A Model for Carbon Monoxide Binding in the Absence of DPG

The model which describes ligand binding to DPG-complexed hemoglobin does not account for the data obtained when DPG was absent. The spectra obtained at pH 6.75 and 7.40 in the absence of DPG were superficially similar to the other experiments (Figure 3). Three peaks were observed, and the liganded and intermediate species did not appear until $Y > 0.15$. The relative magnitude of I was greater by as much as factor of two when DPG was absent. The major differences introduced by removal of DPG became evident only in the log-log plots of population ratios versus ligand pressure. As is shown in Figure 9, at pH 7.40 the slope of the L/D line was again near four (4.1). However, the slope of I/D was 1.9, and the slope of L/I was 2.2. This result indicated that I contained only two ligands.

The model outlined in Figure 8 must be modified to account for this result. The first ligand still must bind to an α^*. However, in the absence of DPG the affinity of the β chains apparently is very

similar to that of the remaining α chain. The remaining three ligands may bind randomly or in any of the alternative sequences. The only requirement imposed by the data is that the last two ligands must bind almost simultaneously. If that were not the case, then either the three-liganded species would be detectable under the L peak (if it were $\alpha^{L}\alpha^{*}\beta_{2}^{L}$) producing an L/D slope lower than 4, or the slope of L/I would increase toward 3 at high ligand pressures (if the species were $\alpha_{2}^{L}\beta^{L}\beta^{*}$). The several possible binding sequences cannot be distinguished from the available data, so the intermediate species under these conditions could be produced by exchange between $\alpha_{2}^{L}\beta_{2}^{*}$ and $\alpha_{2}^{L}\beta_{2}^{L}$ or between $\alpha^{L}\alpha^{*}\beta^{L}\beta^{*}$ and $\alpha^{L}\alpha^{*}\beta^{L}\beta^{*}$, or among all of them.

At pH 6.75 in the absence of DPG, the data are consistent with a similar model. The slope of L/D versus ligand pressure was near 4 for $Y < 0.80$, falling off toward 3 at higher Y values. The slope of I/D was 2.2, beginning at about 2.6 for $Y < 0.50$ and decreasing to 2. The slope of L/I was between one and two, decreasing with increasing Y. Under these conditions, the data indicate that the first ligand again associates with an α chain. A slight increase in the relative concentration of singly liganded tetramers is apparent at high Y. The intermediate appears to contain two ligands except at large Y, where the slope of L/I approaches 1. Thus the final ligand apparently binds to β^{*}. The binding order of the other α and β chains is not evident from the data. The differences between these results and the results at pH 7.4 are readily understood

if the Bohr groups lower the ligand affinity of β chains more than that of α chains (Perutz, 1970).

Conclusion

The data obtained from concurrent observation of nmr and visible spectra of hemoglobin have made it possible to specify the apparent order of carbon monoxide binding under some conditions (including a condition very similar to that of the normal erythrocyte, e.g., 0.1 M salt, pH 7.4, and a one to one molar ratio of DPG to hemoglobin). The apparent sensitivity of the binding order to the pH and DPG concentration of the solution shows that the affinities of the chains are quite similar (at least in human hemoglobin), as well as extremely interdependent.

The model which is consistent with these data is not in complete agreement with any of the currently contested kinetic models of allostery. It resembles the sequential model in the following important respects:

1) the binding of ligands to each chain increases the ligand affinity of neighboring chains;

2) there exists a high affinity deoxy form of the β chain whose conformation is different from that of the ligand chain.

On the other hand, as in the most recent versions of the concerted model:

1) low and high affinity forms exist in the absence of ligand;

2) the structural change which occurs simultaneously with the expulsion of DPG (the "quaternary" structural change) has a singular role in the cooperative process, since the conformational equilibrium

of more than one chain is thus driven toward a high affinity form.

References

Adair, G. S. (1925), J. Biol. Chem., 63, 529.

Davis, D. G., Lindstrom, T. R., Mock, N. H., Baldassare, J. J., Charache, S., Jones, R. T., and Ho, C. (1971), J. Mol. Biol., 60, 101.

Gibson, Q. H. (1959), Progr. Biophys. Chem., 9, 1.

Hopfield, J. J., Schulman, R. G., and Ogawa, S. (1971), J. Mol. Biol., 61, 425.

Kilmartin, J. V., and Wootton (1970), Nature, 228, 766.

Koshland, D. E., Nemethy, G., and Filmer, D. (1966), Biochemistry, 5, 365.

Lindstrom, T. R., Olson, J. S., Mock, N. H., Gibson, Q. H., and Ho, C. (1971), Biochem. Biophys. Res. Commun., 45, 22.

MacQuarrie, R. A., and Gibson, Q. H. (1971), J. Biol. Chem., 246, 517.

Monod, J., Wyman, J., and Changeux, J. P. (1965), J. Mol. Biol., 12, 88.

Ogata, R. T., and McConnell, H. M. (1972), Proc. Natl. Acad. Sci., 69, 335.

Olson, J. S., and Gibson, Q. H. (1971), J. Biol. Chem., 246, 5241.

Ogawa, S., and Schulman, R. G. (1971), Biochem. Biophys. Res. Commun., 42, 9.

Perutz, M. (1970), Nature, 228, 726.

Figure 1. Combination nmr tube/cuvette used for concurrent observation of nmr and visible spectra.

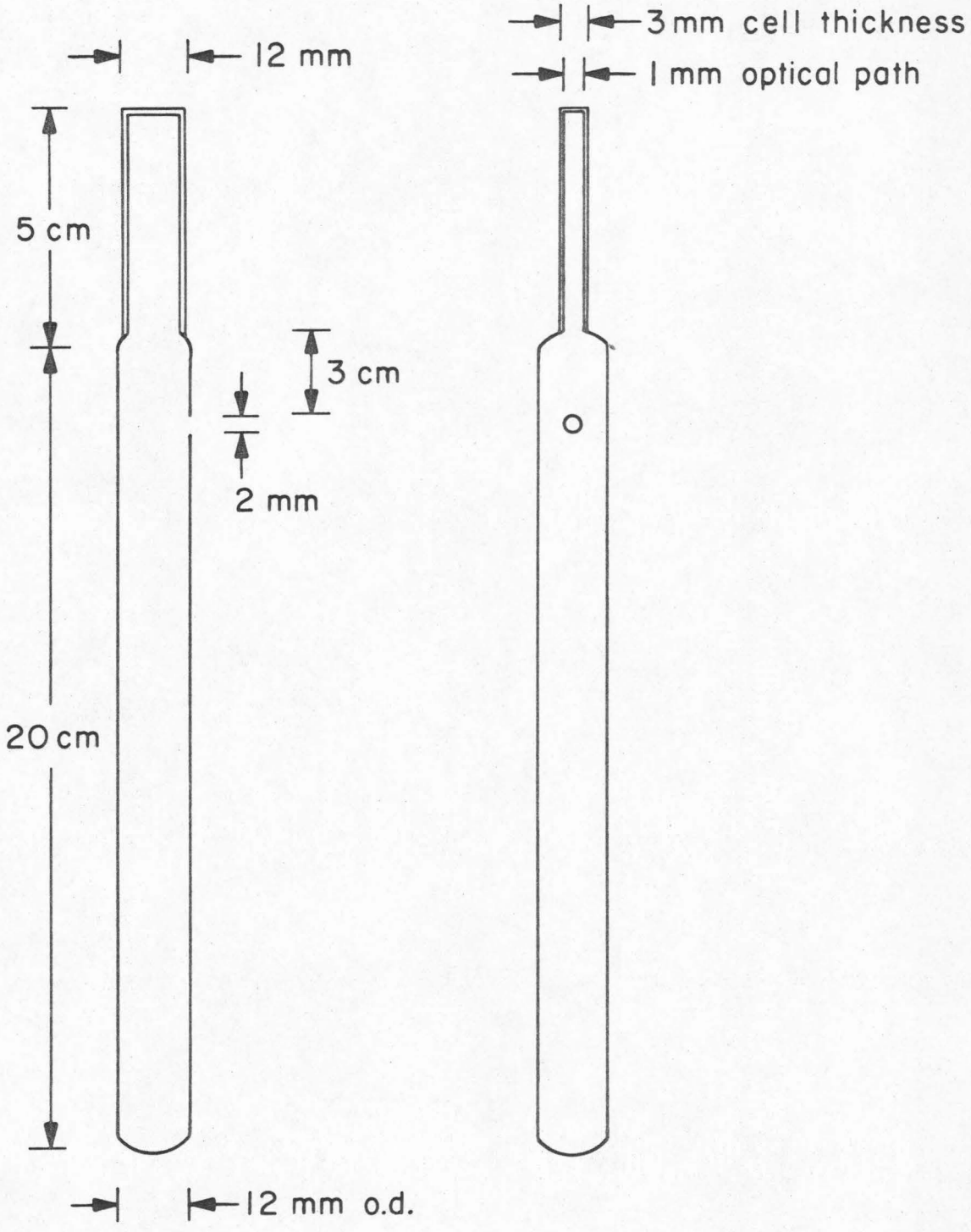
12 mm
3 mm cell thickness
1 mm optical path
5 cm
3 cm
2 mm
20 cm
12 mm o.d.

Figure 2. Nmr spectrum of Hb^{TFA} as a function of increasing fraction bound to carbon monoxide (Y). Peak D is the absorbance due to Hb^{TFA}-deO_2; L is due to Hb^{TFA}-CO; I is due to a partially liganded intermediate species. The arrow "H" marks the chemical shift position of the high affinity (β^*) unliganded form. Spectra were recorded at pH 7.40.

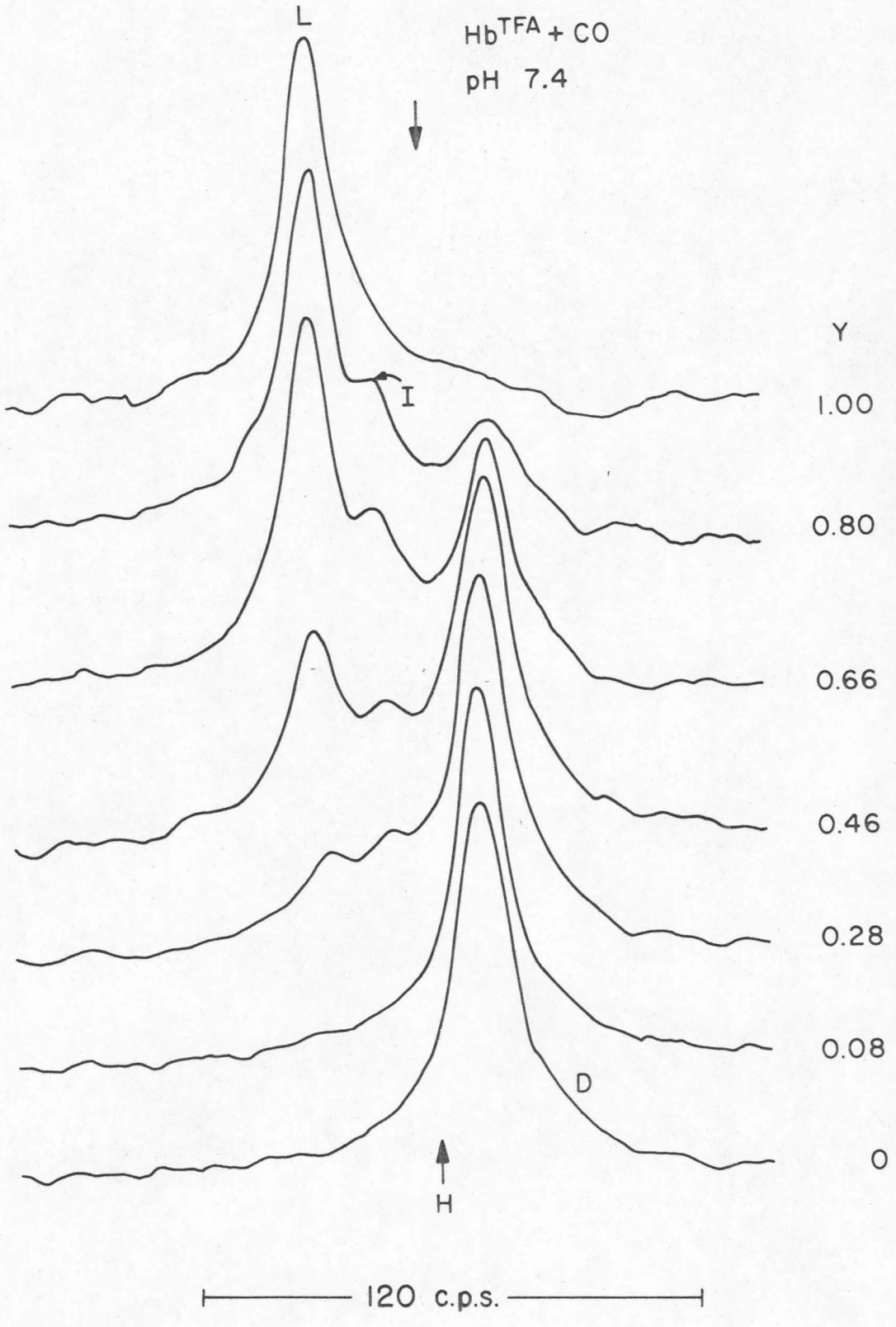
L
Hb^TFA + CO
pH 7.4
I
Y
1.00
0.80
0.66
0.46
0.28
0.08
0
D
H
120 c.p.s.

Figure 3. Carbon monoxide binding curves observed concurrently in visible and nmr spectra. -o-, Y; -●-, Y_{β}.

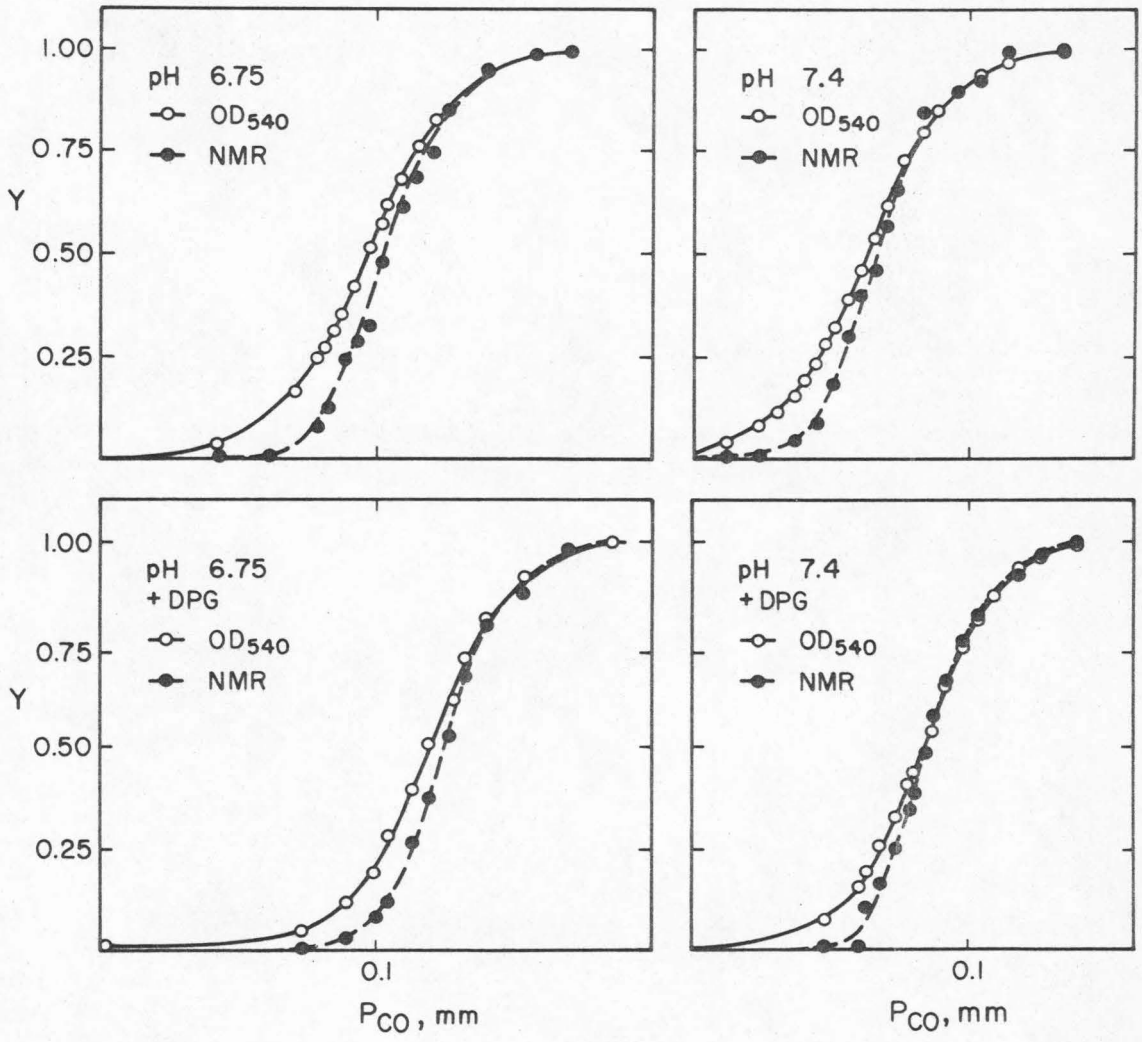
1.00
0.75
0.50
0.25
Y
pH 6.75
OD540
NMR
pH 7.4
OD540
NMR
pH 6.75
+ DPG
OD540
NMR
pH 7.4
+ DPG
OD540
NMR
0.1
PCO, mm
0.1
PCO, mm

Figure 4. Populations of the species observed in the nmr spectrum as functions of Y. ●, fraction of total integral in peak D; o, fraction in peak L; x, fraction in peak I.

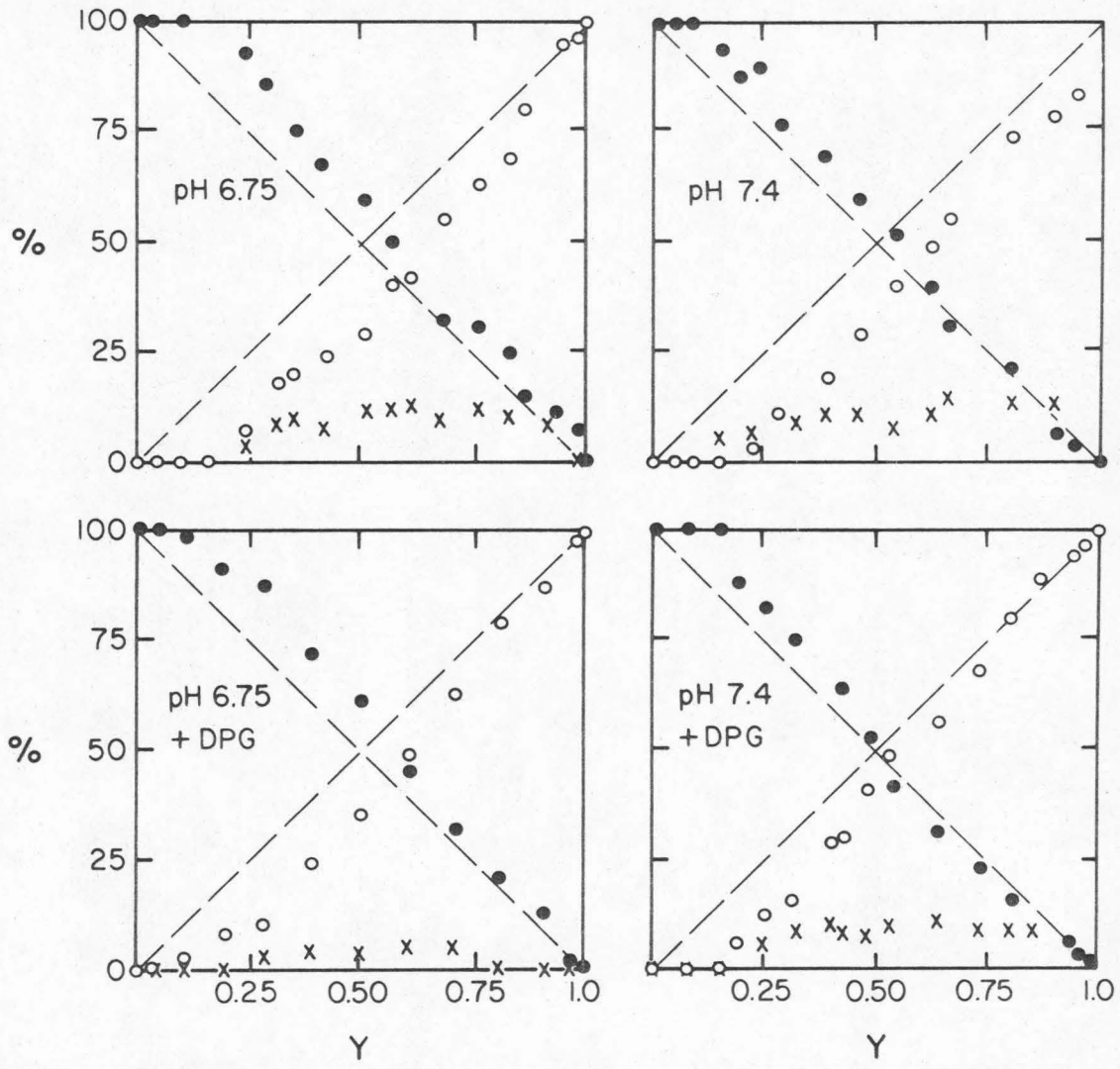
100
75
50
25
0
%
pH 6.75
pH 7.4
pH 6.75
+ DPG
pH 7.4
+ DPG
0.25
0.50
0.75
1.0
Y

Figure 5. n-Butyl isocyanide binding curves observed concurrently in visible and nmr spectra -o-, Y; -●-, Y_{β}.

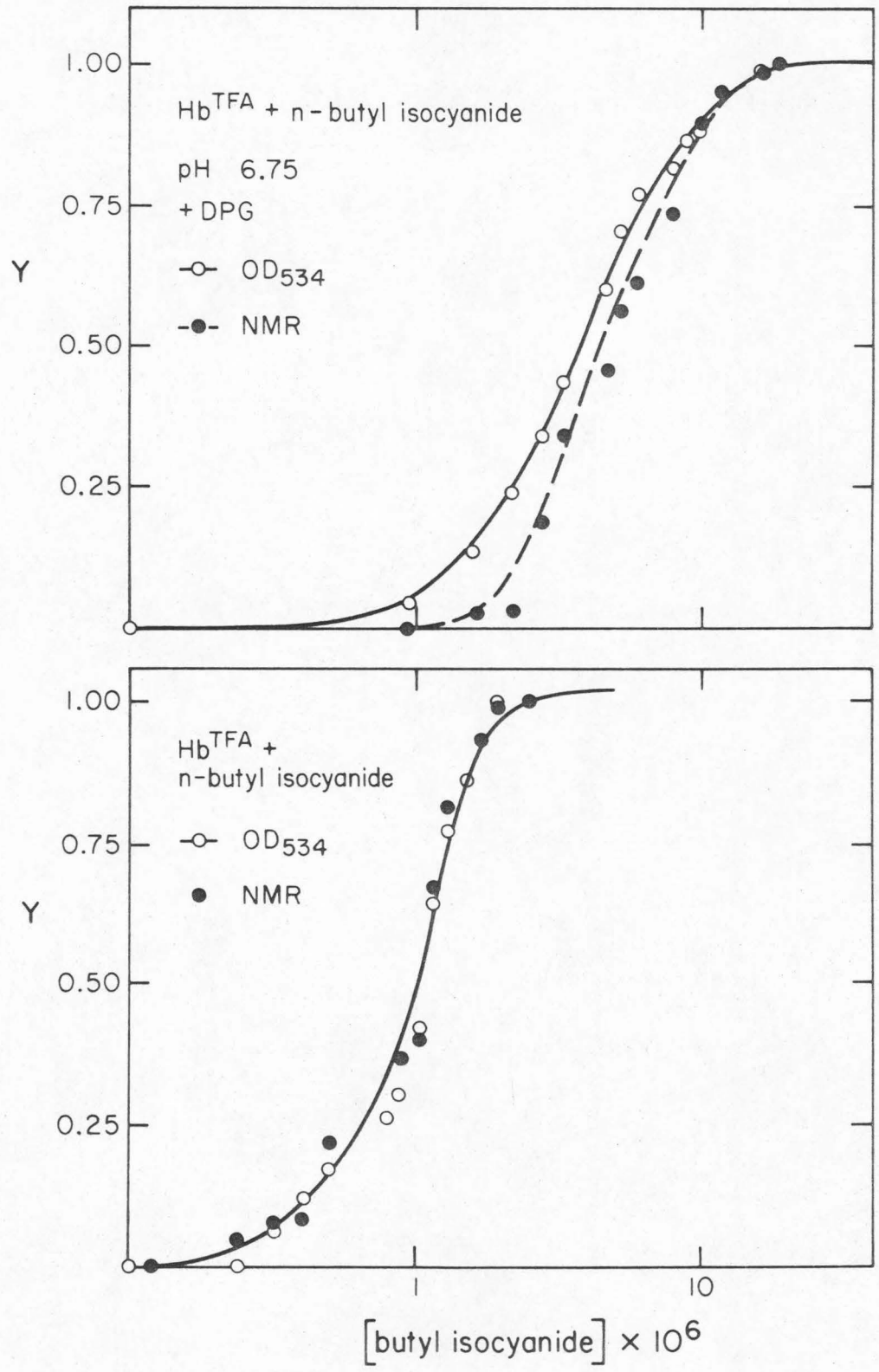
1.00
0.75
0.50
0.25
Y
Hb^TFA + n-butyl isocyanide
pH 6.75
+ DPG
OD534
NMR
1.00
0.75
0.50
0.25
Y
Hb^TFA +
n-butyl isocyanide
OD534
NMR
1
10
[butyl isocyanide] × 10^6

Figure 6. Dependence of the nmr populations on P_{CO} at pH 7.4, in the presence of DPG. ×, log L/D; o, log I/D; Δ, log L/I. The slopes, determined by least-squares fits, are 4.0, 3.0, and 1.0 ± 0.02, respectively.

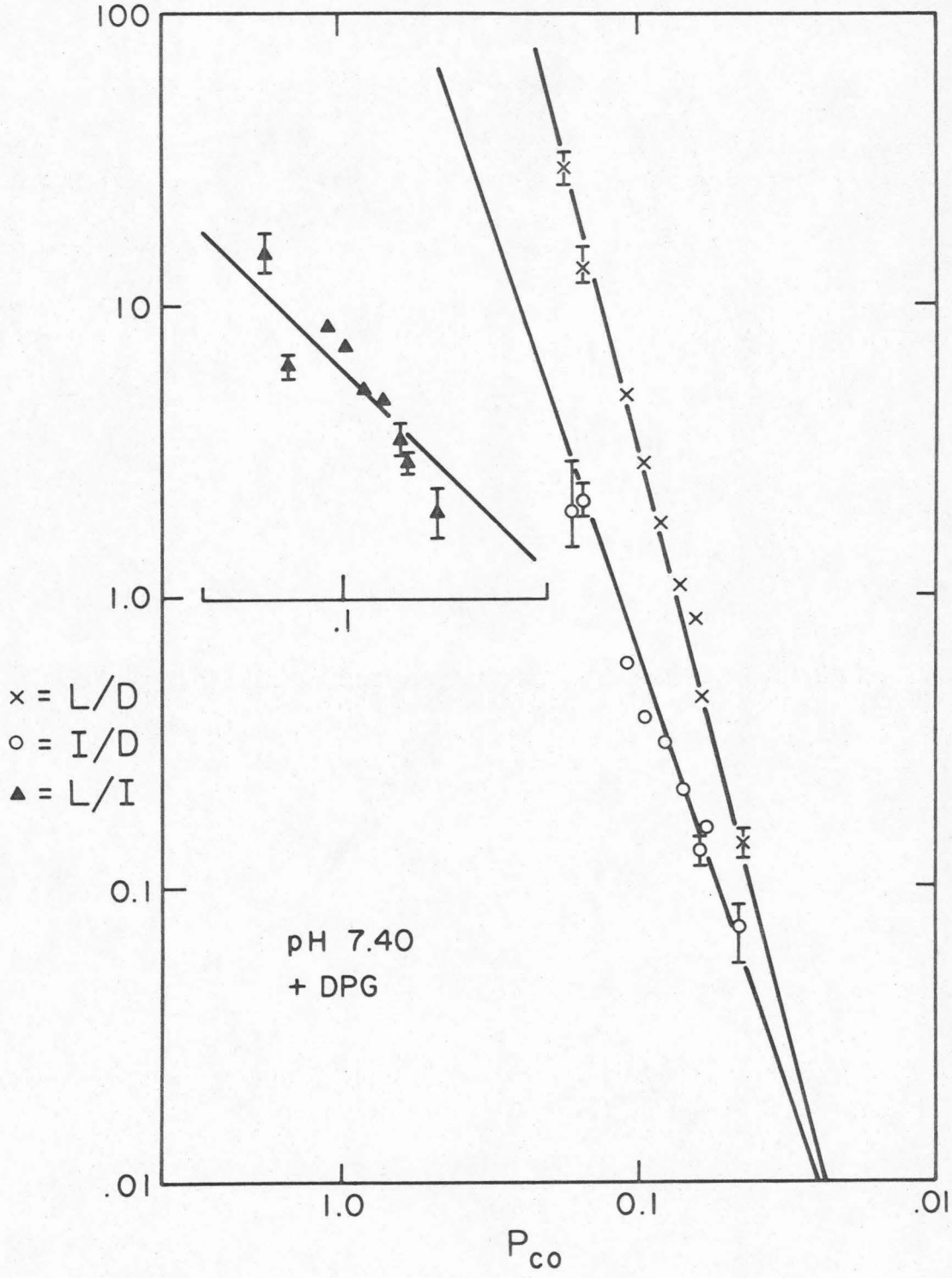
100
10
1.0
0.1
.01
1.0
0.1
.01
.1
× = L/D
○ = I/D
▲ = L/I
pH 7.40
+ DPG
P_{CO}

Figure 7. Dependence of the nmr populations on P_{CO} at pH 6.75 in the presence of DPG. ×, log L/D; o, log I/D; Δ, log L/I. The slopes of the lines, determined from least-squares fits, are 3.9, 2.7, and 1.8 ± 0.05, respectively.

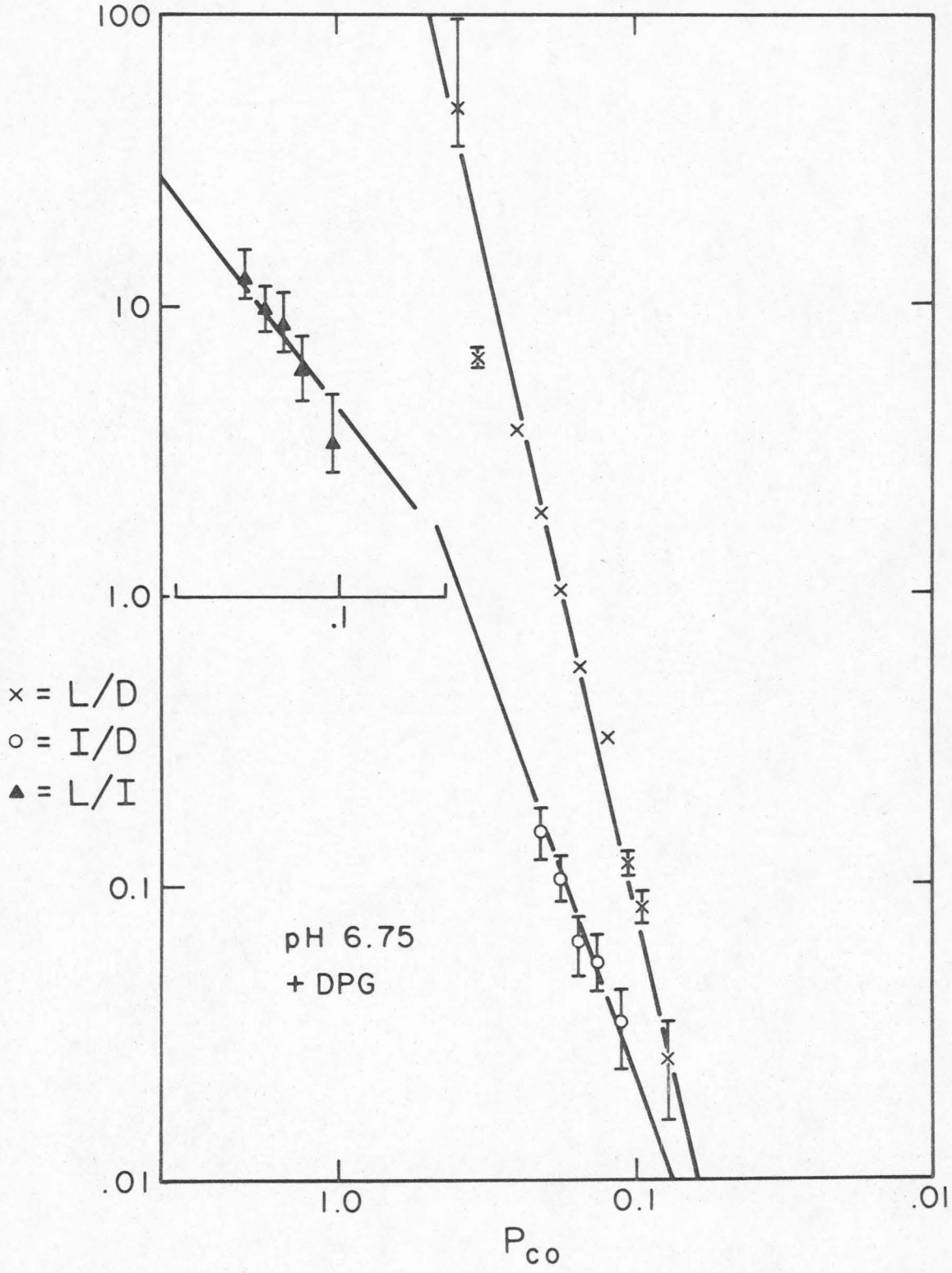
100
10
1.0
0.1
.01
.1
× = L/D
○ = I/D
▲ = L/I
pH 6.75
+ DPG
1.0
0.1
.01
P_{CO}

Figure 8. Proposed model for the binding of carbon monoxide (L) to hemoglobin in the presence of DPG. The species whose nmr absorptions were studied are marked as "D", "H", "I", and "L".

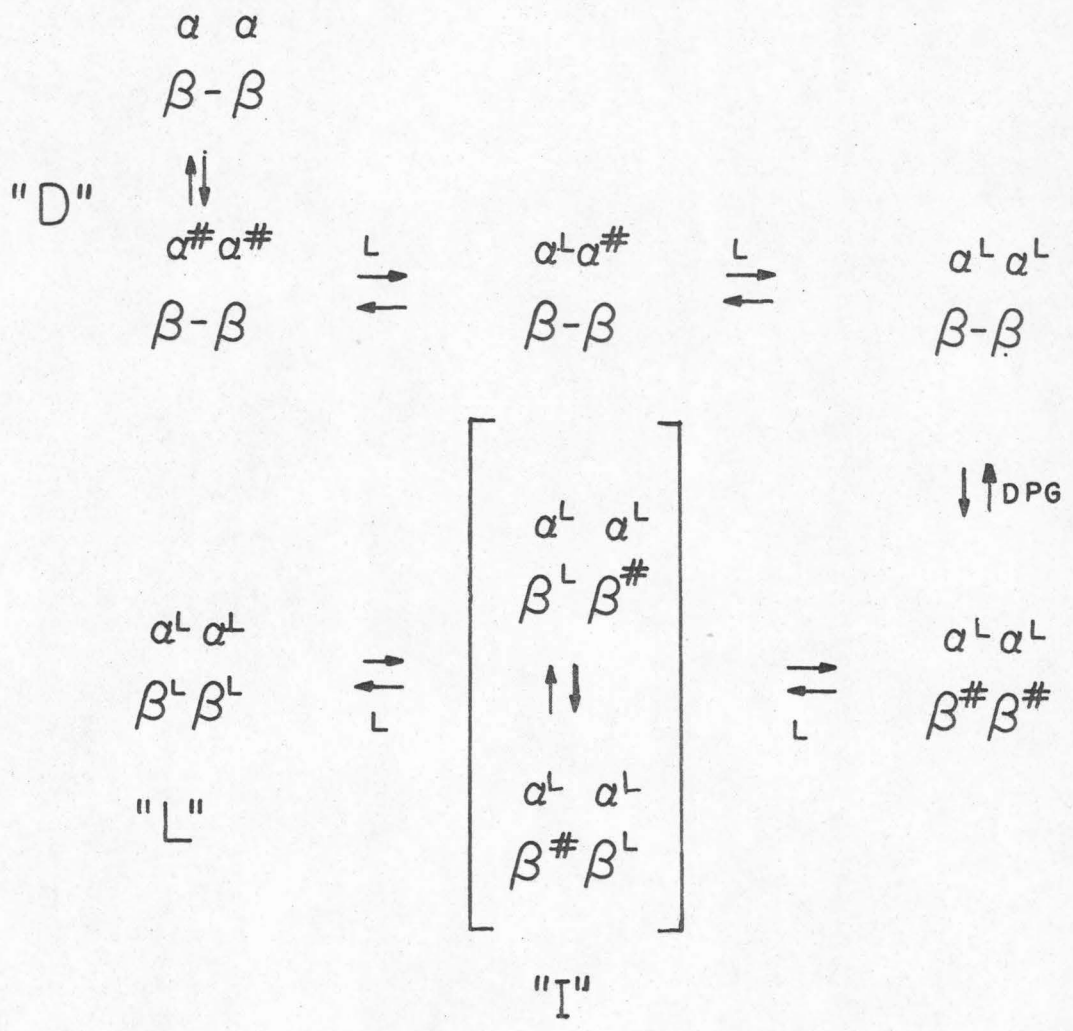
α α
β-β
"D"
α#α#
β-β
L
αLα#
β-β
L
αLαL
β-β
DPG
αL αL
βL βL
L
"L"
αL αL
βL β#
αL αL
β# βL
"I"
L
αL αL
β# β#

Figure 9. Dependence of the nmr populations on P_{CO} at pH 7.4, in the absence of DPG. ×, log L/D; o, log I/D; Δ, log L/I. The slopes of the lines, determined from least-squares fits, are 4.1, 1.9, and 2.2 ± 0.05, respectively.

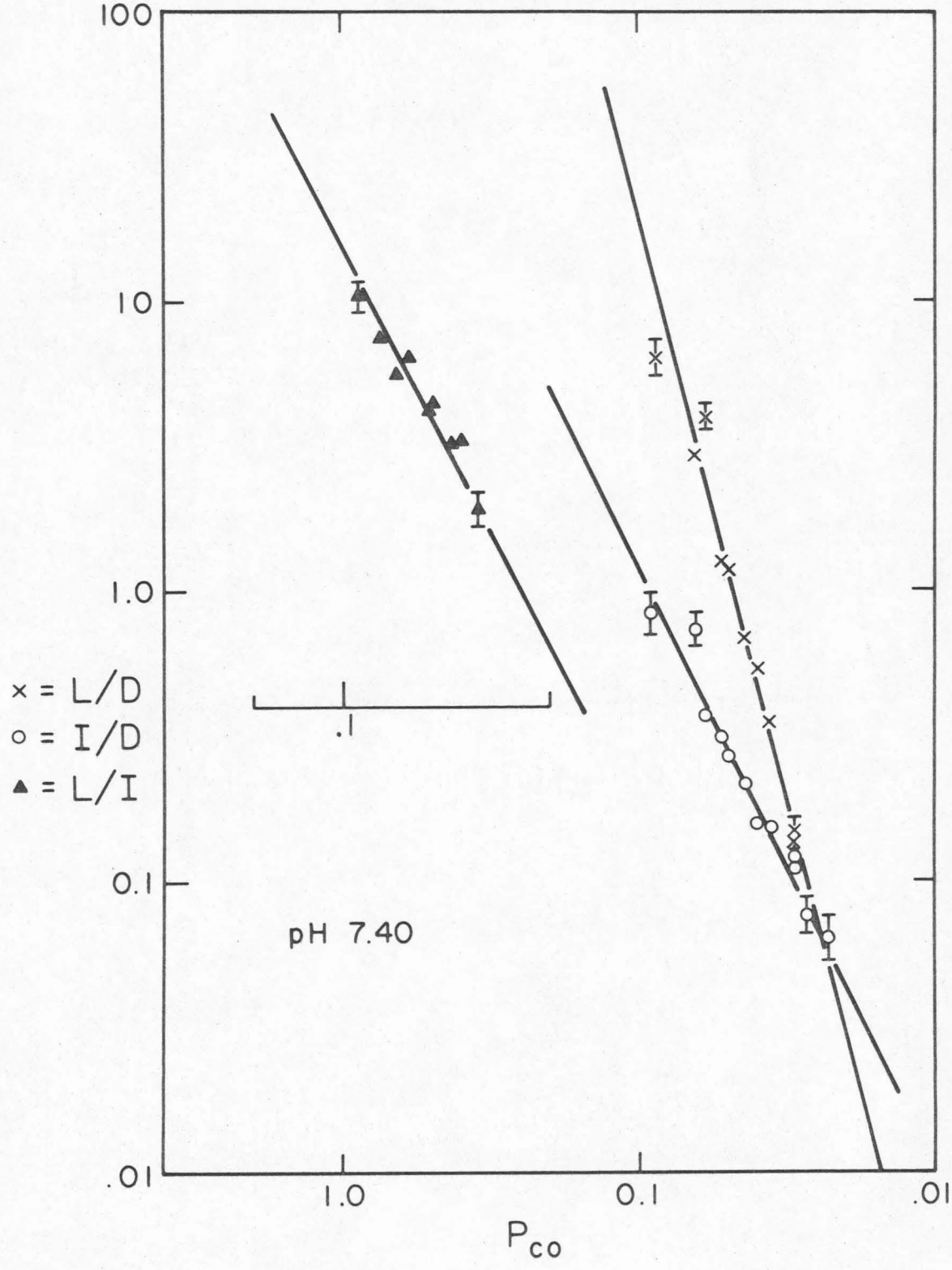
100
10
1.0
0.1
.01
× = L/D
○ = I/D
▲ = L/I
.1
pH 7.40
1.0
0.1
.01
P_{CO}

Figure 10. Dependence of the nmr populations on P_{CO} at pH 6.75, in the absence of DPG. ×, log L/D; o, log I/D; Δ, log L/I. The slopes of the lines, determined from least-squares fits of the points in the range $0.20 < Y < 0.90$, are 4.0, 2.2, and 1.1 ± 0.05, respectively.

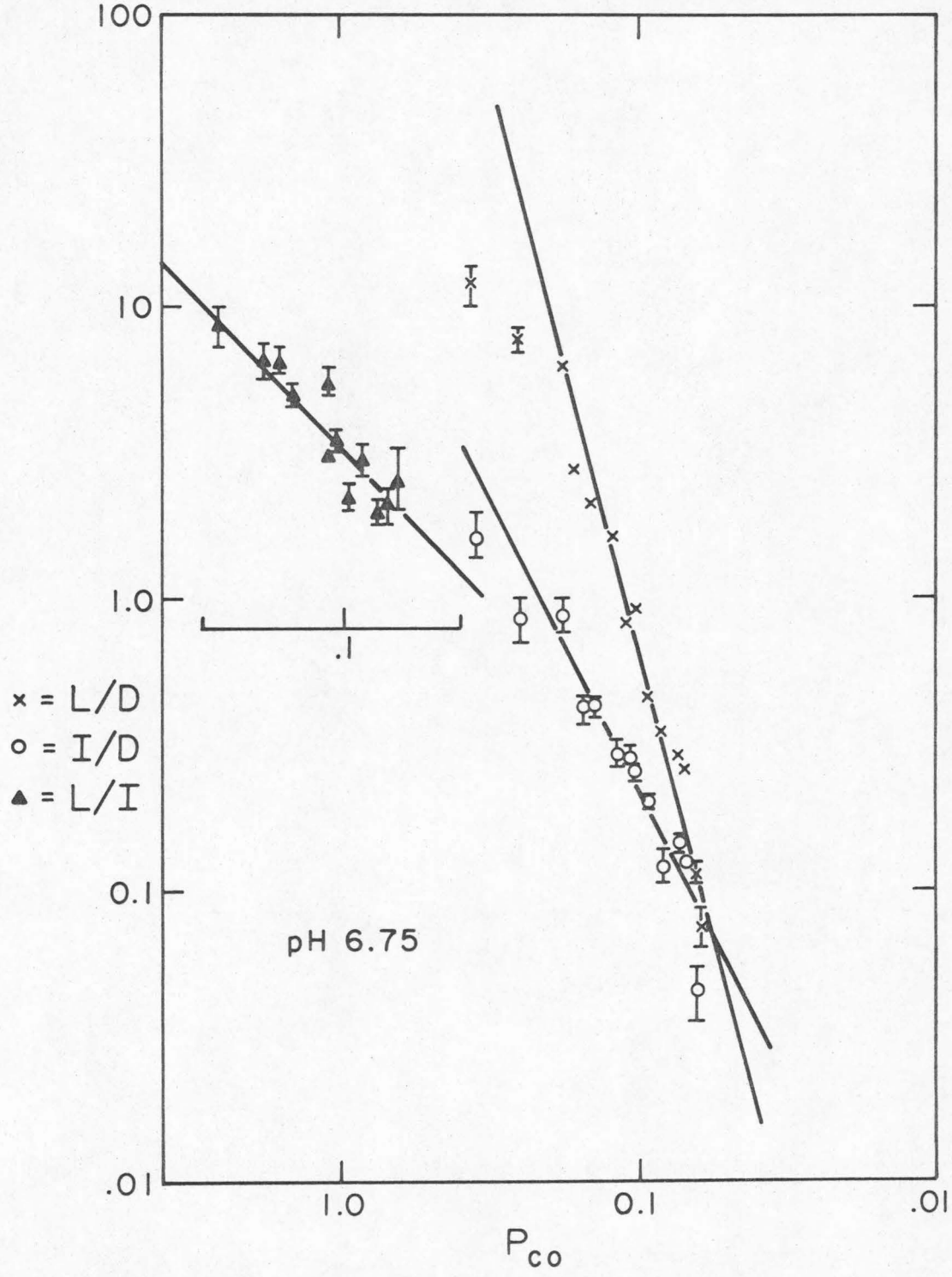
100
10
1.0
0.1
.01
1.0
0.1
.01
.1
× = L/D
○ = I/D
▲ = L/I
pH 6.75
P_{CO}

APPENDIX

Chapter II contains a brief description of coupled ionization systems. In this Appendix, the derivation of Equation (5), which describes the population of observed species as a function of $[H^+]$ and the equilibrium constants, will be reproduced. The analogous equations for three and four equivalent interacting ionizations will be discussed, and finally the identity of these relations with the Hill and Adair equations for oxygen binding to hemoglobin will be demonstrated.

The simplest coupled ionization system consists of two groups, AH and BH, each of which changes the pK_a of the other on ionization.

$$\frac{[H^+][^-A\sim BH]}{[HA\sim BH]} = K_{A_1} \qquad (1)$$

$$\frac{[H^+][^-A\sim B^-]}{[HA\sim B^-]} = K_{A_2} \qquad (2)$$

$$\frac{[H^+][HA\sim B^-]}{[HA\sim BH]} = K_{B_1} \qquad (3)$$

$$\frac{[H^+][^-A\sim B^-]}{[^-A\sim BH]} = K_{B^2} \qquad (4)$$

As is demonstrated in the free energy diagram below, thermodynamic consistency requires that $K_{A_1} K_{B_2} = K_{B_1} K_{A_2}$.

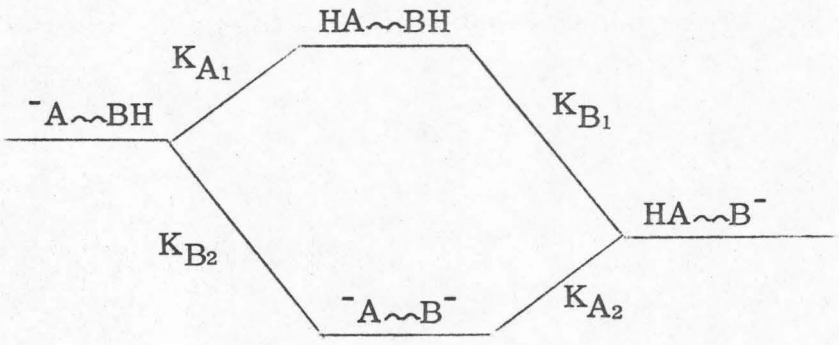

(Protons were omitted for clarity)

The observed parameter is the fraction of group A which is ionized. We wish to express this quantity (N) as a function of the constants and the $[H^+]$.

Let $[H^+] = z$

$[^-A\sim\sim BH] = x$

$[HA\sim\sim B^-] = w$

$[^-A\sim\sim B^-] = y$

$[HA\sim\sim BH] + [^-A\sim\sim BH] + [HA\sim\sim B^-] + [^-A\sim\sim B^-] = Q$

$[HA\sim\sim BH] = Q - x - y - w.$

Then

$$K_{A_1} = \frac{zx}{Q - x - y - w} \qquad (1a)$$

$$K_{A_2} = \frac{zy}{w} \tag{2a}$$

$$K_{B_1} = \frac{zw}{Q - x - y - w} \tag{3a}$$

$$K_{B_2} = \frac{zy}{x} \tag{4a}$$

and

$$N = \frac{x + y}{Q} \equiv \text{fraction of AH ionized.}$$

Let

$$\rho = \frac{K_{A_2}}{K_{B_2}} = \frac{K_{A_1}}{K_{B_1}}$$

$$= \frac{\frac{zx}{Q - x - y - w}}{\frac{zw}{Q - x - y - w}} = \frac{x}{w}$$

$$x = \rho w.$$

From (2a) and (4a)

$$y = \frac{K_{A_2} w}{z} = \frac{K_{B_2} x}{z}.$$

Substituting,

$$K_{A_1} = \frac{zx}{Q - x - \frac{K_{B_2} x}{z} - \frac{x}{\rho}}$$

$$z\,x = K_{A_1}\left(Q - x - \frac{K_{B_2}\,x}{z} - \frac{x}{\rho}\right)$$

$$= K_{A_1}Q - K_{A_1}x\left(1 + \frac{K_{B_2}\,x}{z} + \frac{1}{\rho}\right)$$

$$K_{A_1}Q = K_{A_1}x\left(\frac{z}{K_{A_1}} + 1 + \frac{K_{B_2}}{z} + \frac{1}{\rho}\right)$$

$$\frac{x}{Q} = \frac{1}{z/K_{A_1} + 1 + K_{B_2}/z + 1/\rho} \qquad (5)$$

From Equation (4a)

$$y = \frac{K_{B_2}\,x}{z}.$$

So

$$N = \frac{x+y}{Q} = \frac{1 + K_{B_2}/z}{z/K_{A_1} + 1 + K_{B_2}/z + 1/\rho}$$

$$= \frac{K_{A_1}(z + K_{B_2})}{z^2 + z\,K_{A_1} + K_{A_1}K_{B_2} + z\,K_{B_1}}$$

$$N = \frac{K_{A_1}[H^+] + K_{A_1}K_{B_2}}{[H^+]^2 + (K_{A_1} + K_{B_1})[H^+] + K_{A_1}K_{B_2}}. \qquad (6)$$

In order to keep the fitted nmr plots in the same form as the original Δ vs. pH plots, the curves were fitted from Equation (7):

$$1 - N = S = 1 - \frac{K_{A_1}[H^+] + K_{A_1}K_{B_2}}{[H^+]^2 + (K_{A_1} + K_{B_1})[H^+] + K_{A_1}K_{B_2}}$$

$$S = \frac{[H^+]^2 + [H^+]K_{B_1}}{[H^+]^2 + (K_{A_1} + K_{B_1}) + K_{A_2}K_{B_2}} \qquad (7)$$

Equation (6) is a more convenient form for the purpose of this discussion. A computer analysis was conducted of the titration curves generated by various combinations of the four constants. For the trivial case of $K_{A_1} = K_{A_2} = K_{B_1} = K_{B_2}$, Equation (6) collapses to the

$$N = \frac{K}{[H^+] + K}$$

equation of a normal titration. Normal behavior also results when $K_{B_1} \gg K_{A_1}$, so that titration of B is complete before A begins to ionize, or vice versa. Unusually shaped curves are obtained only when the titration ranges of the groups overlap. Steep curves are produced when $K_{A_1} < K_{A_2}$ and $K_{B_1} < K_{B_2}$, that is, when HA becomes a stronger acid during its ionization. When $K_{A_1} > K_{A_2}$ and $K_{B_1} > K_{B_2}$, both groups become weaker acids during titration and the observed change in $[HA]$ with pH is more gradual than normal. When the groups are equivalent, i.e., $K_{A_1} = K_{B_1}$ and $K_{A_2} = K_{B_2}$, effects of interaction are at a maximum and the observed titration of HA is perfectly symmetrical. If the interacting groups are non-equivalent, an asymmetric curve is obtained, the shape of which

depends on the spacing of the constants.

Systems of three and four interacting ionizations were analyzed as for the doubly coupled system. These models are prohibitively complicated for nonequivalent groups, so systems of equivalent groups only were considered. For three equivalent interacting ionizations,

$$N = \frac{K_1[H^+]^2 + 2K_1K_2[H^+] + K_1K_2K_3}{[H^+]^3 + 3K_1[H^+]^2 + 3K_1K_2[H^+] + K_1K_2K_3} \qquad (8)$$

and for four,

$$N = \frac{K_1[H^+]^3 + 3K_1K_2[H^+]^2 + 3K_1K_2K_3[H^+] + K_1K_2K_3K_4}{[H^+]^4 + 4K_1[H^+]^3 + 6K_1K_2[H^+]^2 + 4K_1K_2K_3[H^+] + K_1K_2K_3K_4} \qquad (9)$$

The discussion of the doubly coupled model applies in general to these models. Steeper titration curves are obtained when $K_1 < K_2 < K_3 < K_4$.

The similarity between these coupled ionization systems and models for cooperative oxygen binding to hemoglobin is readily apparent when Equation (9) is compared to the Adair equation (Adair, 1925):

$$y = \frac{4K_1x + 12K_1K_2x^2 + 12K_1K_2K_3x^3 + 4K_1K_2K_3K_4x^4}{1 + 4K_1x + 6K_1K_2x^2 + 4K_1K_2K_3x^3 + K_1K_2K_3K_4x^4}. \qquad (10)$$

This equation describes the four stage binding of a ligand (x) to a protein with four equivalent binding sites. y is the fraction of liganded sites, all four of which are observed. In general, fits of hemoglobin oxygen binding data are obtained for $K_n < K_{n+1}$. Equation (9) describes the dissociation of $[H^+]$ from a network of four equivalent sites, one of which is observed. These equations are identical when the ligand "x" of Equation (9) is expressed as the loss of a proton:

$$\frac{N}{4} = \frac{K_1\left(\frac{1}{[H^+]}\right) + 3K_1K_2\left(\frac{1}{[H^+]}\right)^2 + 3K_1K_2K_3\left(\frac{1}{[H^+]}\right)^3 + K_1K_2K_3K_4\left(\frac{1}{[H^+]}\right)^4}{1 + 4K_1\left(\frac{1}{[H^+]}\right) + 6K_1K_2\left(\frac{1}{[H^+]}\right)^2 + 4K_1K_2K_3\left(\frac{1}{[H^+]}\right)^3 + K_1K_2K_3K_4\left(\frac{1}{[H^+]}\right)^4} \qquad (11)$$

Similarly, the equations for any number of equivalent coupled ionizations can be expressed in the form of the empirical Hill equation (Hill, 1910). Consider a system of n interacting groups.

$$K_i = \frac{[H^+][(ABC\cdots n)^{-i}]}{[(ABC\cdots n)^{-i+1}]}$$

$$K_{i+1} = \frac{[H^+][(ABC\cdots n)^{-(i+1)}]}{[(ABC\cdots n)^{-i}]}$$

and so on. When a product of all equilibria is taken, populations of all intermediate ionization states cancel.

$$\prod_{i=1}^{n} K_i = \frac{[H^+]^n [(ABC\cdots n)^{-n}]}{[(ABC\cdots n)]}$$

Let

$$\prod_{i=1}^{n} K_i = K_0^n$$

$$x = [(ABC\cdots n)^{-n}]$$

$$y = [(ABC\cdots n)]$$

$$s = \frac{y}{x+y} = \text{fraction of unionized A}$$

$$z = \left[\frac{H^+}{K_0}\right]^n$$

Then $$\frac{zx}{y} = 1$$

$$x = y/z$$

$$s = \frac{y}{y/z+y} = \frac{z}{z+1}$$

$$\therefore \quad S = \frac{\left(\frac{H^+}{K_0}\right)^n}{1+\left(\frac{H^+}{K_0}\right)^n} = \frac{[H^+]^n}{K_0 + [H^+]^n} \qquad (12)$$

Equation (12) is exactly analogous to the Hill equation. The exponent n is the familiar Hill coefficient, which describes the degree of cooperativity of the system. For any set of data, the Hill number is the slope of a plot of log s/1-s versus log $[H^+]$. K_0 corresponds

to $p_{1/2}$, or the ligand pressure (concentration) required to produce saturation of half of the binding sites.

The nmr data described in Chapter II were analyzed in this manner. The "Hill coefficients" so obtained were 1.5 for Hb^{TFA}-deO_2 and 4.0 for DPG-complexed Hb^{TFA}-deO_2. pK_0, of course, is 7.4.

References:

Adair, J. G. (1925), J. Biol. Chem., 63, 529.

Hill, A. V. (1910), J. Physiol. (London), 40, iv-vii.